

The Islamic University of Gaza
High Studies Deanery
Faculty of Engineering
Civil Engineering Department
Design and Rehabilitation of Structures



الجامعة الإسلامية بغزة
عمادة الدراسات العليا
كلية الهندسة
قسم الهندسة المدنية
برنامج تصميم وتأهيل المنشآت

Non-linear Finite Element Analysis of Reinforced Concrete Beams Strengthened with Carbon Fiber- Reinforced Polymer (CFRP) Technique

By

Mohammed Rafiq Hammad

Supervised By

Dr. Mohammed Arafa

Dr. Mamoun Al-Qedra

A Thesis Submitted in Partial Fulfillment of the Requirement for the Degree
of Master of Science in Civil Engineering – Design and Rehabilitation of
Structures

1436 هـ - 2015 م

إقرار

أنا الموقع أدناه مقدم الرسالة التي تحمل العنوان:

Non-linear Finite Element Analysis of Reinforced Concrete Beams Strengthened with Carbon Fiber- Reinforced Polymer (CFRP) Technique

أقر بأن ما اشتملت عليه هذه الرسالة إنما هو نتاج جهدي الخاص، باستثناء ما تمت الإشارة إليه
حيثما ورد، وإن هذه الرسالة ككل أو أي جزء منها لم يقدم من قبل لنيل درجة أو لقب علمي أو
بحثي لدى أي مؤسسة تعليمية أو بحثية أخرى.

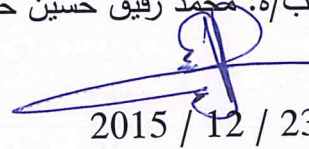
DECLARATION

The work provided in this thesis, unless otherwise referenced, is the
researcher's own work, and has not been submitted elsewhere for any
other degree or qualification

Student's name:

اسم الطالب/ة: محمد رفيق حسين حماد

Signature:

التوقيع: 

Date:

التاريخ: 2015 / 12 / 23



نتيجة الحكم على أطروحة ماجستير

بناءً على موافقة شئون البحث العلمي والدراسات العليا بالجامعة الإسلامية بغزة على تشكيل لجنة الحكم على أطروحة الباحث/ محمد رفيق حسين حماد لنيل درجة الماجستير في كلية الهندسة قسم الهندسة المدنية تصميم وتأهيل المنشآت وموضوعها:

تحليل غير خطي باستخدام طريقة العناصر المحددة للكمرات الخرسانية المسلحة المقواة بتقنية البوليمرات المسلحة بألياف الكربون

Non-linear Finite Element Analysis of Reinforced Concrete Beams Strengthened with Carbon Fiber Reinforced Polymer (CFRP) Technique

وبعد المناقشة العلنية التي تمت اليوم الأحد 10 صفر 1437 هـ، الموافق 2015/11/22م الساعة الواحدة ظهراً بمبنى طيبة، اجتمعت لجنة الحكم على الأطروحة والمكونة من:

.....	مشرفاً و رئيساً	د محمد حسني عرفة
.....	مشرفاً	د. مأمون عبد الحميد القدرة
.....	مناقشاً داخلياً	د. جمال محمد سعيد / الزيدة
.....	مناقشاً خارجياً	د. يوسف صبحي الغريز

وبعد المداولة أوصت اللجنة بمنح الباحث درجة الماجستير في كلية الهندسة / قسم الهندسة المدنية - تصميم وتأهيل المنشآت.

واللجنة إذ تمنحه هذه الدرجة فإنها توصيه بتقوى الله ولزوم طاعته وأن يبخر علمه في خدمة دينه ووطنه.

والله ولي التوفيق ،،،

نائب الرئيس لشئون البحث العلمي والدراسات العليا

أ.د. عبدالرؤف علي المناعمة

ABSTRACT

Strengthening of reinforced concrete beams with carbon fiber reinforced polymer (CFRP) is one of the most used strengthening techniques recently. It offers an attractive solution to enhance shear and flexural capacities of RC beams.

Behavior in shear and flexure of reinforced concrete beams externally strengthened with CFRP is highly affected by the way in which these composites are bonded to the beam.

The main objective of this research is to analyze strengthening of RC beams with CFRP using non-linear finite element models. The research made use of the commercial finite element modeling software (ANSYS) to prepare the finite element models and to study the influence of the important parameters on the overall response of strengthened RC beams in shear and flexure, in order to achieve the optimum utilization of such strengthening technique, in terms of load bearing capacity and possible deflection values. These parameters are: effect of number of CFRP layers, effect of CFRP layer length, and effect of CFRP layer inclination.

The analysis of results proved that the general behavior of the FE models shows a good agreement with corresponding experimental investigations results, and that ANSYS is capable of producing results in good agreement with previously published experimental test results.

The parametric study has proved that increasing the number of CFRP layers bonded to the beam soffit increases the stiffness of the beam, increases its flexural capacity, and decreases mid-span deflection at failure. Further, decreasing the length of the CFRP layer bonded to the beam soffit decreases the ultimate load of the beam with a slight increase in mid-span deflection at failure. Length of CFRP fabric when reaches 50% of beam span length, the increase in ultimate strength of the beam becomes worthless.

Moreover, it has proved that shear strengthening of RC beams with CFRP fabric inclined at an angle of 90° to the beam axis is more efficient than strengthening with CFRP fabric inclined at an angle of 45° . Further, strengthening the RC beams with one layer of U-wrap CFRP fabric inclined at an angle of 45° with an additional layer of CFRP fabric on both sides of the web inclined at an angle of 0° is more efficient than strengthening with one layer of U-wrap CFRP fabric inclined at an angle of 90° with an additional layer of CFRP fabric on both sides of the web inclined at an angle of 0° .

المخلص

تعتبر تقوية الكمرات الخرسانية المسلحة باستخدام ألياف الكربون البوليمرية إحدى أكثر طرق التقوية المستخدمة حالياً، حيث إنها تقدم حلاً جذاباً لزيادة قدرات تحمل الكمرات الخرسانية لقوى القص وعزوم الانحناء التي تتعرض عليها نتيجة الأحمال الواقعة عليها. ويتأثر تصرف الكمرات الخرسانية المسلحة المقواة باستخدام صفائح ألياف الكربون البوليمرية في حالتها قوى القص وعزوم الانحناء بالطريقة التي يتم لصق هذه الصفائح على سطح الكمرات.

تهدف هذه الرسالة إلى تحليل تقوية الكمرات الخرسانية المسلحة المقواة باستخدام ألياف الكربون البوليمرية باستخدام طريقة العناصر المحددة من خلال عمل نماذج غير خطية باستخدام برنامج ANSYS وهو أحد أشهر البرامج المستخدمة في هذا المجال. الهدف من عملية النمذجة وتحليل النماذج هو دراسة تأثير بعض العوامل المهمة التي تؤثر على سلوك هذه الكمرات في حالتها قوى القص وعزوم الانحناء، للمحاولة في إيجاد أفضل الطرق لاستخدام هذه الصفائح في تقوية الكمرات الخرسانية المسلحة، من حيث أقصى حمل يمكن أن تتحمله الكمرات قبل الفشل وأقل قيم ترخيم يمكن أن تتعرض لها، هذه العوامل هي: عدد صفائح ألياف الكربون، طول صفائح ألياف الكربون، وزاوية ميل صفائح ألياف الكربون بالنسبة لمحور الكمرات.

تحليل النماذج أظهر تقارباً جيداً بين نتائج التحليل باستخدام نماذج العناصر المحددة اللاخطية وبين النتائج التي تم الحصول عليها عملياً، مما يؤكد قدرة برنامج ANSYS على إخراج نتائج مقارنة لنتائج الاختبارات العملية المنشورة سابقاً في هذا المجال.

أظهرت عملية تحليل النماذج أن زيادة عدد صفائح ألياف الكربون البوليمرية الملصقة لسطح الكمرات الخرسانية السفلي (منطقة الشد) يؤدي إلى زيادة قساوة الكمرات وزيادة قدرة تحمل الكمرات وتقليل قيم الترخيم لحظة الانهيار. كما أظهرت أن تقليل طول صفيحة ألياف الكربون البوليمرية الملصقة بسطح الكمرات الخرسانية السفلي يؤدي إلى تقليل قدرة تحمل الكمرات وزيادة قيم الترخيم لحظة الانهيار، وأن استخدام هذه الصفائح يصبح غير مجدياً من حيث قدرة تحمل الكمرات إذا قل طول الصفيحة عن نصف مسافة البحر للكمرات.

أظهرت الدراسة أيضاً أن تقوية الكمرات الخرسانية المسلحة في حالة قوى القص باستخدام صفائح ألياف الكربون ملصقة على جوانب الكمرات بزاوية ميل 90 مع محور الكمرات أفضل من تقويتها باستخدام صفائح ملصقة على جوانب الكمرات بزاوية 45 مع محور الكمرات. بينما تقويتها باستخدام طبقة أولى من الصفائح مائلة بزاوية 45 مع محور الكمرات ثم طبقة ثانية مائلة بزاوية صفر أفضل من تقويتها بطبقة أولى من الصفائح مائلة بزاوية 90 ثم طبقة ثانية مائلة بزاوية 0.

ACKNOWLEDGEMENTS

I would like to express my sincere gratitude to my thesis supervisors, Dr. Mohammed Arafa and Dr. Mamoun Alqedra, Department of Civil Engineering, Islamic University of Gaza, for their gracious efforts and keen pursuit, which has remained a valuable asset for the successful completion of this work.

I would like to give my special thanks to my beloved parents, brothers, and sisters who have supported me the entire way.

I also extend my heartiest gratitude to my wife, Eng. Abeer Thaher, for here constant encouragement and advice. This thesis would not have been possible without her love and support.

Mohammed Hammad
Gaza - 2015

TABLE OF CONTENTS

ABSTRACT.....	I
الملخص.....	II
ACKNOWLEDGEMENTS.....	III
TABLE OF CONTENTS.....	IV
LIST OF TABLES.....	VII
LIST OF FIGURES.....	VIII
LIST OF SYMBOLS.....	XI
CHAPTER 1: INTRODUCTION.....	1
1.1 General.....	1
1.2 Problem Statement.....	1
1.3 Research Aim and Objectives.....	2
1.4 Methodology.....	2
1.5 Contents of the Thesis.....	3
CHAPTER 2: STRENGTHENING OF RC BEAMS WITH CFRP.....	4
2.1 Introduction.....	4
2.2 Constituents of Fiber Reinforced Polymers.....	4
2.3 Advantages and Disadvantages of Fiber Reinforced Polymers.....	4
2.4 Types of FRP Materials Used in Construction Applications....	5
2.4.1 Glass Fibers.....	5
2.4.2 Carbon Fibers.....	5
2.4.3 Aramid Fibers.....	6
2.5 FRP Applications for External Strengthening of RC Beams....	6
2.5.1 Flexural Strengthening.....	6
2.5.2 Shear Strengthening.....	7
2.6 Installation Techniques of FRP in Strengthening Applications.....	7
2.6.1 Pre-cured Laminates and Strip Systems.....	8
2.6.2 Fabric Systems.....	9
2.7 Previous Works in the FE Modeling of RC Beams Strengthened with CFRP.....	12
CHAPTER 3: MECHANICAL BEHAVIOR AND FINITE ELEMENT MODELING OF MATERIALS.....	15
3.1 Introduction.....	15
3.2 Concrete.....	15
3.2.1 Mechanical Behavior of Concrete.....	15
3.2.1.1 Uniaxial Compressive Stress.....	15

3.2.1.2 Uniaxial Tensile Stress.....	16
3.2.2 Finite Element Modeling of Concrete.....	16
3.2.3 Finite Element Modeling of Cracks in Concrete.....	18
3.2.3.1 Discrete Crack Model.....	18
3.2.3.2 Smearred Crack Model.....	19
3.2.4 Finite Element Failure Criteria of Concrete.....	19
3.3 Steel Reinforcement.....	21
3.3.1 Mechanical Behavior of Steel Reinforcement.....	21
3.3.2 Finite Element Modeling of Steel Reinforcement.....	22
3.3.2.1 Smearred Steel Approach.....	22
3.3.2.2 Embedded Steel Approach.....	22
3.3.2.3 Discrete Steel Approach.....	23
3.4 Fiber Reinforced Polymer (FRP).....	23
3.4.1 Mechanical Behavior of FRP.....	23
3.4.2 Finite Element Modeling of FRP.....	25
3.4.3 Finite Element Failure Criteria of FRP.....	26
CHAPTER 4: BUILDING OF ANSYS FINITE ELEMENT MODELS	27
4.1 Introduction.....	27
4.2 Description of Experimental Beams.....	27
4.2.1 Flexure Beam	27
4.2.1.1 Flexure Control Beam.....	27
4.2.1.2 Flexure Strengthened Beam	28
4.2.2 Shear Beam	28
4.2.2.1 Shear Control Beam.....	28
4.2.2.2 Shear Strengthened Beam.....	29
4.3 Modeling Assumptions.....	29
4.4 Selection of Element Types Using ANSYS	30
4.4.1 Concrete.....	30
4.4.2 Steel Reinforcement.....	31
4.4.3 Loading and Supporting Steel Plates.....	31
4.4.4 Carbon Fiber Reinforced Polymer (CFRP).....	31
4.5 Real Constants.....	33
4.5.1 Flexure Beam Model.....	33
4.5.2 Shear Beam Model.....	34
4.6 Material Properties.....	35
4.6.1 Concrete.....	35
4.6.1.1 Linear Isotropic Properties of Concrete.....	35
4.6.1.2 Multilinear Isotropic Properties of Concrete	35
4.6.1.3 Failure Criteria of Concrete.....	38
4.6.2 Steel Reinforcement.....	40
4.6.3 Loading and Supporting Steel Plates.....	41
4.6.4 Carbon Fiber Reinforced Polymer (CFRP).....	42

4.6.4.1 Linear Orthotropic Properties.....	43
4.6.4.2 Section Properties.....	44
4.6.4.3 Failure Criteria of CFRP.....	44
4.7 Geometry.....	44
4.7.1 Flexure Beam.....	44
4.7.2 Shear Beam Model.....	45
4.8 Meshing.....	46
4.8.1 Concrete and Steel Plates.....	46
4.8.2 Reinforcement.....	48
4.8.3 CFRP Fabric Layer.....	50
4.9 Loads and Boundary Conditions.....	53
4.10 Setting Nonlinear Solution Parameters.....	57
CHAPTER 5: VERIFICATION OF ANSYS FINITE ELEMENT MODELS AND PARAMETRIC STUDY.....	60
5.1 Introduction.....	60
5.2 Verification of ANSYS Finite Element Models.....	60
5.2.1 Load - Mid Span Deflection Curves.....	60
5.2.1.1 Flexure Beam.....	60
5.2.1.2 Shear Beam.....	64
5.2.3 Crack Patterns.....	68
5.2.3.1 Crack Patterns for Flexure Beam.....	68
5.2.3.2 Crack Patterns for Shear Beam.....	72
5.2.4 Loads and Deflection at Failure.....	78
5.2.5 Maximum Stresses in CFRP Fabric.....	81
5.2.6 Maximum Strain in CFRP Fabric.....	83
5.3 Parametric Study.....	84
5.3.1 Effect of Number of CFRP Layers – Flexure Beam.....	84
5.3.2 Effect of CFRP Length – Flexure Beam.....	86
5.3.3 Effect of CFRP Inclination – Shear Beam.....	87
CHAPTER 6: CONCLUSIONS AND FUTURE WORKS.....	91
6.1 Introduction.....	91
6.2 Conclusions.....	91
6.3 Recommendations.....	93
REFERENCES.....	95

LIST OF TABLES

Table (3-1):	Typical Properties of FRP Materials.....	25
Table (4-1):	Element Types for ANSYS Flexure and Shear Beams Models.....	32
Table (4-2):	Real Constants for ANSYS Flexure Beam Model.....	33
Table (4-3):	Real Constants for ANSYS Shear Beam Model.....	34
Table (4-4):	Material Properties of Concrete for ANSYS Flexure Beam Model	37
Table (4-5):	Material Properties of Concrete for ANSYS Shear Beam Model...	38
Table (4-6):	Material Properties of Steel Reinforcement for ANSYS Flexure Beam Model.....	40
Table (4-7):	Material Properties of Steel Reinforcement for ANSYS Flexure Beam Model.....	41
Table (4-8):	Material Properties of Steel Plates for ANSYS Flexure Beam and Shear Beam Models.....	42
Table (4-9):	Material Properties of CFRP for ANSYS Flexure Beam Model.....	42
Table (4-10):	Material Properties of CFRP for ANSYS Shear Beam Model.....	43
Table (4-11):	Dimensions of Volumes and Areas - Flexure Beam Model.....	44
Table (4-12):	Dimensions of Volumes and Areas – Shear Beam Model.....	45
Table (4-13):	Mesh Attributes – Flexure Beam Model.....	50
Table (4-14):	Mesh Attributes – Shear Beam Model.....	51
Table (4-15):	Nonlinear Analysis Control Commands.....	57
Table (4-16):	Output Control Commands.....	58
Table (4-17):	Nonlinear Algorithm and Convergence Criteria Parameters.....	58
Table (4-18):	Advanced Nonlinear Control Settings.....	58
Table (4-19):	ANSYS Analysis Statistics.....	59
Table (5-1):	Comparisons Between Experimental and ANSYS Results – Failure Loads.....	78
Table (5-2):	Comparisons Between Experimental and ANSYS Results – Mid- Span Deflection.....	78
Table (5-3):	Effect of Increasing Number of CFRP Layers – Comparison of ANSYS Results.....	85
Table (5-4):	Effect of CFRP Length – Comparison of ANSYS Results.....	87
Table (5-5):	Effect of CFRP Inclination – Comparison of ANSYS Results.....	90

LIST OF FIGURES

Figure (2-1):	Constituents of Fiber Reinforced Polymers Materials.....	4
Figure (2-2):	FRP Products Currently Used for Reinforcement or Rehabilitation of Concrete Structures.....	6
Figure (2-3):	Typical Flexural Strengthening of a Reinforced Concrete T- beam Using Externally Bonded FRP Reinforcement.....	7
Figure (2-4):	Two-Way Flexural Strengthening of a Reinforced Concrete Slab Using Carbon FRP Strips.....	7
Figure (2-5):	Typical Shear Strengthening Schemes of a Reinforced Concrete T-Beam Using Externally Bonded FRP Reinforcement.....	8
Figure (2-6):	Shear Strengthening of a Reinforced Concrete Bridge Girder Using CFRP Sheets.....	8
Figure (2-7):	Pressing a Carbon FRP Strip into Adhesive.....	9
Figure (2-8):	Application of Epoxy Primer.....	9
Figure (2-9):	Application of Epoxy Putty.....	10
Figure (2-10):	Application of Epoxy Saturant Layer.....	10
Figure (2-11):	Impregnating of CFRP Fabric with Epoxy.....	11
Figure (2-12):	Layers of Materials in a Typical Lay-up Application of an Externally-Bonded FRP System.....	11
Figure (3-1):	Uniaxial Compressive Behavior of Concrete.....	15
Figure (3-2):	Uniaxial Tensile Behavior of Concrete.....	16
Figure (3-3):	Uniaxial Stress-Strain Behavior of Concrete.....	17
Figure (3-4):	Modified Hognestad Model Used in the Present Study.....	17
Figure (3-5):	Discrete Crack Model: (a) Inter-element Crack Approach, (b) Intra-element Crack Approach.....	18
Figure (3-6):	Smeared Crack Model.....	19
Figure (3-7):	3D failure Surface for Concrete.....	20
Figure (3-8):	Tensile Stress-strain Curve for Typical Reinforcing Steel Bar.....	21
Figure (3-9):	Idealized Stress-Strain Curve for Reinforcing Steel.....	22
Figure (3-10):	Modeling of Reinforcement: (a) Distributed Steel Approach, (b) Embedded Steel Approach, (c) Discrete Steel Approach...	23
Figure (3-11):	Stress-Strain Relationships for FRP.....	24
Figure (3-12):	Stress-Strain Plots for Various FRP Strengthening Systems...	24
Figure (3-13):	Schematic of FRP Composites.....	26
Figure (4-1):	Description of Flexure Control Beam Model.....	28
Figure (4-2):	Description of Flexure Strengthened Beam Model.....	28
Figure (4-3):	Description of Shear Control Beam Model.....	29
Figure (4-4):	Description of Shear Strengthened Beam Model.....	29
Figure (4-5):	Solid65 Geometry.....	30
Figure (4-6):	Link180 Geometry.....	31

Figure (4-7):	SOLID185 Homogeneous Structural Solid Geometry.....	32
Figure (4-8):	Shell181 Geometry.....	32
Figure (4-9):	Compressive Uniaxial Stress-Strain Curve for Concrete – Flexure Beam Model.....	36
Figure (4-10):	Compressive Uniaxial Stress-Strain Curve for Concrete – Shear Beam Model.....	36
Figure (4-11):	Stress-Strain Curve for Steel Reinforcement.....	41
Figure (4-12):	Volumes Created in ANSYS - Flexure Beam Model.....	45
Figure (4-13):	Volumes Created in ANSYS - Shear Beam Model.....	46
Figure (4-14):	Mesh of the Concrete Beam and Steel Plates – Flexure Beam Model.....	47
Figure (4-15):	Mesh of the Concrete Beam and Steel Plates – Shear Beam Model.....	47
Figure (4-16/a):	Reinforcement Configuration– Flexure Beam Model.....	48
Figure (4-16/b):	Reinforcement Configuration– Flexure Beam Model.....	49
Figure (4-17/a):	Reinforcement Configuration– Shear Beam Model.....	49
Figure (4-17/b):	Reinforcement Configuration– Shear Beam Model.....	50
Figure (4-18):	Meshing of CFRP Layer in ANSYS – Flexure Beam Model....	51
Figure (4-19):	Meshing of CFRP Layer in ANSYS – Shear Beam Model.....	52
Figure (4-20):	The Overall Meshing of the Model – Flexure Beam Model....	52
Figure (4-21):	The Overall Meshing of the Model – Shear Beam Model.....	53
Fig. (4-22):	Plane of Symmetry – Flexure Beam Model	54
Fig. (4-23):	Plane of Symmetry – Shear Beam Model	54
Fig. (4-24):	Beam Support Plate – Flexure Beam Model	55
Fig. (4-25):	Beam Support Plate – Shear Beam Model	55
Fig. (4-26):	Loading Plate – Flexure Beam Model	56
Fig. (4-27):	Loading Plate - Shear Beam Model	56
Figure (5-1):	Comparison of Experimental Load Deflection Curves for Flexure Beam.....	60
Figure (5-2):	Comparison of ANSYS Load Deflection Curves for Flexure Beam.....	61
Figure (5-3):	Comparison of Load Deflection Curves – Flexure Control Beam.....	62
Figure (5-4):	Reinforcement Elastic Stress at Yielding Load– Flexure Control Beam.....	62
Figure (5-5):	Comparison of Load Deflection Curves – Flexure Strengthened Beam.....	63
Figure (5-6):	Reinforcement Elastic Stress at Yielding Load – Flexure Strengthened Beam.....	64
Figure (5-7):	Comparison of ANSYS Load Deflection Curves for Shear Beam.....	65
Figure (5-8):	Load Deflection Curve – Shear Control Beam.....	65
Figure (5-9):	Reinforcement Elastic Stress at Yielding Load – Shear	66

	Control Beam.....	67
Figure (5-10):	Comparison of Load Deflection Curves – Shear Strengthened Beam.....	67
Figure (5-11):	Reinforcement Elastic Stress at Yielding Load – Shear Strengthened Beam.....	67
Figure (5-12):	Crack Propagations – Flexure Control Beam.....	70
Figure (5-13):	Crack Propagations – Flexure Strengthened Beam.....	71
Figure (5-14):	Crack Propagations – Shear Control Beam.....	74
Figure (5-15):	Crack Propagations – Shear Strengthened Beam.....	77
Figure (5-16):	Deflection Contour Results at Failure – Flexure Control Beam.....	79
Figure (5-17):	Deflection Contour Results at Failure – Flexure Strengthened Beam.....	80
Figure (5-18):	Deflection Contour Results at Failure – Shear Control Beam.....	80
Figure (5-19):	Deflection Contour Results at Failure – Shear Strengthened Beam.....	81
Figure (5-20):	Stress of CFRP Fabric at Failure – Flexure Strengthened Beam.....	82
Figure (5-21):	Stress of CFRP Fabric at Failure – Shear Strengthened Beam.....	82
Figure (5-22):	Strain of CFRP Fabric at Failure – Flexure Strengthened Beam.....	83
Figure (5-23):	Strain of CFRP Fabric at Failure – Shear Strengthened Beam.....	84
Figure (5-24):	Bonding Multiple CFRP Layers to the Flexure Beam.....	84
Figure (5-25):	Effect of Increasing Number of CFRP Layers Bonded to the Flexure Beam– Load Deflection Curves.....	85
Figure (5-26):	Effect of Changing Length of CFRP Layer – Load Deflection Curves.....	86
Figure (5-27):	Decreasing length of CFRP Layer Bonded to Flexure Beam...	87
Figure (5-28):	Effect of CFRP Inclination – First Configuration.....	87
Figure (5-29):	Effect of CFRP Inclination – Second Configuration.....	88
Figure (5-30):	Effect of CFRP Inclination – Third Configuration.....	88
Figure (5-31):	Effect of CFRP Inclination – Fourth Configuration.....	89
Figure (5-32):	Effect of CFRP Inclination – Load Deflection Curves.....	90

LIST OF SYMBOLS

f_c'	Concrete compressive strength.
E_c	Modulus elasticity of concrete.
F	Function of the principal stress state (σ_{xp} , σ_{yp} , σ_{zp}).
S	Failure surface of concrete expressed in terms of principal stresses and five input parameters f_t , f_c , f_{cb} , f_1 and f_2 .
f_c	Uniaxial crushing strength of concrete.
σ_{xp}	Principal stresses in x direction.
σ_{yp}	Principal stresses in y direction.
σ_{zp}	Principal stresses in z direction.
f_t	Ultimate uniaxial tensile strength of concrete.
f_c	Ultimate uniaxial compressive strength of concrete.
f_{cb}	Ultimate biaxial compressive strength of concrete.
σ_h^a	Ambient hydrostatic stress state.
f_1	Ultimate compressive strength of concrete for a state of biaxial compression superimposed on hydrostatic stress state σ_h^a .
f_2	Ultimate compressive strength of concrete for a state of uniaxial compression superimposed on hydrostatic stress state.
E_s	Modulus elasticity of steel.
f_y	Yield strength of steel.
ε_y	The strain at which steel yields.
f_u	Peak strength of steel.
ε_u	The strain at which peak strength of steel is achieved.
f_s	The strain at which steel failure occurs.
ε_{max}	The strain at which fracture of steel occurs.
f_s	The strain at which steel failure occurs.
ν	Poisson's ratio.
EX	Modulus of elasticity in x-direction.
EY	Modulus of elasticity in y-direction.
EZ	Modulus of elasticity in z-direction.
PRXY	Poisson's ratio in xy-plane.
PRYZ	Poisson's ratio in yz-plane.
PRXZ	Poisson's ratio in xz-plane.
GXY	Shear modulus in xy-plane.
GYZ	Shear modulus in yz-plane.
GXZ	Shear modulus in xz-plane.
TK	Thickness of CFRP layer.
THETA	Angle of orientation of CFRP layer.
Stress –XTEN	Maximum stress of CFRP in fiber direction.
Strain – XTEN	Maximum strain of CFRP in fiber direction.

CHAPTER 1

INTRODUCTION

1.1 General

Strengthening with fiber reinforced polymer (FRP) is one of most used strengthening techniques of reinforced concrete beams due to a number of advantages, such as excellent strength to self-weight ratio, high tensile strength, large fatigue resistance capacity, and high durability, (Jayajothi, 2013, Camata, 2007).

Reinforced concrete (RC) beams with carbon and glass fiber-reinforced polymer (CFRP and GFRP) composites offer an attractive solution to enhance shear and flexural capacities and ductility, as well as altering the mode of rupture, (Vijayakumar, 2012, Chansawat, 2009).

Investigation of the behavior of FRP retrofitted reinforced concrete structures has in the last decade become a very important research field. In terms of experimental application, several studies were performed to study the behavior of retrofitted beams and how various parameters influence its behavior, (Basappa, 2013, Santhakumar, 2004).

While experimental methods of investigation are extremely useful in obtaining information about the composite behavior of FRP and reinforced concrete, the use of numerical models helps in developing a good understanding of the behavior at lower costs, (Elyasian, 2006, Supaviriyakit, 2004).

In this research, non-linear finite element analysis models for strengthening of reinforced concrete beams with carbon fiber reinforced polymers (CFRP) have been presented. The research made use of the commercial Finite Element modeling software (ANSYS) to study the effects of some parameters that are important in the response of the strengthened concrete beams in shear and flexure.

1.2 Problem Statement

Behavior in shear and flexure of reinforced concrete beams strengthened externally with carbon fiber reinforced polymers (CFRP) is highly affected by the way in which these composites are applied (bonded) to the beam, (Vijayakumar, 2012, Chansawat, 2009, Santhakumar, 2004).

In this research, the influence of some important parameters on the overall response of the strengthened RC beams has been investigated, in order to

achieve the optimum utilization of such strengthening technique, in terms of load bearing capacity and possible deflection values.

1.3 Research Aim and Objectives

The aim of this research is to develop nonlinear finite element models of reinforced concrete beams externally strengthened with carbon fiber reinforced polymers (CFRP) using the commercial finite element modeling software (ANSYS); in order to investigate the effect of different parameters on the behavior of these beams.

Objectives of this research are to:

- 1- Identify the suitable consecutive element types available in ANSYS library that are capable of modeling the behavior of RC beams externally strengthened with CFRP. (Concrete, steel reinforcement bars, interface between concrete and steel, loading plates, supporting plates, CFRP fabrics, and interface between concrete and CFRP fabrics).
- 2- Develop non-linear three dimensional finite element models to simulate the behavior of simply supported reinforced concrete beams externally strengthened in flexure and shear with CFRP.
- 3- Verify the finite element models by comparing results obtained from the models with results obtained from experimental tests available in the literature.
- 4- Conduct a parametric study using the verified model to evaluate the effect of different parameters on the behavior of strengthened beams.

1.4 Methodology

The following methodology was followed in this research to achieve the research objectives:

a- Review of available literature related to the research subject: A review for available literature for the finite element modeling and experimental works related to external strengthening of reinforced concrete beams with Carbon Fiber-Reinforced Polymers (CFRP) was conducted.

b- Development of the Finite Element models using ANSYS: Non-linear three dimensional finite element models were developed to simulate the behavior of simply supported reinforced concrete beams externally strengthened with Carbon Fiber-Reinforced Polymers (CFRP), using the commercial finite element modeling software (ANSYS). Unstrengthened flexure control beam, strengthened flexure beam, unstrengthened shear control beam, and strengthened shear beam were modeled. This step included the following tasks:

- a- Modeling of properties of concrete, steel reinforcement bars, interface between concrete and steel, loading plates, supporting plates, CFRP fabrics, and interface between concrete and CFRP fabrics.
- b- Preparing the model geometry and selection of element types based on the real materials properties and the element types available in ANSYS.
- c- Determination of boundary conditions that were used in the model.
- d- Fixing of analysis assumptions (where needed).
- e- Carrying out the nonlinear analysis.
- f- Getting the analysis results.

c- Models Verification: Finite element models were calibrated with experimental results available in the literature based on the following criteria:

- a- Load – mid span deflection curves.
- b- Loads and deflection at failure.
- c- Maximum stresses in CFRP fabric.
- d- Maximum strains in CFRP fabric

d- Performing a Parametric Study: After verification of Finite Element models, a parametric study was performed using ANSYS to evaluate the effect of the following parameters on the behavior of strengthened beams:

- a- Effect of number of CFRP layers.
- b- Effect of CFRP length.
- c- Effect of CFRP inclination.

e- Conclusion and Recommendations: Results and recommendations of this research were presented.

1.5 Contents of the Thesis

This thesis consists of six chapters: Chapter 1: Introduction, Chapter 2: Strengthening of RC Beams with CFRP, Chapter 3: Mechanical Behavior and Finite Element Modeling of Materials, Chapter 4: Building of ANSYS Finite Element Models, Chapter 5: Verification of ANSYS Finite Element Models and Parametric Study, and Chapter 6: Conclusions and Recommendations

CHAPTER 2

STRENGTHENING OF RC BEAMS WITH CFRP

2.1 Introduction

In this chapter, a background about Fiber Reinforced Polymers FRP (constituents, advantages, disadvantages, types) is presented. Typical applications of CFRP for external flexural and shear strengthening of RC beams, installation techniques of CFRP in strengthening applications, and finally, literature works about FE analysis of RC beams strengthened with CFRP using ANSYS are presented.

2.2 Constituents of Fiber Reinforced Polymers

FRP materials are composed of high strength fibers embedded in a polymer matrix. The fibers, which have very small diameters and are generally considered continuous, provide the strength and stiffness of the composite, while the matrix, which has comparatively poor mechanical properties, separates and disperses the fibers. The primary function of the matrix is to transfer loads to the fibers through shear stresses that develop at the fiber-matrix interface, although it is also important for environmental protection of the fibers. Figure (2-1) illustrates the basic material components that are combined to create an FRP composite, [Kaw, 2006].

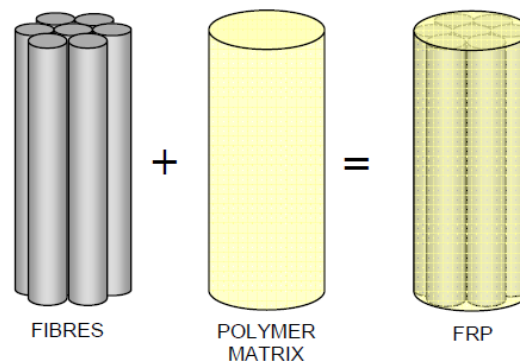


Fig. (2-1): Constituents of Fiber Reinforced Polymers Materials, [Kaw, 2006].

2.3 Advantages and Disadvantages of Fiber Reinforced Polymers

FRP materials for use in concrete strengthening applications have a number of key advantages over conventional reinforcing steel. Some of the most important advantages include [CSC.TR-No55, 2000]:

1. Do not corrode electrochemically, and have demonstrated excellent durability in a number of harsh environmental conditions.

2. Have extremely high strength-to weight ratios (typically weigh less than one fifth the weight of steel, with tensile strengths that can be as much as 8 to 10 times as high).
3. Their installation is easy and simple with no need for temporary support.
4. Have low thermal conductivity.

FRP materials also have a number of potential disadvantages [CSC.TR-No55, 2000]:

1. The relatively high cost of the materials.
2. The risk of fire, vandalism or accidental damage, unless the strengthening is protected.
3. The relatively low elastic modulus of FRPs as compared with steel.

2.4 Types of FRP Materials Used in Construction Applications

Many different types of fibers are available for use. In construction applications, the three most commonly used fiber types are: Glass, Carbon, and Aramid, [ACI 440R, 2007, Kaw, 2006, ISIS-EC-2, 2006].

2.4.1 Glass Fibers

Glass fibers are the most inexpensive, and consequently the most commonly used, fibers in structural engineering applications. Glass fibers are characterized by their high strength, moderate modulus of elasticity and density, and by their low thermal conductivity.

Glass fibers are often chosen for structural applications that are not weight critical (glass FRPs are heavier than carbon or aramid) and that can tolerate the larger deflections resulting from the comparatively low elastic modulus of the glass fibers. Glass fibers are often used in the manufacture of FRP reinforcing bars, pultruded FRP structural sections, FRP wraps for seismic upgrade, and filament wound FRP tubes.

2.4.2 Carbon Fibers

Several classes of carbon fibers are available, differentiated based on their elastic moduli. Although considerably more expensive than glass fibers, carbon fibers are beginning to see widespread use in structural FRP wraps for repair and strengthening of reinforced concrete beams, columns, and slabs.

Their steadily increasing use can be attributed to their steadily decreasing cost, their high elastic moduli and available strengths, their low density (low weight), and their outstanding resistance to thermal, chemical, and

environmental effects. Carbon fibers are an ideal choice for structures which are weight and/or deflection sensitive.

2.4.3 Aramid Fibers

Aramid fibers are characterized by high strength, moderate elastic modulus, and low density. In addition, FRPs manufactured from aramid fibers have low compressive and shear strengths as a consequence of the unique anisotropic properties of the fibers. Aramid fibers are also susceptible to degradation from exposure to ultraviolet radiation and/or moisture.

Figure (2-2) shows various FRP products currently used for reinforcement or rehabilitation of concrete structures.



Fig. (2-2): FRP Products Currently Used for Reinforcement or Rehabilitation of Concrete Structures, [ISIS-EC-2, 2006].

2.5 FRP Applications for External Strengthening of RC Beams

2.5.1 Flexural Strengthening

In this application, FRP materials are bonded to the tension and/or side faces of a concrete beam to provide additional tensile reinforcement and to increase the strength of the member in bending (Fig. 2-3). The fibers are oriented along the longitudinal axis of the beam, [CSC.TR-No55, 2000, ISIS-EC-4, 2004].

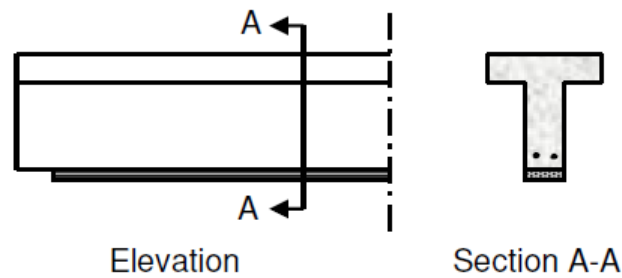


Fig. (2-3): Typical Flexural Strengthening of a Reinforced Concrete T-beam Using Externally Bonded FRP Reinforcement, [CSC.TR-No55, 2000].

Figure (2-4) provides an actual application of the use of externally-bonded FRPs in flexural strengthening applications.



Fig. (2-4): Two-Way Flexural Strengthening of a Reinforced Concrete Slab Using Carbon FRP Strips, [ISIS-EC-4, 2004].

2.5.2 Shear Strengthening

In this application, FRP materials are bonded to the side faces of a concrete beam to provide shear reinforcement which supplements that provided by the internal steel stirrups (Fig. 2-5). The fibers are oriented perpendicular to the longitudinal axis of the beam, [CSC.TR-No55, 2000, ISIS-EC-4, 2004].

Figure (2-6) provides an actual application of the use of externally-bonded FRPs in shear strengthening applications.

2.6 Installation Techniques of FRP in Strengthening Applications

Several methods are currently available to bond FRP materials to concrete members. The two most common methods involve the use of adhesively bonded pre-cured laminates or laid-up fabric systems, [CSC.TR-No55, 2000, ISIS-EC-6, 2006].

2.6.1 Pre-cured Laminates and Strip Systems

A layer of mixed adhesive, typically 1 mm to 3 mm thick, is applied to both the substrate (over the area to be bonded) and the FRP strip. The FRP is then carefully placed in position on the concrete member and is pressed against its surface using a hard rubber roller to achieve a void-free bond line with a thickness of between 2 mm and 3 mm, (Fig.2-7).

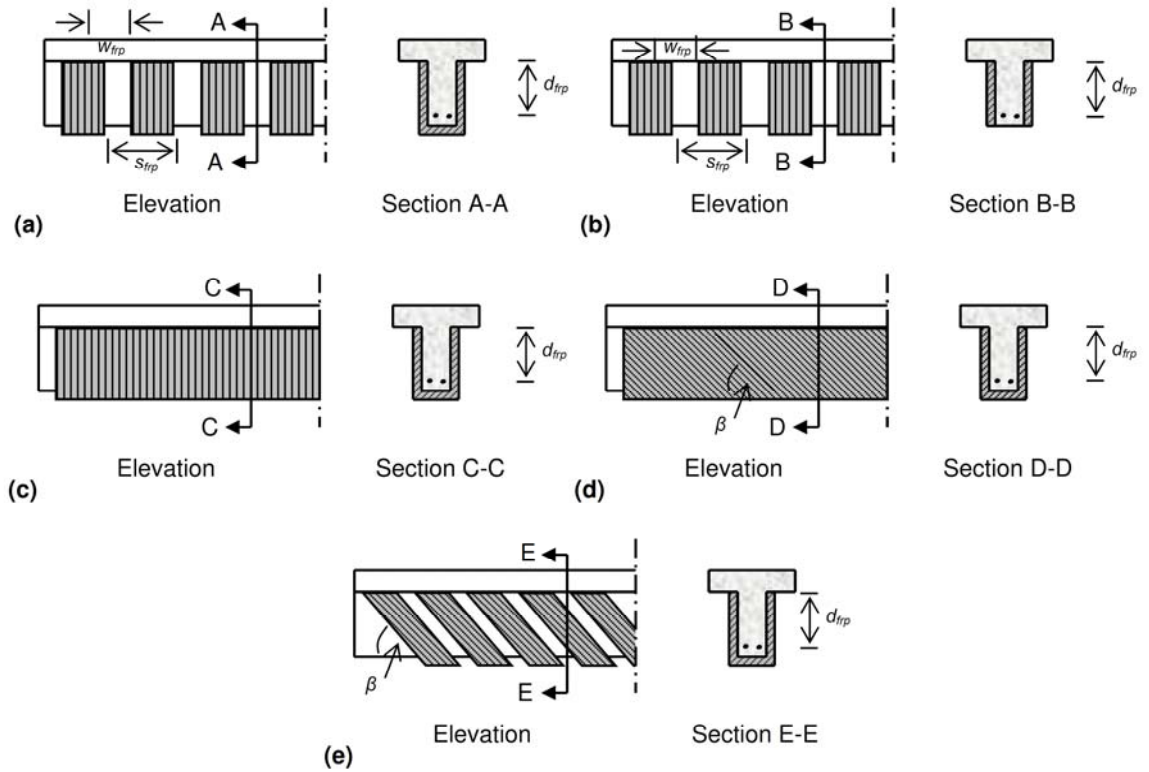


Fig. (2-5): Typical Shear Strengthening Schemes of a Reinforced Concrete T-Beam Using Externally Bonded FRP Reinforcement, [CSC.TR-No55, 2000].



Fig. (2-6): Shear Strengthening of a Reinforced Concrete Bridge Girder Using CFRP Sheets, [ISIS-EC-2, 2006].

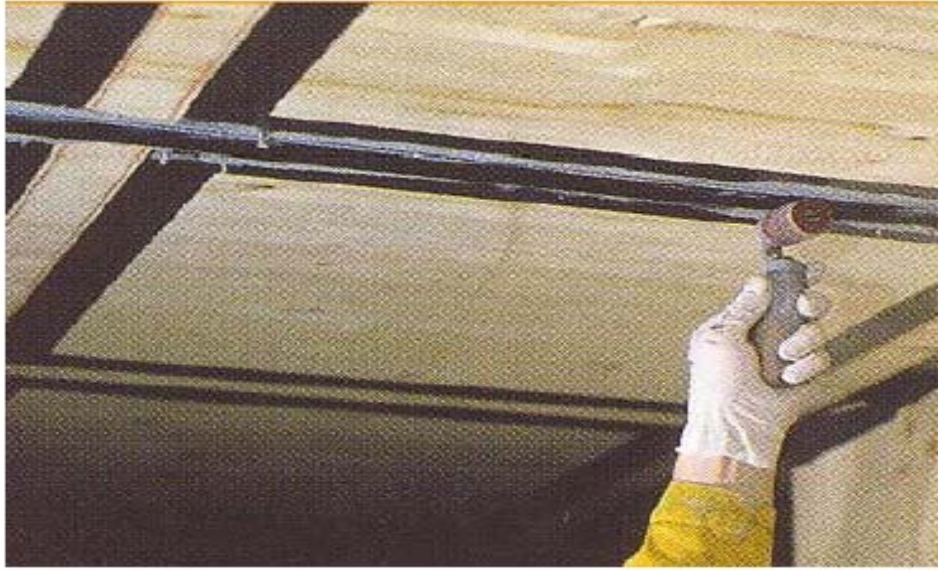


Fig. (2-7): Pressing a Carbon FRP Strip into Adhesive, [ISIS-EC-6, 2006].

2.6.2 Fabric Systems

Two different methods are available for the application of FRP fabric strengthening systems for concrete, namely wet lay-up and dry lay-up. These two techniques are similar, however, and consist of the following steps:

1. A low viscosity epoxy primer is applied to the concrete, using a standard paint roller, to seal and strengthen the concrete surface and to provide the optimal surface for bonding to the FRP material. (Fig.2-8)



Fig. (2-8): Application of Epoxy Primer, [ISIS-EC-6, 2006].

2. The surface of the concrete is leveled, where necessary, with a squeegee or trowel using non-sag epoxy putty. Any minor voids or surface irregularities should be leveled, (Fig.2-9).



Fig. (2-9): Application of Epoxy Putty, [ISIS-EC-6, 2006].

3. A layer of mixed epoxy resin saturant is applied to the surface of the concrete member using a brush, roller, or trowel, (Fig.2-10).



Fig. (2-10): Application of Epoxy Saturant Layer, [ISIS-EC-6, 2006].

4. The FRP material is bonded to the surface of the concrete using the wet or dry lay up technique:
 - **Wet Lay-up** – The fiber fabric is saturated with resin before being bonded to the concrete. The saturated FRP sheet is then placed onto the surface of the concrete and smoothed out by hand or using a squeegee to ensure intimate contact.
 - **Dry Lay-up** – Unsaturated (dry) fiber fabric is placed into the initial layer of saturant applied to the surface of the member. The



Fig. (2-11): Impregnating of CFRP Fabric with Epoxy, [ISIS-EC-6, 2006].

5. A second layer of saturant is applied with a roller over top of the fiber fabric.
6. The process can be repeated for multiple layers of FRP.

Figure (2-12) shows the various layers of materials in a typical lay-up application of an externally-bonded FRP strengthening system.

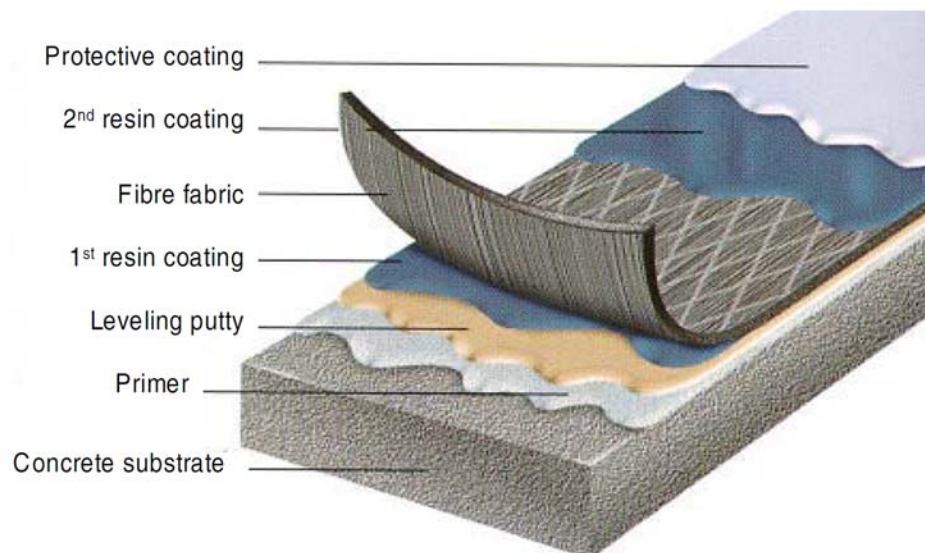


Fig. (2-12): Layers of Materials in a Typical Lay-up Application of an Externally-Bonded FRP System, [CSC.TR-No55, 2000].

2.7 Previous Works in the FE Modeling of RC Beams Strengthened with CFRP

Santhakumar et al. [2004] worked on "Analysis of Retrofitted Reinforced Concrete Shear Beams using Carbon Fiber Composites". They presented a numerical study to simulate the behavior of retrofitted reinforced concrete shear beams. The study was carried out on the unretrofitted RC beam designated as control beam and RC beams retrofitted using carbon fiber reinforced plastic (CFRP) composites with $\pm 45^\circ$ and 90° fiber orientations. The effect of retrofitting on uncracked and precracked beams was studied too. The finite elements adopted by ANSYS were used in this study. The load deflection plots obtained from numerical study showed good agreement with the experimental plots reported by Tom Norris, et al.

Amer et al. [2009] worked on "Finite Element Analysis of RC Beams Strengthened with CFRP in Flexure". They performed numerical analysis using ANSYS to simulate reinforced concrete beams strengthened by CFRP applied at the bottom of these beams. Nonlinear material behavior was simulated using appropriate constitutive models. The results showed that the general behavior of the finite element models represented by the load-deflection curves at mid-span showed good agreement with the test data from the previous researches. Also the crack patterns at the failure loads from the finite element models corresponded well with the observed failure modes of the experimental beams.

Amer et al. [2009] worked on "Finite Element Modeling of Reinforced Concrete Beams Strengthened with FRP Laminates". They presented an analysis model for reinforced concrete beams externally reinforced with fiber reinforced polymer (FRP) laminates using ANSYS. The finite element models were developed using a smeared cracking approach for concrete and 3D layered elements for the FRP composites. The results obtained from the ANSYS finite element analysis were compared with the experimental data for six beams with different conditions from researches (all beams are deficient shear reinforcement). The comparisons were made for load-deflection curves at mid-span; and failure load. The accuracy of the finite element models is assessed by comparison with the experimental results, which were to be in good agreement. The load-deflection curves from the finite element analysis agreed well with the experimental results in the linear range, but the finite elements results were slightly stiffer than that from the experimental results. He concluded that the addition of FRP reinforcement to the control beam shifted the behavior of the control beams from shear failure near the ends of the beam to flexure failure at the mid-span.

Abbas [2010] worked on "Non-linear Analysis of RC Beams Strengthened with Steel and CFRP Plates". He conducted a 3D nonlinear finite element analysis of reinforced concrete beams strengthened with bonding steel or carbon-fiber reinforcement plates using ANSYS and a smeared crack approach for concrete, to obtain the response of the strengthened beams with steel and CFRP plates in terms of applied load -deflection, tension force distribution in the strengthening plates along the reinforced concrete beams, and bond force distribution in the beam with CFRP plate and beam with steel plate. It was found the general behavior of the finite element models represented by the load-deflection plots at mid-span showed good agreement with the experimental results and other available numerical results. The average strength for beams strengthened with steel plate showed larger increasing than the average strength for the beams strengthened with CFRP plates and the failure in all cases was due to debonding of plates.

Fathelbab et al. [2011] worked on "Finite Element Modeling of Strengthened Simple Beams using FRP Techniques". They studied analytically the strengthening of a simple reinforced concrete *T-beams* due to excessive uniform loads in flexure, shear and a combination of flexure and shear, using externally bonded FRP sheets technique. ANSYS was used to perform a structural linear and non-linear analysis for several models using several schemes of FRP sheets. A parametric study was performed for a lot of strengthened beams. FE models studied a main parameter of different schemes of FRP sheets in flexure, shear and combination flexure/shear. Comparing the results with a control beam model – simple reinforced concrete beam without strengthening – it was concluded that the strengthening of beam in both flexure and shear gives a higher ultimate load capacity, delays the failure and prevents debonding failure up to a level at which debonding occurs in both longitudinal and wrapped jackets CFRP sheets

Jayajothi et al. [2013] worked on "Finite Element Analysis of FRP Strengthened RC Beams using ANSYS". They presented a nonlinear finite element analysis to simulate the behavior of failure modes of Reinforced Concrete beams strengthened in flexure and shear by Fiber Reinforced Polymer laminates. Four beams were modeled in FEM software using ANSYS. In those four beams, two beams were control beams without FRP and other two beams were Carbon Fiber Reinforced Polymer (CFRP) strengthened beams. The load deflection plots obtained from numerical studies show good agreement with the experimental results. There was a difference in behavior between the RC beams strengthened with and without CFRP layers. The crack patterns obtained in FEA in the beams were also presented. The ultimate load carrying capacity of all the strengthened beams was higher when compared to the control beams

and CFRP fabric properly bonded to the tension face of RC beams can enhance the flexural strength substantially.

Umesh et al. [2013] worked on "Modeling of CFRP strengthened RCC beam using the nonlinear finite element method". They performed a 3D nonlinear finite element analysis using ANSYS to predict the flexural cracking behavior of CFRP strengthened RCC beams. The behavior RC beam with and without hangers was compared with experimental results. Later, the crack patterns for the various area of steel reinforcement were simulated to judge the failure pattern of RC beam with hanger bars. A parametric study was made for various lengths of CFRP used for post strengthening of the flexural capacity of RCC beam with and without hanger bars.

In the present study, three dimensional nonlinear finite element models of reinforced concrete beams externally strengthened with carbon fiber reinforced polymers (CFRP) are developed using the commercial finite element modeling software (ANSYS), and then, a parametric study with different CFRP strengthening schemes are performed; in order to study the effect of these schemes on the overall response of RC strengthened beams in flexure and shear.

CHAPTER 3

MECHANICAL BEHAVIOR AND FINITE ELEMENT MODELING OF MATERIALS

3.1 Introduction

In this chapter, the mechanical behavior and finite element modeling basics of different related materials as concrete, steel reinforcement, and carbon fiber reinforced polymer (CFRP) are presented. Further, failure criteria and modeling approaches for each material are introduced.

3.2 Concrete

3.2.1 Mechanical Behavior of Concrete

3.2.1.1 Uniaxial Compressive Stress

Concrete exhibits many micro-cracks during loading due to different stiffness of aggregates and mortar, which significantly affects its mechanical behavior. It shows a linear elastic behavior up to 30-40% of its compressive strength (f_{cu}) and beyond that, bond cracks are formed. Then until stresses about 70-90% of the compressive strength, micro-cracks opens and join to the bond cracks which makes continuous cracks. After reaching the peak stress (f_{cu}), strain softening which depends on the size of specimen and the strength of the concrete occurs. As shown in Fig. (3-1), the softening part of the stress-strain curve for long specimens are sharper than for short specimens which is due to deformation localization in some regions during unloading of other parts, [Chong, 2004, Kaufmann, 1998, Kostovos 1995].

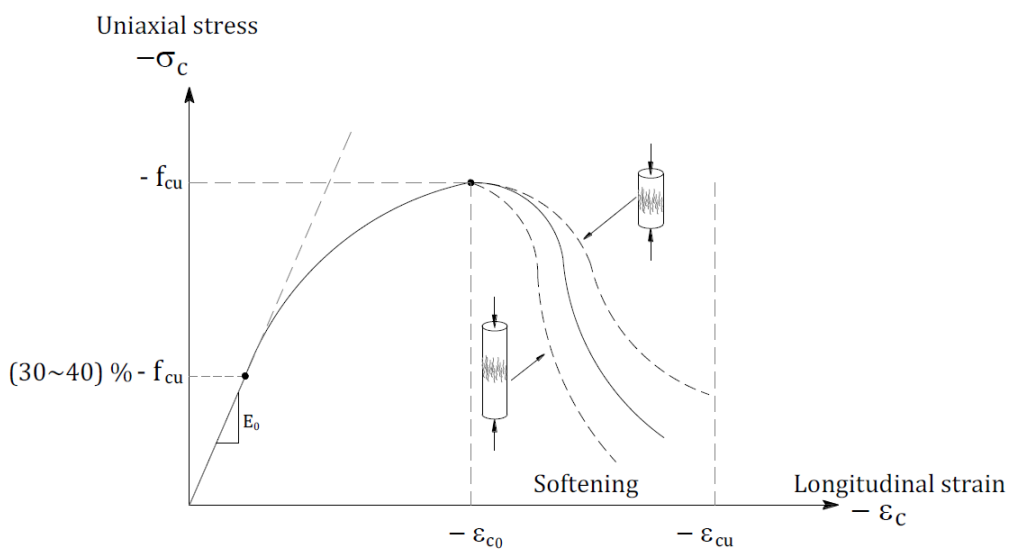


Fig. (3-1): Uniaxial Compressive Behavior of Concrete, [Chong, 2004].

3.2.1.2 Uniaxial Tensile Stress

Concrete exhibits a linear response in uniaxial tension up to stresses about 60-80% of the tensile strength when micro-cracks form and then concrete behaves softer and highly non-linear. As shown in Fig. (3-2), beyond the tensile strength, the tensile stress does not suddenly drop to zero due to the quasi brittle nature of concrete. On the contrary, in the weakest regions damage initiates during unloading of the other parts. Due to interlocking of aggregates, stress can be transferred in the fracture zone across the crack opening direction, until a complete crack is formed which cannot transfer any stress and then complete tensile failure occurs. The concrete during this process undergoes tension softening, [Chong, 2004, Kaufmann, 1998, Kostovos 1995].

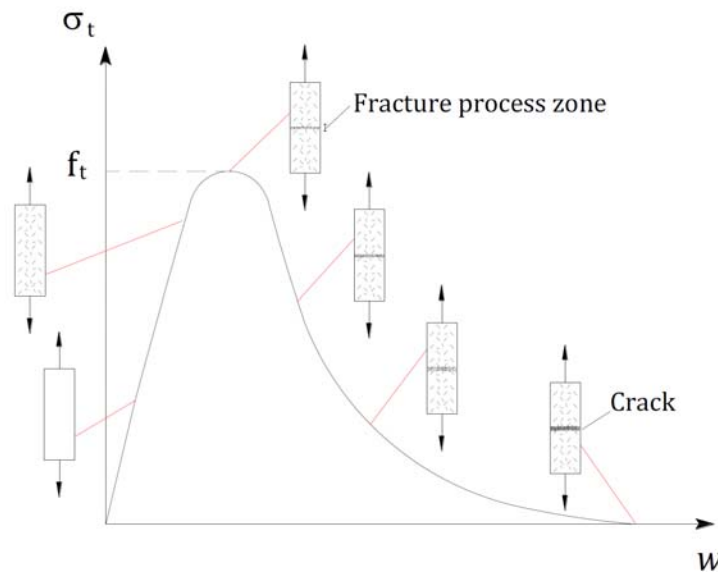


Fig. (3-2): Uniaxial Tensile Behavior of Concrete, [Chong, 2004].

3.2.2 Finite Element Modeling of Concrete

The uniaxial stress-strain behavior of concrete in compression is shown in Figure (3-3). Various mathematical models are available to approximate this nonlinear behavior namely: linearly elastic-perfectly plastic model, inelastic-perfectly plastic, Hognestad, and piecewise linear model. In the present study a modified Hognestad mathematical model (Fig. 3-4) has been used for the approximation of the stress-strain behavior of concrete, [MacGregor, 1997, Kostovos 1995].

1. Initial tangent modulus of elasticity increases with an increase in compressive strength. So, the elastic modulus (E_c) is given by (ACI 8.5.1):

$$E_c = 4700 \sqrt{f'_c} \quad (3-1)$$

Where f'_c is compressive strength of concrete at 28 days in MPa. The stress-strain relation initially must satisfy the Hooke's law.

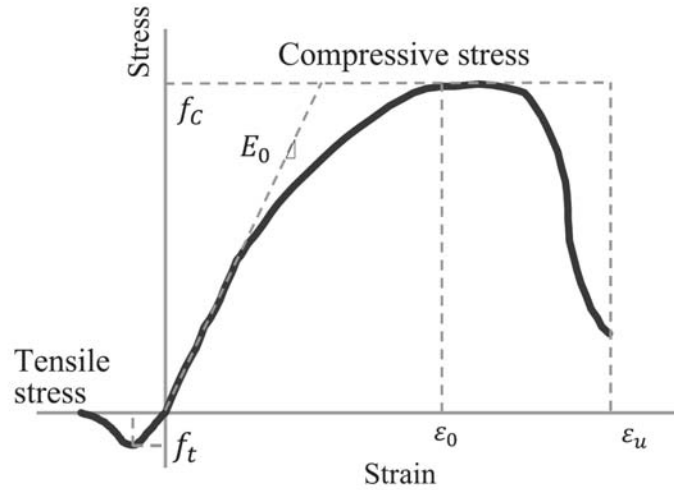


Fig. (3-3): Uniaxial Stress-Strain Behavior of Concrete, [Basappa et al., 2013]

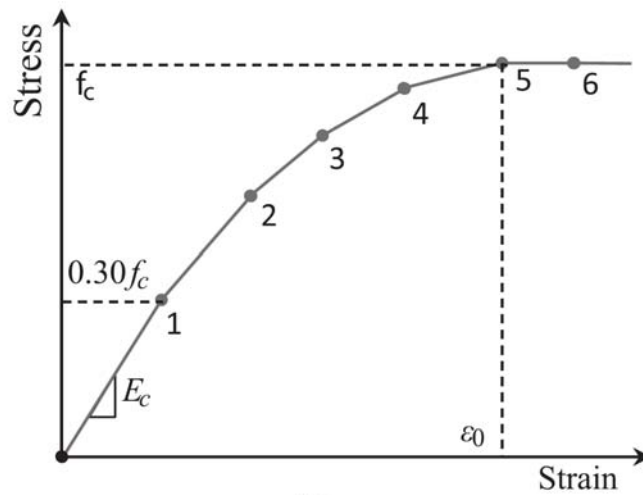


Fig. (3-4): Modified Hognestad Model, [Basappa et al., 2013]

2. The strain at maximum stress increases as the compressive strength increases:

$$\epsilon_0 = \frac{2f_c}{E_c} \quad (3-2)$$

3. The raising portion of the stress strain curve resembles a parabola with vertex at the maximum stress:

$$f = \frac{E_c \epsilon}{1 + \frac{\epsilon^2}{\epsilon_0^2}} \quad (3-3)$$

Where, (f) is stress for a value of strain in stress-strain relationship of concrete.

The stress-strain behavior of concrete under tension includes raising part and descending part. The raising part is slightly curved, approximated either as straight lines or parabola. The descending part drops rapidly with increased elongation after the maximum stress is crossed.

3.2.3 Finite Element Modeling of Cracks in Concrete

To accurately evaluate the structural behavior of concrete structures, the FE method should be coupled with precise representation of concrete cracking. For modeling of concrete cracking, the two major methods are the discrete crack approach and the smeared crack approach.

3.2.3.1 Discrete Crack Model

This model is based on propagation of discontinuities in the structure with either an inter-element crack approach or an intra-element crack approach. The inter-element crack approach, as shown in Figure (3-5-a), means modeling of cracks by disjunction of element edges. This approach has two drawbacks; crack path is limited because it has to follow the predefined boundaries of inter-elements and also, when cracks open, separated nodes make extra degree of freedom, which increases the computation time and cost and decreases the efficiency.

In the intra-element crack approach the cracks can propagate through the finite elements, as shown in Figure (3-5-b). This approach has two available types. First type is embedded discontinuity model which early was used for strain localization problems like shear band in metal and then developed for cohesive material like concrete, and the second type based on partition-of-unity concept which uses discontinuous shape function and with adding degrees of freedom in nodes represents the displacement appears across the crack. The discrete crack method is useful in structures which suffer large localized cracking but in other cases the smeared crack method is more efficient, [Zihai, 2009, Chong, 2004, Kostovos 1995].

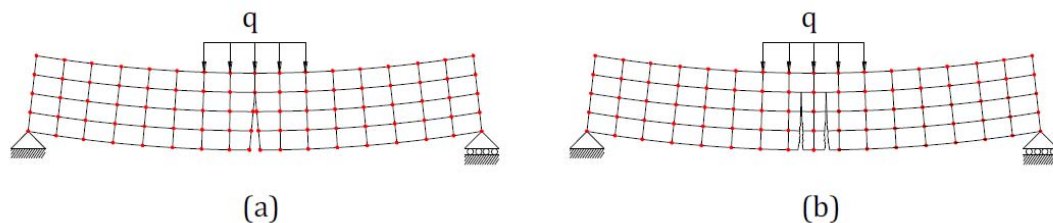


Fig. (3-5): Discrete Crack Model: (a) Inter-element Crack Approach, (b) Intra-element Crack Approach, [Hamedani et al., 2012].

3.2.3.2 Smearred Crack Model

Smearred crack method assumes cracks smearred in a certain volume of the material, as shown in Figure (3-6), which reduces the average material stiffness in the direction of the major principal stresses. The advantage of this method is that when cracks are developed and propagared, it does not need a new mesh which simplifies numerical implementation.

Nevertheless, this model has its deficiencies especially for localized cracking. In fracture problems, the smearred crack model localizes the cracks into a single row of elements, which causes mesh sensitivity and leads to inappropriate results beyond the ultimate tensile strength. In addition, the smearred crack approach predicts the cracks propagation in alignment with mesh direction due to its mesh directional bias, [Zihai, 2009, Chong, 2004, Kostovos 1995,].

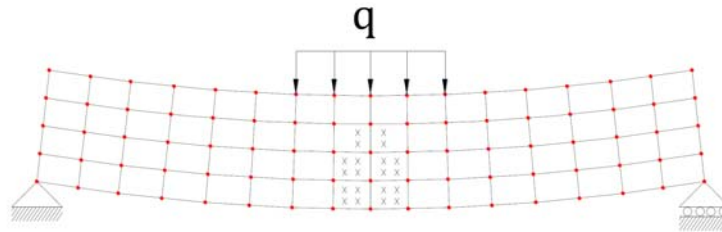


Fig. (3-6): Smearred Crack Model. [Hamedani et al., 2012].

3.2.4 Finite Element Failure Criteria of Concrete

The criterion for failure of concrete due to a multiaxial stress state can be expressed in the form [Willam and Warnke, 1974]. If Equation (3-4) is satisfied, the material will crack or crush.

$$\frac{F}{f_c} - S \geq 0 \quad (3 - 4)$$

Where:

F = a function of the principal stress state (σ_{xp} , σ_{yp} , σ_{zp})

S = failure surface expressed in terms of principal stresses and five input parameters f_t , f_c , f_{cb} , f_1 and f_2 .

f_c = uniaxial crushing strength.

σ_{xp} , σ_{yp} , σ_{zp} = principal stresses in principal directions.

A total of five input strength parameters are needed to define the failure surface as well as an ambient hydrostatic stress state. These are:

f_t :Ultimate uniaxial tensile strength

f_c :Ultimate uniaxial compressive strength

f_{cb} :Ultimate biaxial compressive strength

σ_h^a :Ambient hydrostatic stress state

- f_1 : Ultimate compressive strength for a state of biaxial compression superimposed on hydrostatic stress state σ_h^a
- f_2 : Ultimate compressive strength for a state of uniaxial compression superimposed on hydrostatic stress state.

However, the failure surface can be specified with a minimum of two constants, f_t and f_c . The other three constants default to [Willam and Warnke, 1974]:

$$f_{cb} = 1.2 f_c \quad (3-5)$$

$$f_1 = 1.45 f_c \quad (3-6)$$

$$f_2 = 1.725 f_c \quad (3-7)$$

However, these default values are valid only for stress states where the following condition is satisfied:

$$|\sigma| \leq \sqrt{3} f_c \quad (3-8)$$

$$\sigma_h = \frac{1}{3} (\sigma_{xp} + \sigma_{yp} + \sigma_{zp}) \quad (3-9)$$

Figure (3-7) represents the 3-D failure surface for states of stress that are biaxial or nearly biaxial. If the most significant nonzero principal stresses are in the σ_{xp} and σ_{yp} directions, the three surfaces presented are for σ_{zp} slightly greater than zero, σ_{zp} equal to zero, and σ_{zp} slightly less than zero. Although the three surfaces, shown as projections on the $\sigma_{xp} - \sigma_{yp}$ plane, are nearly equivalent and the 3-D failure surface is continuous, the mode of material failure is a function of the sign of σ_{zp} . For example, if σ_{xp} and σ_{yp} are both negative and σ_{zp} is slightly positive, cracking would be predicted in a direction perpendicular to the σ_{zp} direction. However, if σ_{zp} is zero or slightly negative the material is assumed to crush, [ANSYS, 2014].

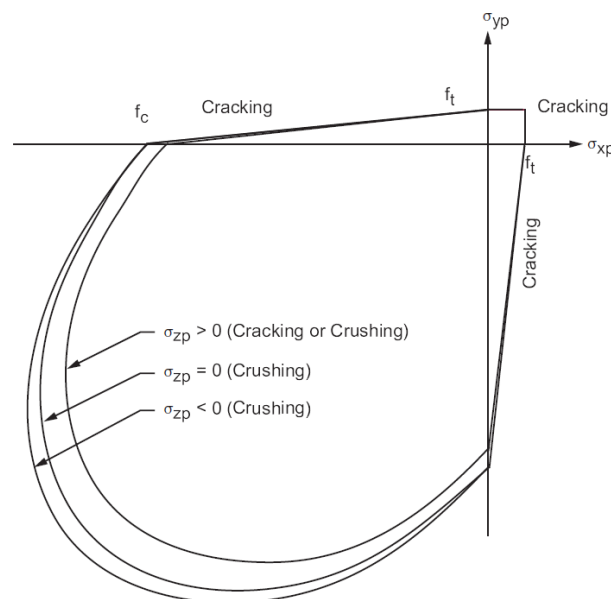


Figure (3-7): 3D failure Surface for Concrete, [ANSYS 2014].

In ANSYS, a concrete element cracks when the principal tensile stress in any direction lies outside the failure surface. After cracking, the elastic modulus of the concrete element is set to zero in the direction parallel to the principal tensile stress direction. Crushing occurs when all principal stresses are compressive and lie outside the failure surface; subsequently, the elastic modulus is set to zero in all directions and the element effectively disappears, [ANSYS, 2014].

3.3 Steel Reinforcement

3.3.1 Mechanical Behavior of Steel Reinforcement

Figure (3-8) shows a typical stress-strain relationship for reinforcing steel. Steel is initially linear-elastic for stress less than the initial yield stress. At ultimate tensile strain, the reinforcement begins to neck and strength is reduced. At a maximum strain, the steel reinforcement fractures and load capacity is lost. This steel response may be defined by a few material parameters. These include the elastic modulus (E_s), the yield strength (f_y), the strain at which peak strength is achieved (ϵ_u), the peak strength (f_u), the strain at which fracture occurs (ϵ_{max}), and the capacity prior to steel fracture (f_s), [ASTM A615].

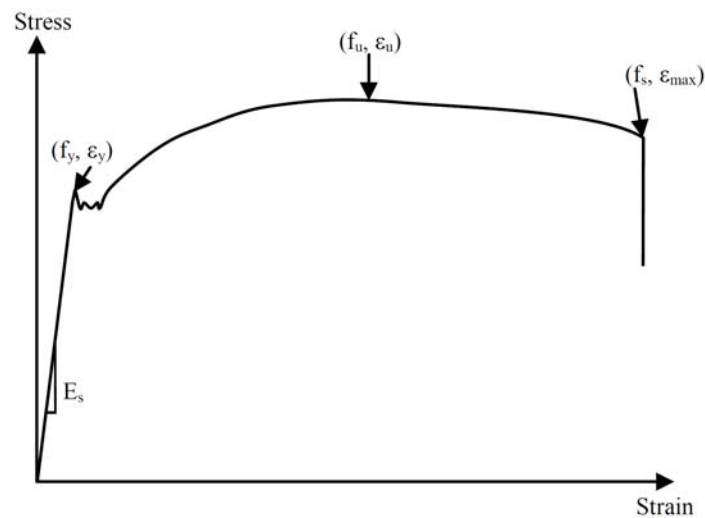


Fig. (3-8): Tensile Stress-strain Curve for Typical Reinforcing Steel Bar, [ASTM A615].

For general engineering applications, an elastic-plastic constitutive relationship, either with or without strain hardening, is normally assumed for ductile reinforcing steel, as shown in Figure (3-9). In an elastic hardening model it is assumed that steel shows some hardening after it yields, [Supaviriyakit et al., 2004]. An elastic-perfectly plastic model generally yields acceptable results for the response prediction of RC members, [Neale et al., 2005].

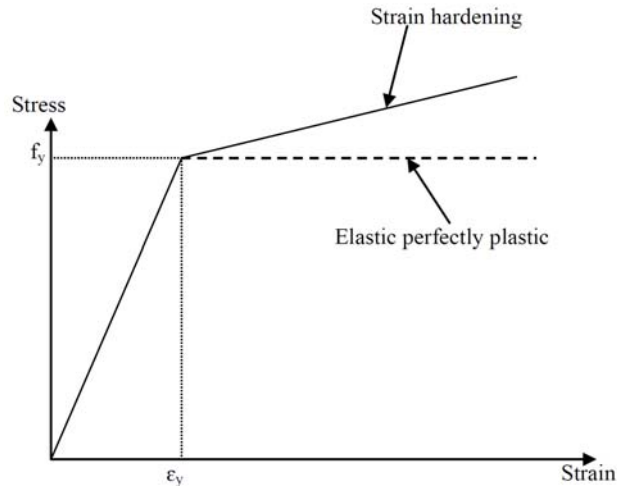


Fig. (3-9): Idealized Stress-Strain Curve for Reinforcing Steel, [Supaviriyakit et al., 2004]

3.3.2 Finite Element Modeling of Steel Reinforcement

Three distinct approaches are available to represent steel reinforcement in reinforced concrete modeling, they are: smeared steel approach, embedded steel approach and discrete steel approach, [Chong, 2004].

3.3.2.1 Smeared Steel Approach

In the smeared steel approach (Figure 3-10-a), reinforcing steel is assumed to be smeared over concrete elements at a particular angle of orientation and is often described by the reinforcement ratio. The total stiffness of a distributed reinforced concrete finite element consists of the stiffness of the concrete and the stiffness contributed by the smeared steel reinforcement. When the reinforcement is assumed to be smeared, a full compatibility between steel and concrete is naturally enforced. This type of formulation is useful for the analysis of reinforced concrete structures with densely distributed reinforcement, since the exact definition of every single reinforcing bar can be avoided.

3.3.2.2 Embedded Steel Approach

In the embedded steel approach (Figure 3-10-b), each reinforcing bar is considered as an axial member incorporated into the concrete element by the principle of virtual work. The displacements of the embedded steel are consistent with the displacements of the concrete element. The major advantage of the embedded steel formulation is that the reinforcing steel can be defined arbitrarily regardless of the mesh shape and size of the base concrete element.

3.3.2.3 Discrete Steel Approach

The discrete steel approach (Figure 3-10-c) is based on the use of separate elements to represent the reinforcing steel. One-dimensional truss elements are commonly adopted since reinforcing steel is usually assumed to carry axial load only. Steel truss elements are overlaid onto the boundary of the concrete elements by connecting the nodal points. This approach greatly facilitates the inclusion of bond-slip effects between steel and concrete, which may be achieved by inserting bond-slip elements between the concrete elements and the steel truss elements. A major disadvantage of this approach is that the mesh boundary of the concrete element must overlap the direction and location of the steel reinforcement. In this study, the discrete steel approach was used, to ensure the full connectivity between concrete and steel reinforcement nodes.

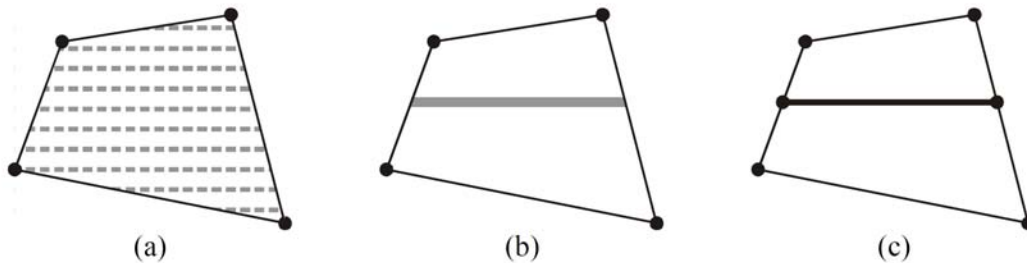


Fig. (3-10): Modeling of Reinforcement: (a) Smeared Steel Approach, (b) Embedded Steel Approach, (c) Discrete Steel Approach, [Chong, 2004].

3.4 Fiber Reinforced Polymer (FRP)

3.4.1 Mechanical Behavior of FRP

FRP composite materials are not homogeneous. Their properties are dependent on many factors, the most important of which are, [ISIS-EC-2, 2006]:

1. The relative proportions of fiber and matrix (volume fractions).
2. The mechanical properties of the constituent materials (fiber, matrix, and any additives).
3. The orientation of the fibers within the matrix.
4. The method of manufacture

Figure (3-11) shows typical stress-strain curves for fibers, matrices, and the FRP materials that result from the combination of fibers and matrix. Unidirectional FRP materials are typically linear elastic up to failure, and do not exhibit the yielding behavior that is displayed by conventional reinforcing steel. Figure (3-12) illustrates the significant differences in the tensile behavior of FRPs as compared with steel, [ISIS-EC-2, 2006].

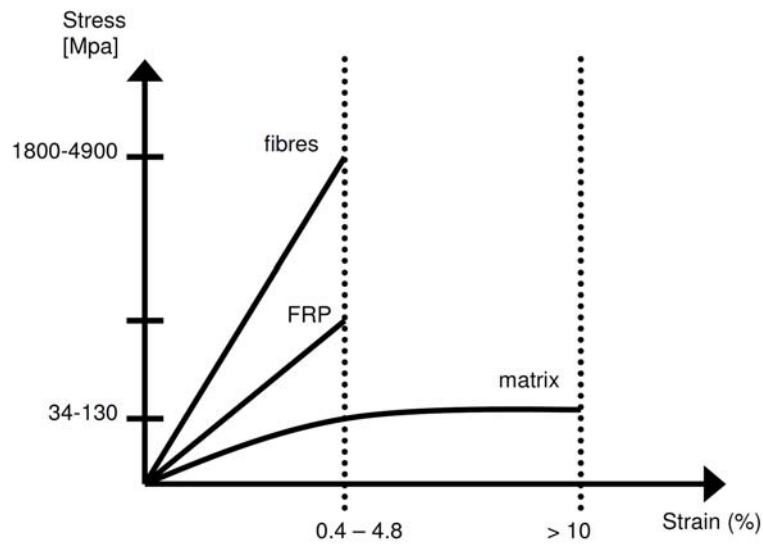


Fig. (3-11): Stress-Strain Relationships for FRP, [ISIS-EC-2, 2006].

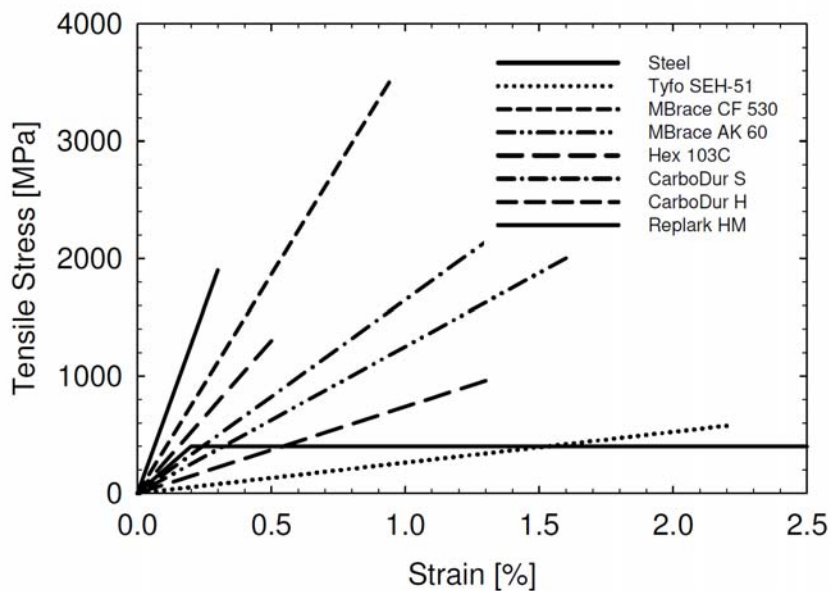


Fig. (3-12): Stress-Strain Plots for Various FRP Strengthening Systems, [ISIS-EC-2, 2006].

FRP materials generally have much higher strengths than the yield strength of steel, although they do not exhibit yield, and have strains at failure that are much less. Table (3-1) gives typical properties of various types of FRP materials.

FRP System	Fiber Type	Weight (g/m ²)	Thickness (mm)	Tensile Strength (MPa)	Tensile Elastic Modulus (GPa)	Strain at Failure (%)
Fyfe Co.LLC						
Tyfo SHE-51	Glass	930	1.3	575	26.1	2.2
Tyfo SCH-35	Carbon	-	0.89	991	78.6	1.3
Mitsubishi						
Replark 20	Carbon	200	0.11	3400	230	1.5
Replark 30	Carbon	300	0.17	3400	230	1.5
Replark MM	Carbon	-	0.17	2900	390	0.7
Replark KM	Carbon	200	0.14	1900	640	0.3
Sika						
Hex 100G	Glass	913	1	600	26.1	2.2
Hex 103G	Carbon	618	1	960	73.1	1.3
CarboDur S	Carbon	2240	1.2-1.4	2800	165	1.7
CarboDur M	Carbon	2240	1.2	2400	210	1.2
CarboDur H	Carbon	2240	1.2	1300	300	0.5
Degussa Building Systems						
Mbrace EG 900	Glass	900	0.35	1517	72.4	2.1
Mbrace CF 530	Carbon	300	0.17	3500	373	0.94
Mbrace AK 60	Aramid	600	0.28	2000	120	1.6

Table (3-1): Typical Properties of FRP Materials, [ACI 440R, 2007]

3.4.2 Finite Element Modeling of FRP

As shown in Figure (3-13), the unidirectional lamina has three mutually orthogonal planes of material properties (i.e., xy , xz , and yz planes). The xyz coordinate axes are referred to as the principal material coordinates where the x direction is the same as the fiber direction, and the y and z directions are perpendicular to the x direction. It is a so-called orthotropic material, [Barbero, 2014, Kaw, 2006].

CFRP composites can be modeled either using isotropic linear elastic model or orthotropic linear elastic model, [Camata et al., 2007, Hu et al., 2006]. In this study, the properties of the CFRP composites were nearly the same in any direction perpendicular to the fibers. Thus, the properties in the y direction were the same as those in the z direction. Orthotropic linear elastic model for CFRP composites was used throughout this study.

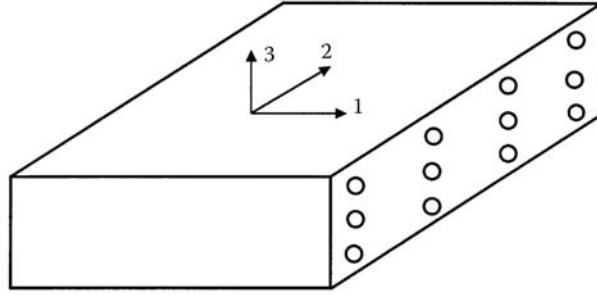


Fig. (3-13): Schematic of FRP Composites, [Kaw, 2006].

3.4.3 Finite Element Failure Criteria of FRP

Failure criteria are used to assess the possibility of failure of a material. Doing so allows the consideration of orthotropic materials, which might be much weaker in one direction than another, (ANSYS, 2014).

Failure criteria are used to learn if a layer has failed due to the applied loads. Many failure criteria are used in FE software packages for composite materials. The most used criteria are: maximum strain failure criteria, maximum stress failure criterion, Tsai-Wu failure criteria, and physical failure criteria, like: Hashin fiber failure criterion, Hashin matrix failure criterion, Puck fiber failure criterion, and Puck matrix failure criterion [Barbero, 2014, ANSYS, 2014].

In the present study, maximum strain failure criterion and maximum stress failure criterion were used, based on the longitudinal tensile strength and maximum strain of the used CFRP fabrics.

CHAPTER 4

BUILDING OF ANSYS FINITE ELEMENT MODELS

4.1 Introduction

The finite element method is a numerical analysis technique for obtaining approximate solutions to a wide variety of engineering problems. ANSYS is a general purpose finite element modeling package for numerically solving a wide variety of problems which include static/dynamic structural analysis (both linear and nonlinear), heat transfer and fluid problems, as well as acoustic and electro-magnetic problems. The external strengthening of reinforced concrete beams with carbon fiber reinforced polymers (CFRP) had been analyzed using finite element models in ANSYS 14. Many self-learning tutorials and manuals were used as references in preparing the FE models using ANSYS, like: Lawrence, (2012), Moaveni, (2008), Nakasone et al. (2006), Madenci et al. (2006), and ANSYS manuals set.

Two different experimental investigations were used to model and verify the strengthening of RC beams with CFRP using ANSYS. The first one was for flexure strengthening (Balamuralikrishnan et al., 2009), and the second one was for shear strengthening (Alagusundaramoorthy et al., 2002).

4.2 Description of Experimental Beams

In this section the configuration and geometric details of flexure beam and shear beam models are presented. Each beam has a control beam model and a strengthened beam model.

4.2.1 Flexure Beam

The experimental investigation of Balamuralikrishnan et al. [2009] was used to simulate the flexure strengthening model in ANSYS. The details of control and strengthened beam models are presented.

4.2.1.1 Flexure Control Beam

The beam is a simply supported beam with a total length of 3200 mm, and a clear span of 3000 mm. The beam has a rectangular cross section with 125 mm width and 250 mm height and a concrete cover of 25 mm was assumed. The beam was subjected to two concentrated static loads, spaced 1000 mm.

Tension reinforcement of the beam is $2\Phi 12$ mm. Compression reinforcement of the beam is $2\Phi 10$ mm. And shear reinforcement of the beam is 6 mm diameter stirrups spaced at 150 mm, as shown in Figure (4-1).

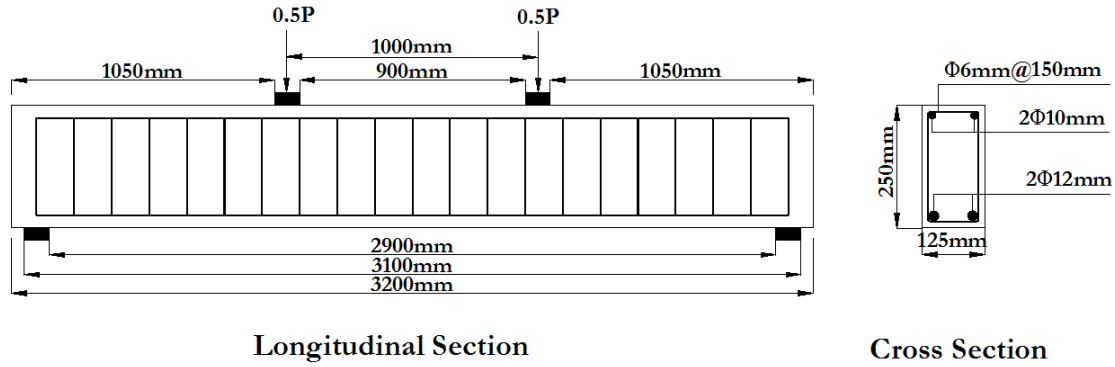


Fig. (4-1): Description of Flexure Control Beam Model, [Balamuralikrishnan et al., 2009]

4.2.1.2 Flexure Strengthened Beam

The control beam was externally strengthened by bonding a 2900 mm single layer of CFRP fabric with 0.3mm thickness (Nitowrap EP-CF from Fosroc Chemicals Limited) [FOSROC Constructive Solutions] to the beam soffit parallel to its axis, as shown in Figure (4-2).

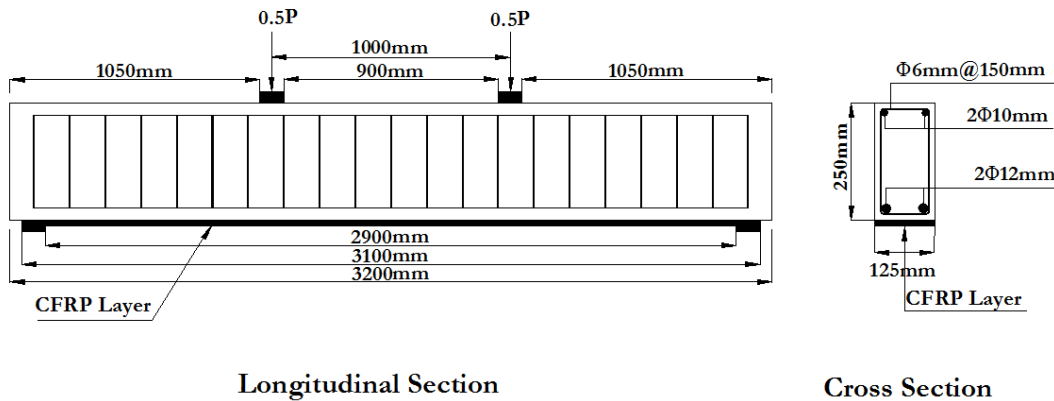


Fig. (4-2): Description of Flexure Strengthened Beam Model, [Balamuralikrishnan et al., 2009]

4.2.2 Shear Beam

The experimental investigation of Alagusundaramoorthy et al. [2002] was used to simulate the shear strengthening model in ANSYS. The details of control and strengthened beam models are presented.

4.2.2.1 Shear Control Beam

The beam is a simply supported beam with a total length of 2130 mm, and a clear span of 1830 mm. The beam has a rectangular cross section with 230 mm width and 280 mm height, and a concrete cover of 25 mm was assumed. The beam was subjected to a concentrated static load at the middle of the beam.

Tension reinforcement of the beam is $2\Phi 25$ mm. Compression reinforcement of the beam is $2\Phi 10$ mm. And shear reinforcement of the beam is 10 mm diameter stirrups spaced at 300 mm, as shown in Figure (4-3).

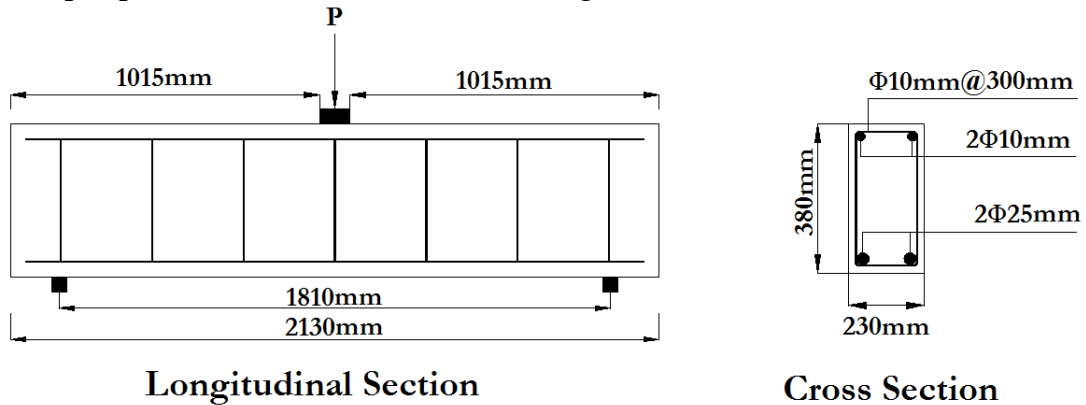


Fig. (4-3): Description of Shear Control Beam Model, [Alagusundaramoorthy et al., 2002]

4.2.2.2 Shear Strengthened Beam

The control beam was externally strengthened by bonding a single U-wrap layer of CFRP fabric with 0.18mm thickness inclined at an angle of 90° to the longitudinal axis of the beam, as shown in Figure (4-4).

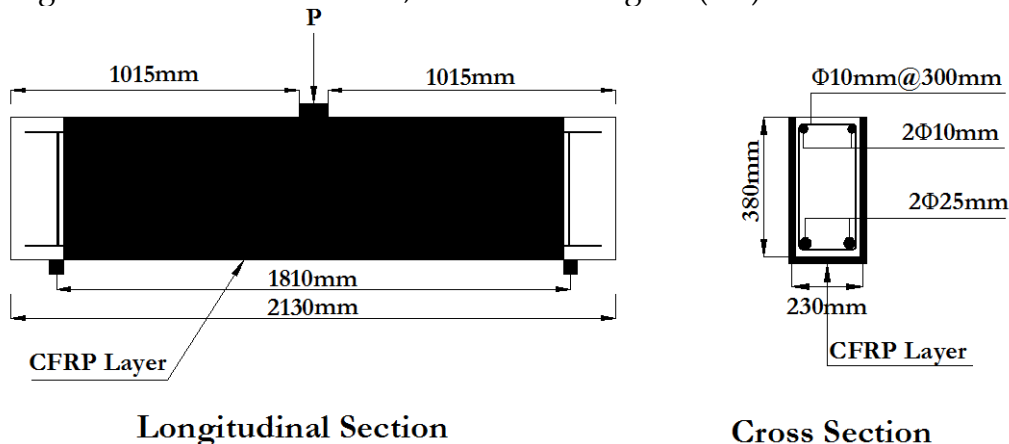


Fig. (4-4): Description of Shear Strengthened Beam Model, [Alagusundaramoorthy et al., 2002]

4.3 Modeling Assumptions

The following are the modeling assumptions made for the flexure beam and shear beam models in the present study to provide reasonably good simulations for the complex behavior:

1. Concrete and steel are modeled as isotropic and homogeneous materials.
2. Poisson's ratio is assumed to be constant throughout the loading history.
3. Steel is assumed to be an elastic-perfectly plastic material and identical in tension and compression.
4. Perfect bond exists between concrete and steel reinforcement.

5. Perfect bond exists between concrete and CFRP fabric. The perfect bond assumption used in the structural modeling doesn't cause a significant error in the predicted load-deflection response, [Isenburg, 1993].
6. The CFRP material is assumed to be especially orthotropic-transversely isotropic. That is, the material properties in the two directions that are both perpendicular to the fiber direction are identical.
7. The CFRP fabric is assumed to carry stress along its axis only.
8. Time-dependent nonlinearities such as creep, shrinkage, and temperature change are not included in this study.

4.4 Selection of Element Types Using ANSYS

In this section, the description of element types used for all materials used in ANSYS models is presented. These materials are: concrete, steel reinforcement, loading and supporting plates, and carbon fiber reinforced polymer (CFRP). Elements used in thesis models are widely used and recommended by ANSYS and previous researchers, [Jayajothi et al., 2013, Vijayakumar et al., 2012, Fathelbab et al., 2011, Abbas, 2010, Amer et al., 2009, Elyasian et al., 2006, Santhakumar et al., 2004, Supaviriyakit et al., 2004,]

4.4.1 Concrete

An eight-node solid element, Solid65, was used to model the concrete. The solid element has eight nodes with three degrees of freedom at each node: translations in the nodal local x , y , and z directions. The element is capable of plastic deformation, cracking in three orthogonal directions, and crushing. The geometry and node locations for this element type are shown in Figure (4-5), [ANSYS 2014].

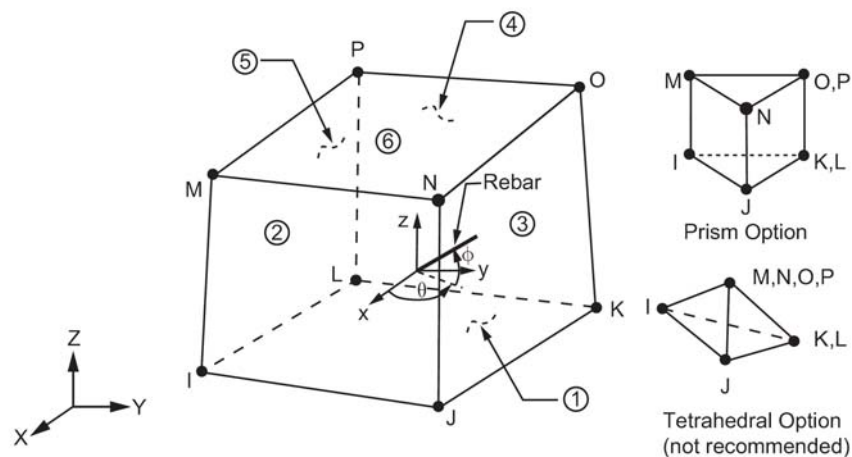


Fig. (4-5): Solid65 Geometry, [ANSYS, 2014].

4.4.2 Steel Reinforcement

A Link180 element was used to model steel reinforcement. The element is a uniaxial tension-compression element with three degrees of freedom at each node: translations in the nodal x , y , and z directions. Plasticity, creep, rotation, large deflection, and large strain capabilities are included. This element is shown in Figure (4-6), [ANSYS, 2014].

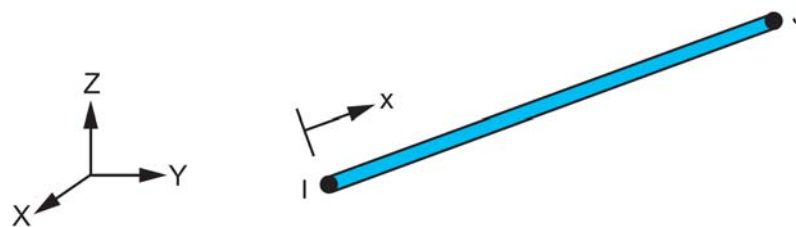


Fig. (4-6): Link180 Geometry, [ANSYS, 2014].

4.4.3 Loading and Supporting Steel Plates

The Solid185 element is used for the modeling of loading and supporting steel plates. This element is defined by eight nodes having three degrees of freedom at each node: translations in the nodal x , y , and z directions. The element is capable of plasticity, hyperelasticity, stress stiffening, creep, large deflection, and large strain capabilities.

SOLID185 is available in two forms:

- Homogeneous Structural Solid (default); and
- Layered Structural Solid.

Homogeneous Structural Solid with simplified enhanced strain formulation is used to model loading and supporting steel plates. This element is shown in Figure (4-7). Solid185 is a current-technology element and is preferred over the legacy element, Solid45, as suggested by ANSYS.

4.4.4 Carbon Fiber Reinforced Polymer (CFRP)

Shell181 element is used for the modeling Carbon Fiber Reinforced Polymer (CFRP). It is a four-node element with six degrees of freedom at each node: translations in the x , y , and z directions, and rotations about the x , y , and z -axes. SHELL181 is well-suited for linear, large rotation, and/or large strain nonlinear applications. The geometry, node locations, and the coordinate system are shown in Figure (4-8), [ANSYS, 2014].

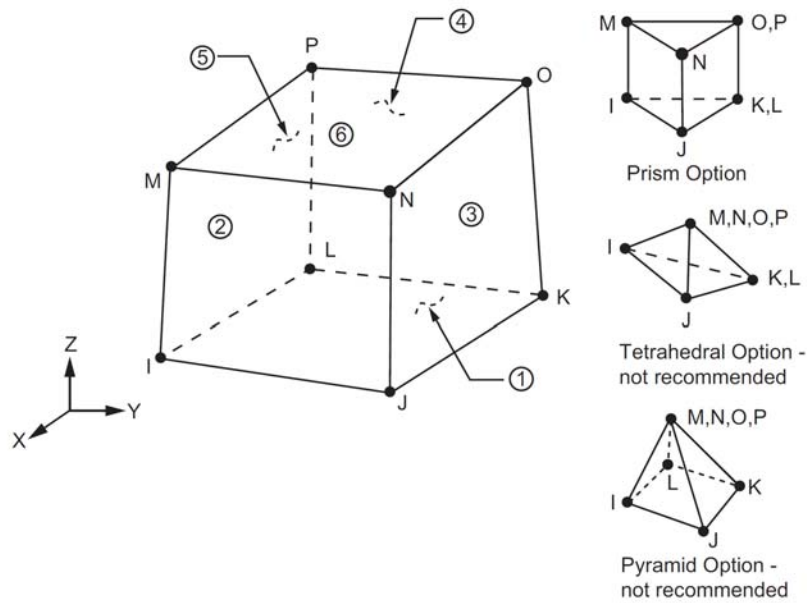


Fig. (4-7): SOLID185 Homogeneous Structural Solid Geometry, [ANSYS, 2014].

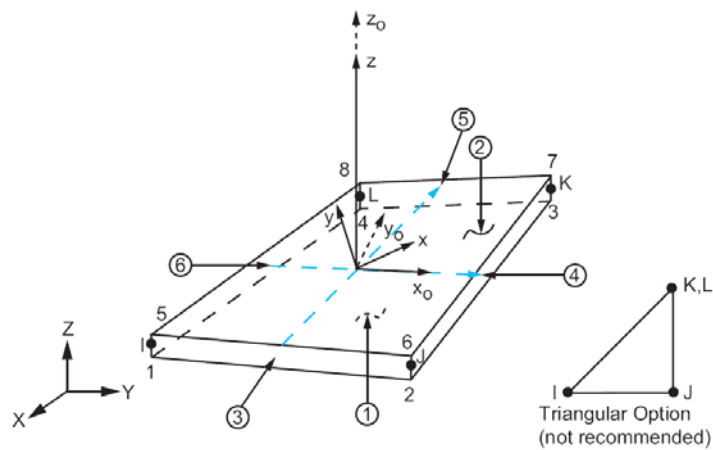


Fig. (4-8): Shell181 Geometry, [ANSYS, 2014].

The element types used for modeling of flexure and shear models are summarized in Table (4-1).

Material Type	ANSYS Element
Reinforced Concrete	Soild65
Steel Reinforcement	Link180
Loading and Supporting Steel Plates	SOLID185 (Homogeneous Structural Solid)
Carbon Fiber Reinforced Polymer(CFRP)	Shell181

Table (4-1): Element Types for ANSYS Flexure and Shear Beams Models.

4.5 Real Constants

4.5.1 Flexure Beam Model

The real constants for this model are shown in Table (4-2). Note that individual elements contain different real constants.

Real Constant Set	Element Type	Real Constants				Notes
			Real Constants for Rebar 1	Real Constants for Rebar 2	Real Constants for Rebar 3	
1	Solid65	Material Number	0	0	0	Concrete
		Volume Ratio	0	0	0	
		Orientation Angle	0	0	0	
		Orientation Angle	0	0	0	
2	Link180	Cross-sectional Area (mm ²)	113.009		Tension Reinf.	
		Initial Strain (mm/mm)	0			
3	Link180	Cross-sectional Area (mm ²)	78.479		Comp. Reinf.	
		Initial Strain (mm/mm)	0			
4	Link180	Cross-sectional Area (mm ²)	28.252		Stirrups	
		Initial Strain (mm/mm)	0			
5	Link180	Cross-sectional Area (mm ²)	14.126		Half Stirrup	
		Initial Strain (mm/mm)	0			

Table (4-2): Real Constants for ANSYS Flexure Beam Model

Real Constant Set 1 is used for the Solid65 element. It requires real constants for rebar assuming a smeared model. Values can be entered for Material Number, Volume Ratio, and Orientation Angles. The material number refers to the type of material for the reinforcement. The volume ratio refers to the ratio of steel to concrete in the element. The orientation angles refer to the orientation of the reinforcement in the smeared model. ANSYS [ANSYS 2014] allows the user to enter three rebar materials in the concrete. Each material corresponds to x, y, and z directions in the element (Figure 4-1). The reinforcement has uniaxial stiffness and the directional orientation is defined by the user. In the present study the beam is modeled using discrete reinforcement. Therefore, a value of

zero was entered for all real constants which turned the smeared reinforcement capability of the Solid65 element off, [Wolanski, 2004, Kachlakev et al., 2001].

Real Constant Sets 2, 3, 4, and 5 are defined for the Link180 element. Values for cross-sectional area and initial strain were entered. Cross-sectional areas in sets 2, 3 and 4 refer to the reinforcement of 12 mm, 10 mm, and 6 mm diameter bars respectively. Due to symmetry, set 5 is half of set 4 because half of the stirrup at the mid-span of the beam is cut off resulting from symmetry. A value of zero was entered for the initial strain because there is no initial stress in the reinforcement. No real constants set exist for the Solid185 and Shell181 elements, which were used for modeling of loading and supporting plates and CFRP respectively.

4.5.2 Shear Beam Model

The real constants for this model are shown in Table (4-3).

Real Constant Set	Element Type	Real Constants			Notes
			Real Constants for Rebar 1	Real Constants for Rebar 2	
1	Solid65	Material Number	0	0	Concrete
		Volume Ratio	0	0	
		Orientation Angle	0	0	
		Orientation Angle	0	0	
2	Link180	Cross-sectional Area (mm ²)	490.492		Tension Reinf.
		Initial Strain (mm/mm)	0		
3	Link180	Cross-sectional Area (mm ²)	63.568		Comp. Reinf. & Stirrups
		Initial Strain (mm/mm)	0		
4	Link180	Cross-sectional Area (mm ²)	31.784		Half Stirrup
		Initial Strain (mm/mm)	0		

Table (4-3): Real Constants for ANSYS Shear Beam Model.

As in flexure beam model, Real Constant Set 1 is used for the Solid65 element, and, a value of zero was entered for all real constants which turned the smeared reinforcement capability of the Solid65 element off.

Real Constant Sets 2, 3, and 4 are defined for the Link180 element. Values for cross-sectional area and initial strain were entered. Cross-sectional areas in sets 2 and 3 refer to the reinforcement of 25 mm, and 9 mm diameter bars respectively. Due to symmetry, set 4 is half of set 3 because half of the stirrup at the mid-span of the beam is cut off resulting from symmetry. A value of zero was entered for the initial strain because there is no initial stress in the reinforcement. No real constants set exist for the Solid185 and Shell181 elements, which were used for modeling of loading and supporting plates and CFRP respectively.

4.6 Material Properties

4.6.1 Concrete

Material Model Number 1 refers to the Solid65 element. The Solid65 element requires linear isotropic and multilinear isotropic material properties, in addition to selection of failure criteria of concrete.

4.6.1.1 Linear Isotropic Properties of Concrete

EX is the modulus of elasticity of the concrete (E_c). It was based on equation (3-1), with a value of f_c' equal to 27.54 MPa for flexure beam, and 31 MPa for shear beam. PRXY is the Poisson's ratio (ν). Poisson's ratio was assumed to be 0.25 for flexure beam, and 0.2 for shear beam.

4.6.1.2 Multilinear Isotropic Properties of Concrete

Modified Hognestad mathematical model (See Fig. 3-8) has been used for the approximation of the stress-strain behavior of concrete. Equations (3-2) and (3-3) were used to predict the multilinear isotropic stress strain curve for the concrete. The multilinear curve was used to help with convergence of the nonlinear solution algorithm, [Wolanski, 2004].

Figures (4-9) and (4-10) show the stress-strain relationship used in this study for ANSYS flexure beam and shear beam models respectively. The curve starts at zero stress and strain. Point 2, defined as $0.3f_c'$, was calculated in the linear range. Points from 3 to 21 were calculated from Eq. (3-3) with ϵ_0 obtained from Eq. (3-2). Strains were selected and the stress was calculated for each strain. Point 22 is at f_c' . After Point 22, perfectly plastic behavior of concrete was assumed.

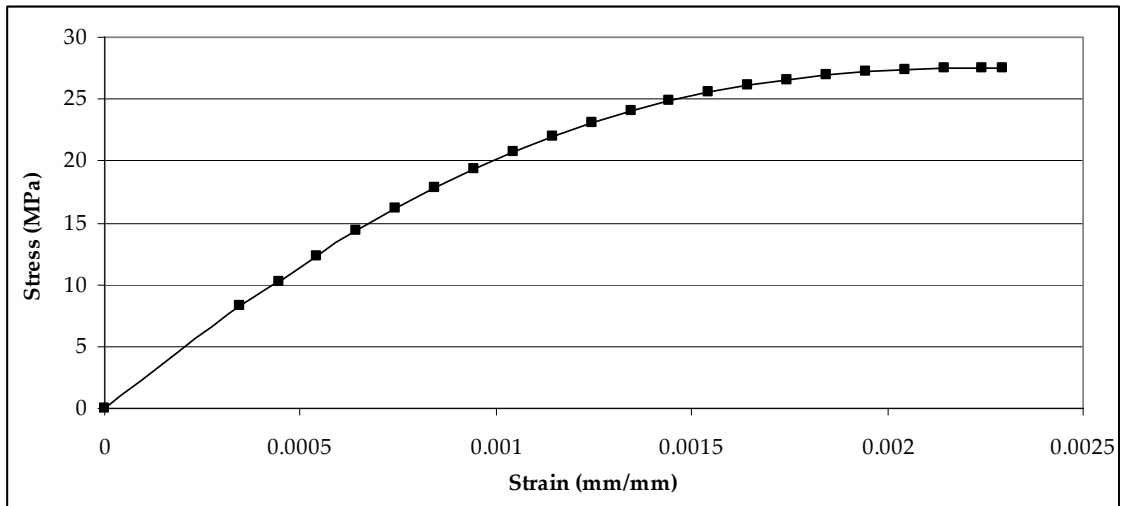


Fig. (4-9): Compressive Uniaxial Stress-Strain Curve for Concrete – Flexure Beam Model

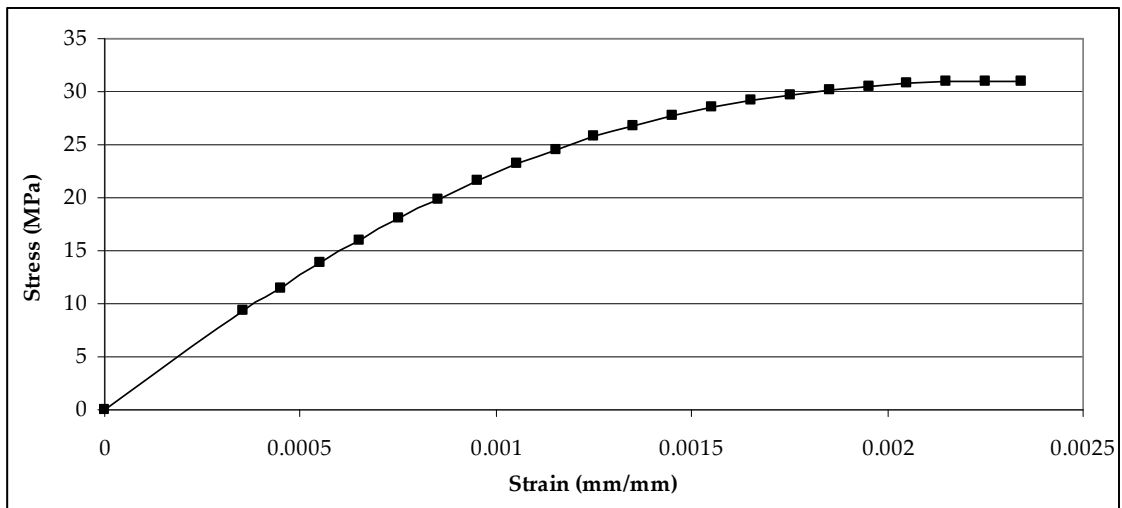


Fig. (4-10): Compressive Uniaxial Stress-Strain Curve for Concrete – Shear Beam Model

Parameters needed to define the material model for concrete in ANSYS models of flexure beam and shear beam are shown in Tables (4-4) and (4-5).

Material Model Number	Element Type	Material Properties			
		Linear Isotropic			
1	Soild65	EX	24000 (MPa)		
		PRXY	0.25		
		Multilinear Isotropic			
		Point	Strain	Stress (MPa)	
		1	0	0	
		2	0.000344	8.26	

		3	0.000444	10.28
		4	0.000544	12.37
		5	0.000644	14.33
		6	0.000744	16.16
		7	0.000844	17.85
		8	0.000944	19.38
		9	0.001044	20.76
		10	0.001144	21.99
		11	0.001244	23.08
		12	0.001344	24.02
		13	0.001444	24.83
		14	0.001544	25.51
		15	0.001644	26.08
		16	0.001744	26.53
		17	0.001844	26.89
		18	0.001944	27.17
		19	0.002044	27.36
		20	0.002144	27.48
		21	0.002244	27.53
		22	0.002295	27.54
		Concrete		
		Open Shear Transfer Coef.	0.35	
		Closed Shear Transfer Coef.	1	
		Uniaxial Cracking Stress	2.9 MPa	
		Uniaxial Crushing Stress	27.54 MPa	
		Biaxial Crushing Stress	Default	
		Hydrostatic Pressure	Default	
		Hydro Biax Crushing Stress	Default	
		Tensile Crack Factor	0.8	

Table (4-4): Material Properties of Concrete for ANSYS Flexure Beam Model

Material Model Number	Element Type	Material Properties		
1	Soild65	Linear Isotropic		
		EX	26447 (MPa)	
		PRXY	0.2	
		Multilinear Isotropic		
		Point	Strain	Stress (MPa)
		1	0	0
		2	0.000352	9.30

		3	0.000452	11.52
		4	0.000552	13.82
		5	0.000652	16.00
		6	0.000752	18.03
		7	0.000852	19.90
		8	0.000952	21.61
		9	0.001052	23.15
		10	0.001152	24.54
		11	0.001252	25.76
		12	0.001352	26.83
		13	0.001452	27.75
		14	0.001552	28.54
		15	0.001652	29.19
		16	0.001752	29.73
		17	0.001852	30.16
		18	0.001952	30.49
		19	0.002052	30.73
		20	0.002152	30.89
		21	0.002252	30.97
		22	0.002344	31.00
		Concrete		
		Open Shear Transfer Coef.		0.35
		Closed Shear Transfer Coef.		0.8
		Uniaxial Cracking Stress		2.7 MPa
		Uniaxial Crushing Stress		31 MPa
		Biaxial Crushing Stress		Default
		Hydrostatic Pressure		Default
		Hydro Biax Crushing Stress		Default
		Tensile Crack Factor		0.6

Table (4-5): Material Properties of Concrete for ANSYS Shear Beam Model

4.6.1.3 Failure Criteria of Concrete

Implementation of the Willam and Warnke (1975) concrete material model in ANSYS requires that different constants to be defined. These constants are: [ANSYS, 2014]

1. Shear transfer coefficients for an open crack;
2. Shear transfer coefficients for a closed crack;
3. Uniaxial tensile cracking stress;
4. Uniaxial crushing stress (positive);
5. Biaxial crushing stress (positive);
6. Ambient hydrostatic stress state for use with constants 7 and 8;

7. Biaxial crushing stress (positive) under the ambient hydrostatic stress state (constant 6);
8. Uniaxial crushing stress (positive) under the ambient hydrostatic stress state (constant 6);
9. Stiffness multiplier for cracked tensile condition.

- The shear transfer coefficient represents a shear strength reduction factor for subsequent loads that induce sliding (shear) across the crack face, [Chansawat et al., 2009]. Typical shear transfer coefficients range from 0.0 to 1.0, with 0.0 representing a smooth crack (complete loss of shear transfer) and 1.0 representing a rough crack (no loss of shear transfer), [ANSYS 2014]. For an open crack, the shear transfer coefficient varied between 0.05 and 0.50 in many studies of reinforced concrete structures, [Isenberg, 1993]. In this study, many analysis attempts had been done to determine the appropriate values of shear transfer coefficients based on comparison of FE load-displacement values with experimental results. The open and closed cracks shear transfer coefficients used in this study for flexure beam and shear beam models are shown in Tables (4-4) and (4-5).
- The uniaxial cracking stress of concrete (tensile strength) is based upon the modulus of rupture. Modulus of rupture of concrete is a more variable property than the compressive strength and is about 8 to 15 percent of the compressive strength, [MacGregor, 1997]. In ANSYS, when cracking occurs at an integration point of Solid65 element, material properties are adjusted to effectively model a “smeared band” of cracks, rather than discrete cracks. When a principal stress at an integration point in a concrete element exceeds the tensile strength, stiffness is reduced to zero in that principal direction perpendicular to the cracked plane [ANSYS, 2014]. In this study, values of uniaxial cracking stress of concrete used for flexure beam and shear beam models are shown in Tables (4-4) and (4-5).
- In ANSYS, crushing of concrete element occurs when all principal stresses are compressive and lies outside the failure surface; subsequently, the elastic modulus is set to zero in all directions, and the element effectively disappears, [ANSYS, 2014]. The uniaxial crushing stress of concrete is based on the uniaxial compressive strength tested in the experimental investigations, [Balamuralikrishnan et al., 2009] and [Alagusundaramoorthy et al., 2002].

The failure surface of concrete can be specified with a minimum of two constants, f_t and f_c . The remainder of the variables in the concrete model was left to default based on [Willam and Warnke, 1974] equations. (Refer 3.2.1.2 in this study)

4.6.2 Steel Reinforcement

For flexure beam model, material model number 2 and 3 refers to the Link180 element. Material model number 2 is used to model the reinforcement, while material model number 3 is used to model the stirrups.

For shear beam model, material model number 2 refers to the Link180 element. Material model number 2 is used to model the reinforcement and the stirrups.

The Link180 element is assumed to be bilinear isotropic and is based on the von Mises failure criteria, [ANSYS 2014]. The bilinear model requires the Yield Stress (f_y), as well as the Hardening Modulus (tangent modulus of the plastic region) of steel to be defined. Elastic Modulus (EX) was also defined, and Poisson's Ratio (PRXY) was assumed to be 0.3.

Tables (4-6) and (4-7) show material properties of steel reinforcement used for ANSYS flexure beam and shear beam models respectively.

Material Model Number	Element Type	Material Properties	
2 (Tension Reinf. Comp. Reinf.)	Link180	Linear Isotropic	
		EX	200000 MPa
		PRXY	0.3
		Bilinear Isotropic	
		Yield stress	512 MPa
		Tangent Modulus	20 MPa
		Linear Isotropic	
3 (Stirrups)	Link180	EX	200000 MPa
		PRXY	0.3
		Bilinear Isotropic	
		Yield stress	280 MPa
		Tangent Modulus	20 MPa

Table (4-6): Material Properties of Steel Reinforcement for ANSYS Flexure Beam Model

Material Model Number	Element Type	Material Properties	
2 (Tension Reinf. Comp. Reinf. Stirrups)	Link180	Linear Isotropic	
		EX	200000 MPa
		PRXY	0.3
		Bilinear Isotropic	
		Yield stress	414 MPa
		Tangent Modulus	20 MPa

Table (4-7): Material Properties of Steel Reinforcement for ANSYS Shear Beam Model

The steel for the finite element models was assumed to be an elastic-perfectly plastic material and identical in tension and compression. Figure (4-11) shows the assumed stress-strain curve for steel reinforcement, [Wolanski, 2004, Kachlakev et al., 2001].

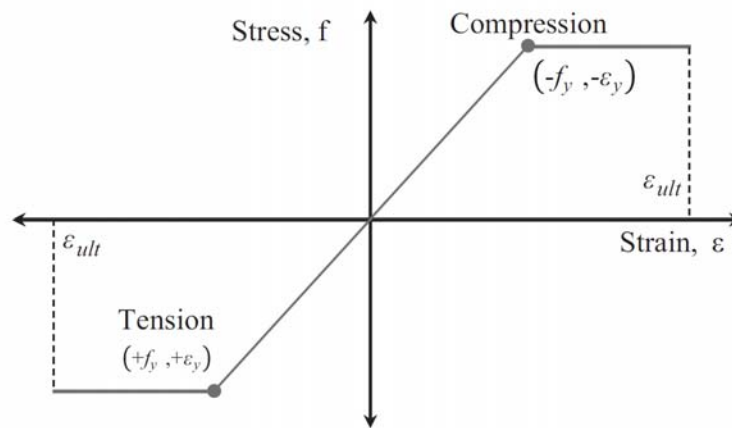


Fig. (4-11): Stress-Strain Curve for Steel Reinforcement, [Kachlakev et al., 2001].

4.6.3 Loading and Supporting Steel Plates

Steel plates were added at support and loading locations in the finite element models - as in the actual beams - to provide an even stress distribution over these locations.

Material model number 4 in flexure beam model and material model number 3 in shear beam model refer to loading and supporting steel plates. These plates were modeled as an elastic linear isotropic material. Table (4-8) shows material properties of steel plates used for ANSYS flexure beam and shear beam models.

Material Model Number	Element Type	Material Properties	
4 (Flexure Beam) 3 (Shear Beam)	Solid185 (Homogeneous Structural Solid)	Linear Isotropic	
		EX	200000 MPa
		PRXY	0.3

Table (4-8): Material Properties of Steel Plates for ANSYS Flexure Beam and Shear Beam Models.

4.6.4 Carbon Fiber Reinforced Polymer (CFRP)

Material model number 5 in flexure beam model and material model number 4 in shear beam model refer to CFRP fabric which was modeled using the shell181 element. CFRP composites were assumed to be especially orthotropic and transversely isotropic; that is, mechanical properties are the same in any direction perpendicular to the fibers. Definition of CFRP in ANSYS model requires definition of linear isotropic material properties, section properties, and failure criteria.

Parameters needed to define the material model for CFRP in ANSYS flexure beam and shear beam models are shown in Tables (4-9) and (4-10).

Material Model Number	Element Type	Material Properties	
5 (Flexure Beam)	Shell181	Linear Orthotropic	
		EX	285000 MPa
		EY	22800 MPa
		EZ	22800 MPa
		PRXY	0.3
		PRYZ	0.45
		PRXZ	0.3
		GXY	13570 MPa
		GYZ	7860 MPa
		GXZ	13570 MPa
		Section (SECID: 1, SECTYPE: Shell)	
		Layer No. 1	
		TK	0.3 mm
		THETA	0 degree
		Failure Criteria	
		Stress – XTEN	3500 MPa
Strain – XTEN	0.015		

Table (4-9): Material Properties of CFRP for ANSYS Flexure Beam Model.

Material Model Number	Element Type	Material Properties	
4 (Shear Beam)	Shell181	Linear Orthotropic	
		EX	228000 MPa
		EY	15200 MPa
		EZ	15200 MPa
		PRXY	0.3
		PRYZ	0.45
		PRXZ	0.3
		GXY	9120 MPa
		GYZ	5241.4 MPa
		GXZ	9120 MPa
		Section (SECID: 1, SECTYPE: Shell)	
		Layer No. 1	
		TK	0.18 mm
		THETA	90 degree
		Failure Criteria	
		Stress – XTEN	490 N/mm ²
		Strain – XTEN	0.018

Table (4-10): Material Properties of CFRP for ANSYS Shear Beam Model.

4.6.4.1 Linear Orthotropic Properties

The stress-strain relationship of CFRP is roughly linear up to failure. In this study, it was assumed that the stress-strain relationship for the CFRP laminates is linearly elastic.

To define the linear orthotropic model of CFRP in ANSYS, the following properties are specified:

- Elastic modulus in three directions (EX, EY and EZ).
- Shear modulus for three planes (GXY, GXZ and GYZ).
- Major Poisson's ratio for three planes (PRXY, PRXZ and PRYZ).

A local coordinate system for the CFRP shell element was defined where the x direction is the same as the fiber direction, while the y and z directions were perpendicular to the x direction.

The elastic modulus in the fiber direction of the unidirectional CFRP material used in the experimental studies was specified by the manufacturer, major Poisson's ratio was assumed, and then, the elastic modulus in directions perpendicular to the fiber direction, minor Poisson' ratio, and shear modulus were predicted using [Piggott, 2002] Rule of Mixture, as shown in tables (4-9) and (4-10).

4.6.4.2 Section Properties

The most important characteristic of a composite material is its layered configuration. Each layer may be made of a different orthotropic material and may have its principal directions oriented differently. For laminated composites, the fiber directions determine layer orientation, [ANSYS 2014]. To define the layered configuration of CFRP fabric, the following shall be specified:

- Number of layers.
- Thickness of each layer (TK).
- Orientation of the fiber direction for each layer (THETA).

4.6.4.3 Failure Criteria of CFRP

CFRP fabrics were modeled as linear elastic materials up to failure. Maximum strain failure criteria and maximum stress failure criteria were used based on the longitudinal tensile strength and maximum strain of the used CFRP fabrics, (Refer section 3.2.3.2 in this study).

4.7 Geometry

By taking advantage of the symmetry of the beams, a half of each full beam was used for modeling. This approach reduced computational time and computer disk space requirements significantly. The concrete beam, and steel loading and supporting plates were modeled as volumes, CFRP layers were modeled as areas, and steel reinforcement were modeled as lines.

4.7.1 Flexure Beam

Since a half of the beam is being modeled, the model is 1600 mm long, with a cross-section of 125 mm x 250 mm. The CFRP fabric layer bonded to the beam soffit was modeled as an area with 125 mm width and 1450 mm length (50 mm far from center of the support plate). Due to symmetry, only one loading plate and one support plate are needed. The steel loading and supporting plates are 100 mm x 25 mm x 125. The dimensions in millimeters for the combined volumes and areas created in the model are shown in Table (4-11).

ANSYS	Concrete		Support Plate		Loading Plate		CFRP Layer	
	Volume (1)		Volume (2)		Volume (3)		Area (1)	
X1, X2 X - Coordinates	0	1600	0	50	1050	1150	150	1600
Y1, Y2 Y- Coordinates	0	250	0	-25	250	275	Y = 0	
Z1, Z2 Z- Coordinates	0	125	0	125	0	125	0	125

Table (4-11): Dimensions of Volumes and Areas - Flexure Beam Model

The half of the entire model including the created volumes for flexure beam model is shown in Figure (4-12).

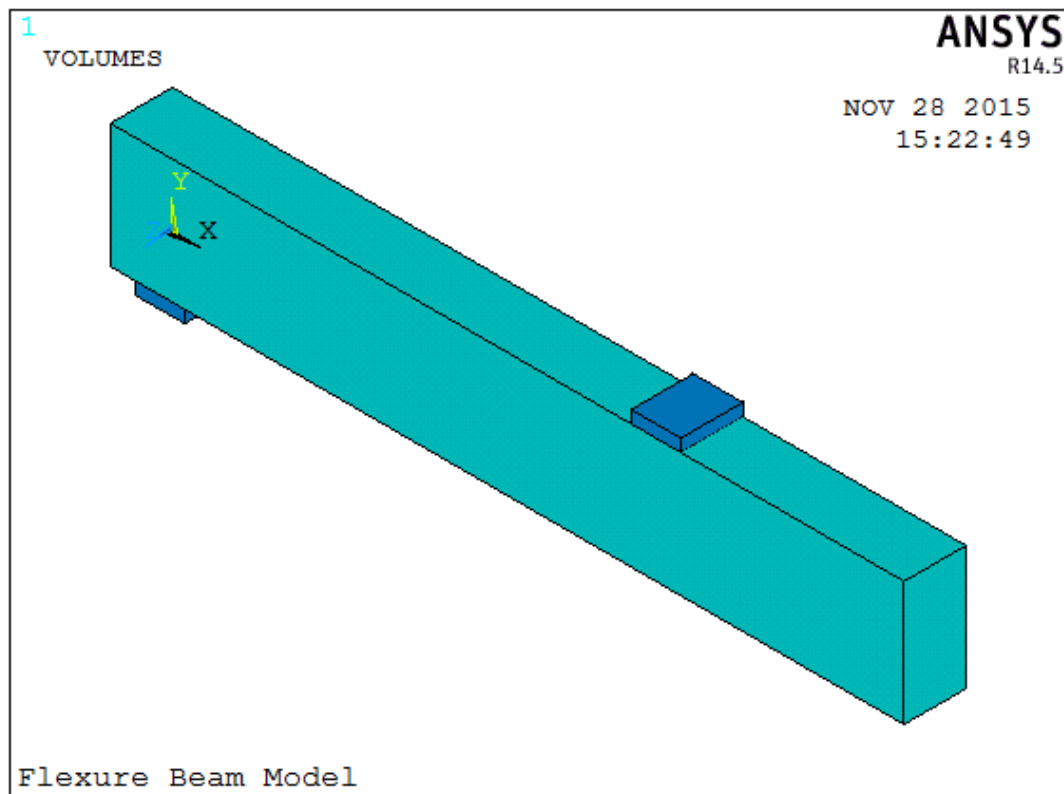


Fig. (4-12): Volumes Created in ANSYS - Flexure Beam Model.

4.7.2 Shear Beam Model

Since a half of the beam is being modeled, the model is 1065 mm long, with a cross-section of 230 mm x 380 mm. The CFRP fabric layer bonded to the beam soffit and sides as U-wrap was modeled as three areas, as shown in Table (4-12). Due to symmetry, only half of loading plate and one support plate are needed. The steel loading and supporting plates are 30 mm x 50 mm x 230. The dimensions for the combined volumes and areas created in the model are shown in Table (4-12).

ANSYS	Concrete		Support Plate		Loading Plate	
	Volume (1)		Volume (2)		Volume (3)	
X1, X2 X-coordinates	0	1065	135	165	1035	1065
Y1, Y2 Y-coordinates	0	380	0	-50	380	430
Z1, Z2 Z-coordinates	0	230	0	230	0	230
	CFRP Layer					
	Area (1)		Area (2)		Area (3)	
X1, X2 X-coordinates	165	1065	165	1065	165	1065
Y1, Y2 Y-coordinates	0	380	0		0	380
Z1, Z2 Z-coordinates	0		0	230	230	

Table (4-12): Dimensions of Volumes and Areas – Shear Beam Model

The half of the entire model including the created volumes for shear beam model is shown in Figure (4-13).

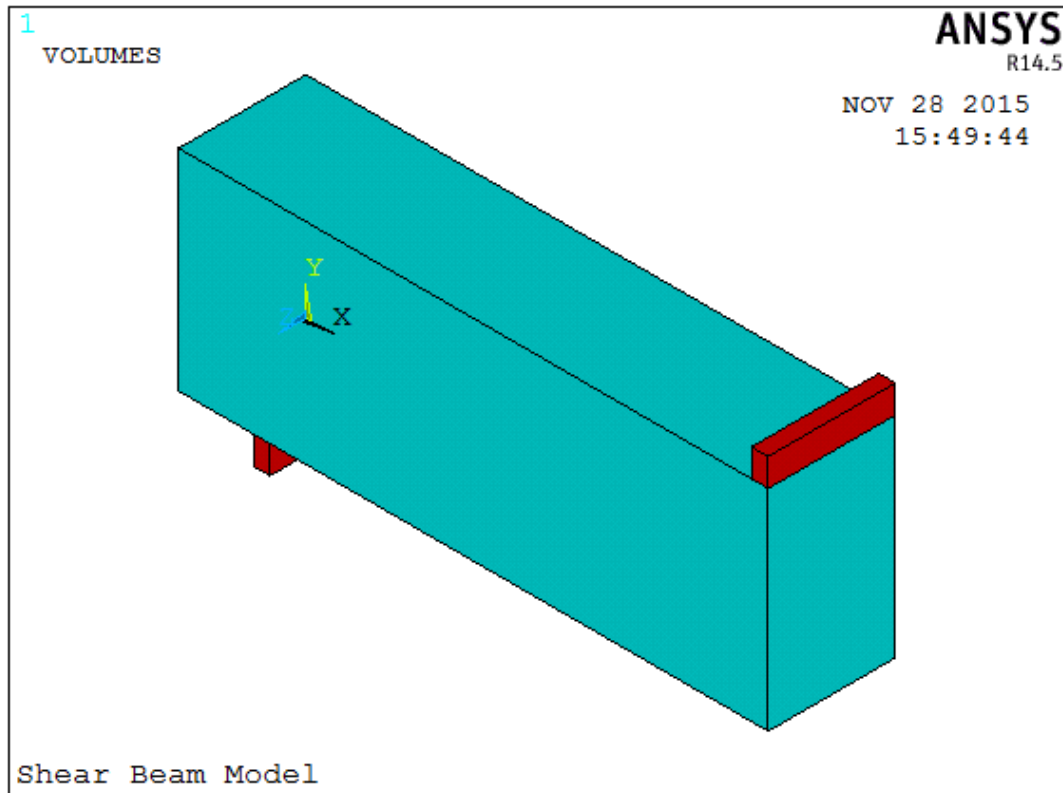


Fig. (4-13): Volumes Created in ANSYS - Shear Beam Model.

4.8 Meshing

4.8.1 Concrete and Steel Plates

To obtain good results from the Solid65 element, the use of a rectangular mesh is recommended (Wolanski, 2004; Kachlakev et al., 2001). Therefore, the mesh is set up such that square or rectangular elements are created. Steel loading and supporting plates were meshed as solid elements in such a way that its nodes were oriented with adjacent concrete solid elements. The command "merge items" was used to merge separate nodes that have the same location.

The overall mesh of the concrete beam and steel plates' volumes for flexure beam model is shown in Figure (4-14)

The overall mesh of the concrete beam and steel plates' volumes for shear beam model is shown in Figure (4-15)

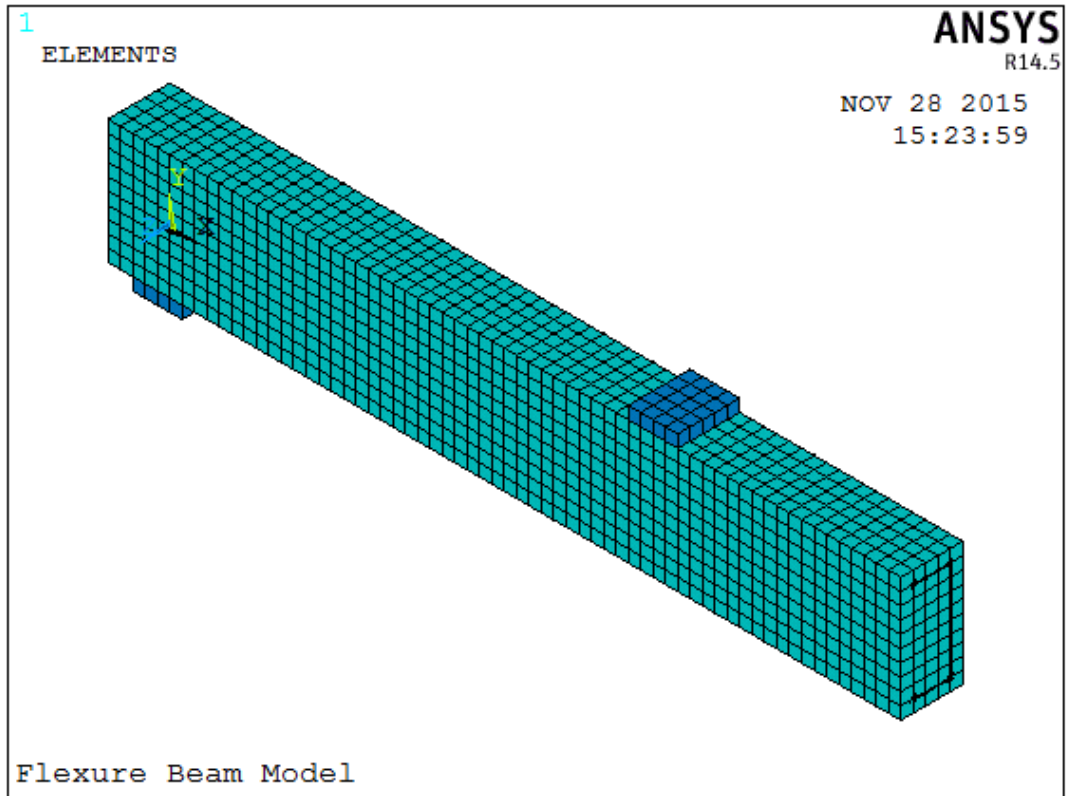


Fig. (4-14): Mesh of the Concrete Beam and Steel Plates – Flexure Beam Model

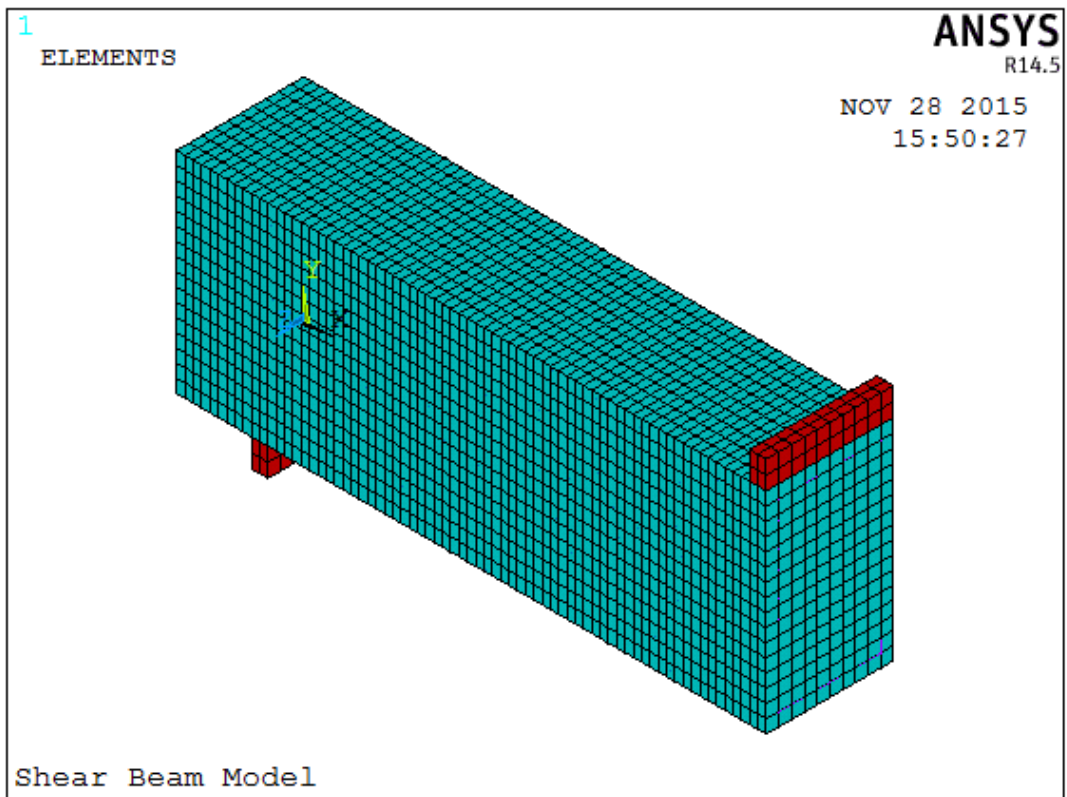


Fig. (4-15): Mesh of the Concrete Beam and Steel Plates – Shear Beam Model

4.8.2 Reinforcement

Ideally, the bond strength between the concrete and steel reinforcement should be considered. However, in this study, perfect bond between materials was assumed. To provide the perfect bond, the link element for the steel reinforcing was connected between nodes of each adjacent concrete solid element, so the two materials shared the same nodes, (Wolanski, 2004; Kachlakev et al., 2001).

The meshing of the reinforcement is a special case compared to the concrete volumes. No mesh of the reinforcement is needed because individual elements are created in the modeling through the nodes created by the mesh of the concrete volumes. However, the necessary mesh attributes need to be set before each section of the reinforcement is created.

Figures (4-16) (a) and (b) illustrate the reinforcement configuration modeled in ANSYS for flexure beam model.

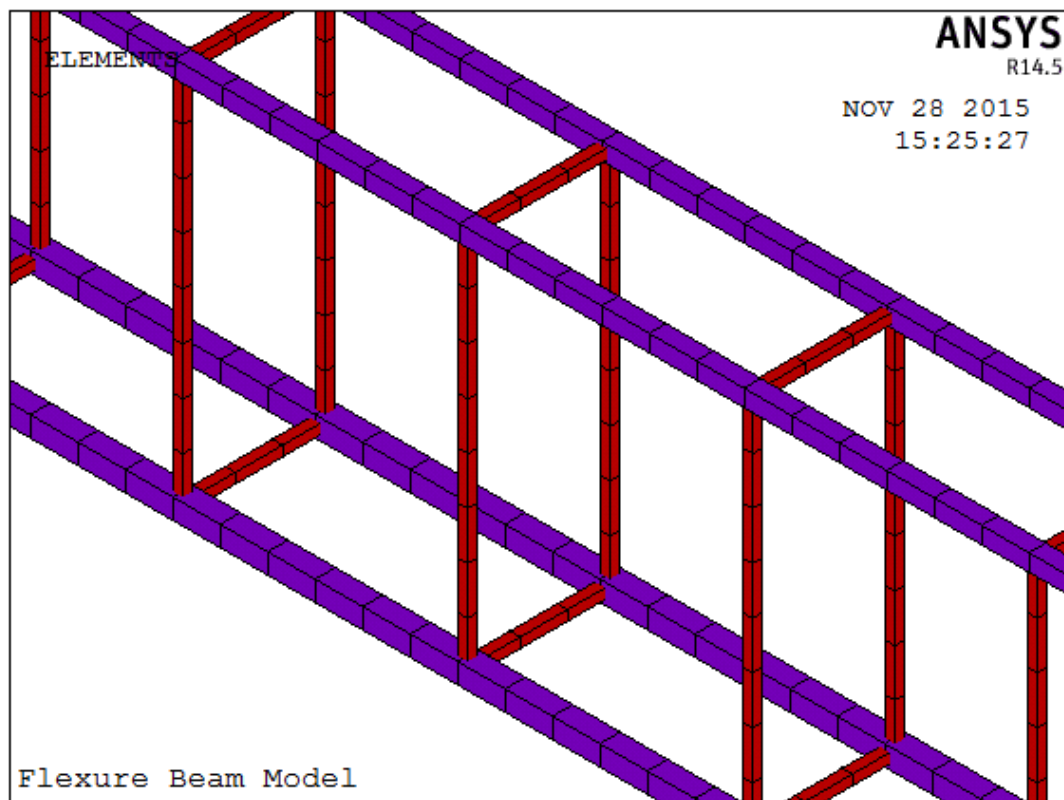


Fig. (4-16/a): Reinforcement Configuration– Flexure Beam Model

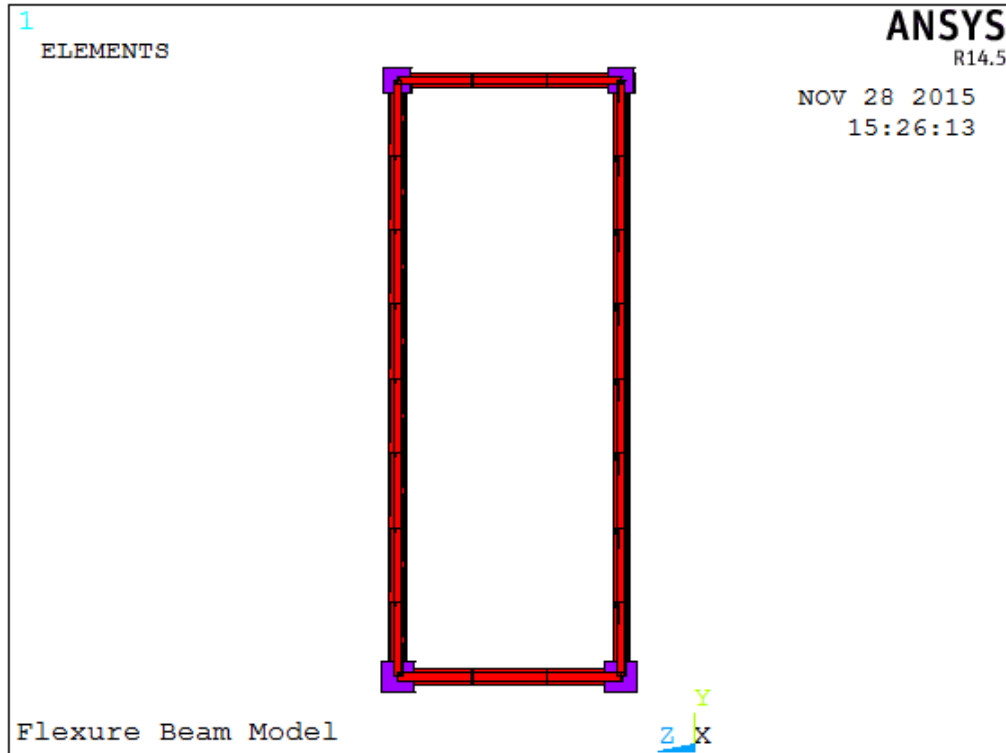


Fig. (4-16/b): Reinforcement Configuration– Flexure Beam Model

Figures (4-17) (a) and (b) illustrate the reinforcement configuration modeled in ANSYS for shear beam model.

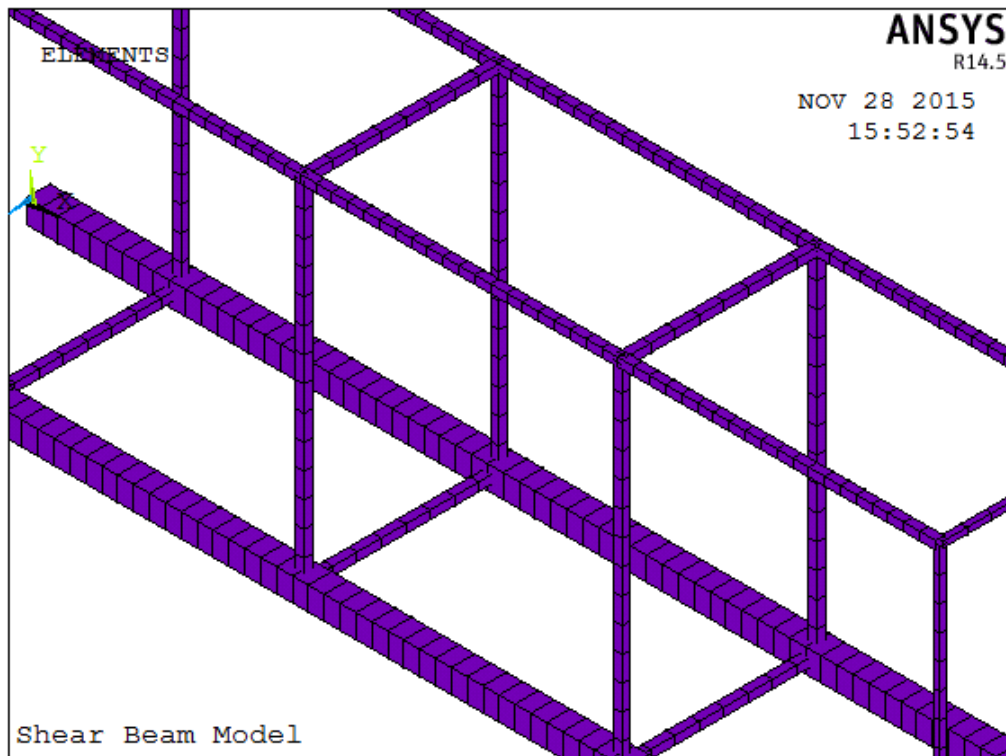


Fig. (4-17/a): Reinforcement Configuration– Shear Beam Model

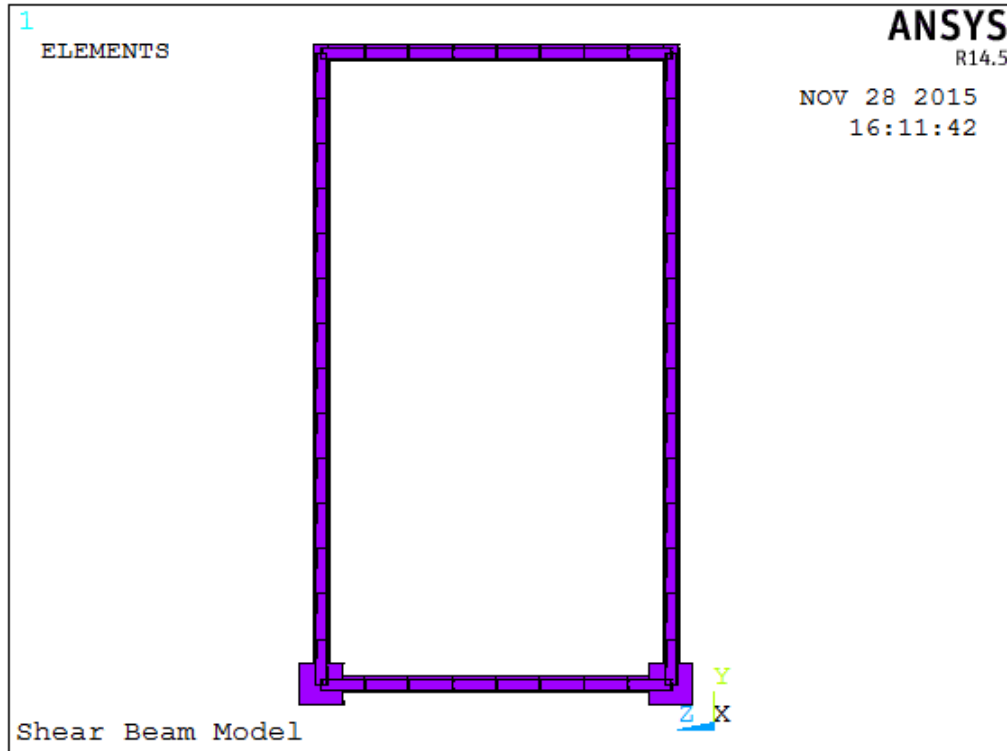


Fig. (4-17/b): Reinforcement Configuration– Shear Beam Model

4.8.3 CFRP Fabric Layer

CFRP sheets were meshed as shell elements in such a way that its nodes were oriented with adjacent concrete solid elements in order to satisfy the perfect bond assumption. The command "merge items" was used to merge separate nodes that have the same location.

The element type number, material number, real constant set number and section ID for the flexure and shear beam models were set for each mesh as shown in Tables (4-13) and (4-14).

Model Component	Element Type	Material Number	Real Constant	SECTION ID
Concrete Beam	1	1	1	N/A
Beam Bot. Rebar	2	2	2	N/A
Beam Top. Rebar	2	2	3	N/A
Stirrups	2	3	4	N/A
Stirrup at Center of Beam	2	3	5	N/A
Steel Loading Plate	3	4	N/A	N/A
Steel Support	3	4	N/A	N/A
CFRP Layer	4	5	N/A	1

Table (4-13): Mesh Attributes – Flexure Beam Model

Model Component	Element Type	Material Number	Real Constant	SECTION ID
Concrete Beam	1	1	1	N/A
Beam Bot. Rebar	2	2	2	N/A
Beam Top. Rebar	2	2	3	N/A
Stirrups	2	2	3	N/A
Stirrup at Center of Beam	2	2	4	N/A
Steel Loading Plate	3	3	N/A	N/A
Steel Support	3	3	N/A	N/A
CFRP Layer	4	4	N/A	1

Table (4-14): Mesh Attributes – Shear Beam Model

Figure (4-18) illustrates the meshing of CFRP fabric layer in ANSYS for flexure beam model.

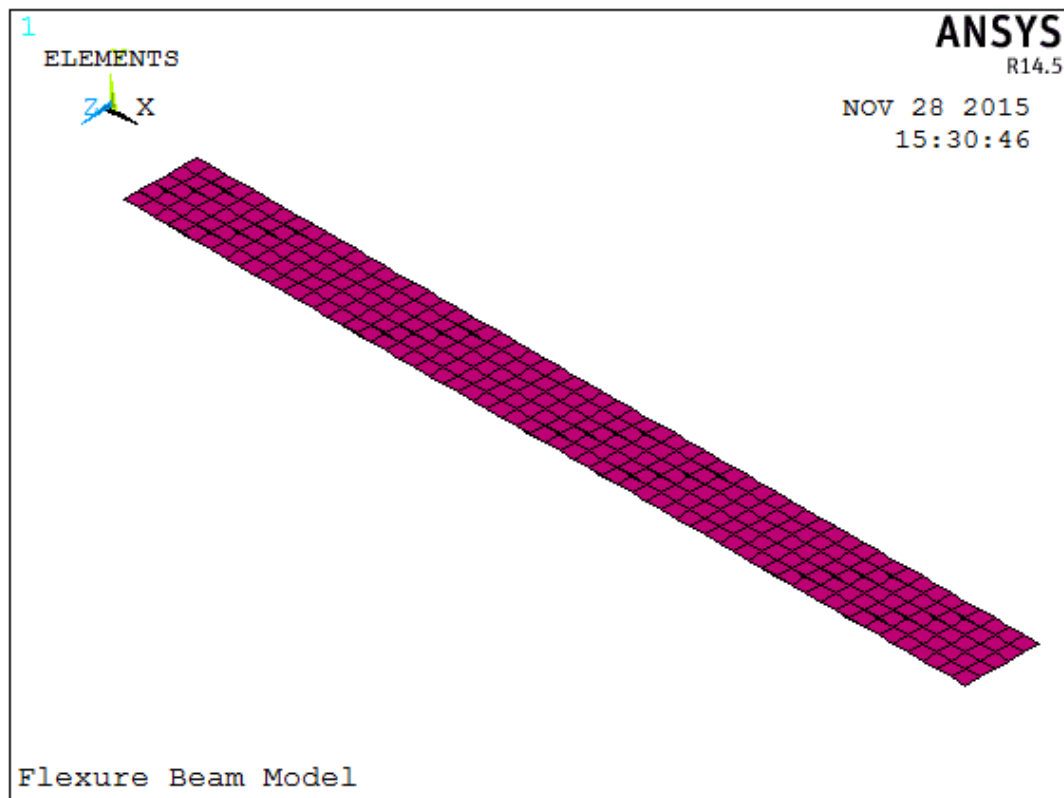


Fig. (4-18): Meshing of CFRP Layer in ANSYS – Flexure Beam Model

Figure (4-19) illustrates the meshing of CFRP fabric layer in ANSYS for shear beam model.

Figures (4-20) and (4-21) show the overall meshing of all model components: concrete beam, steel loading and supporting plates, steel reinforcement, and CFRP layer, for flexure beam and shear beam models respectively

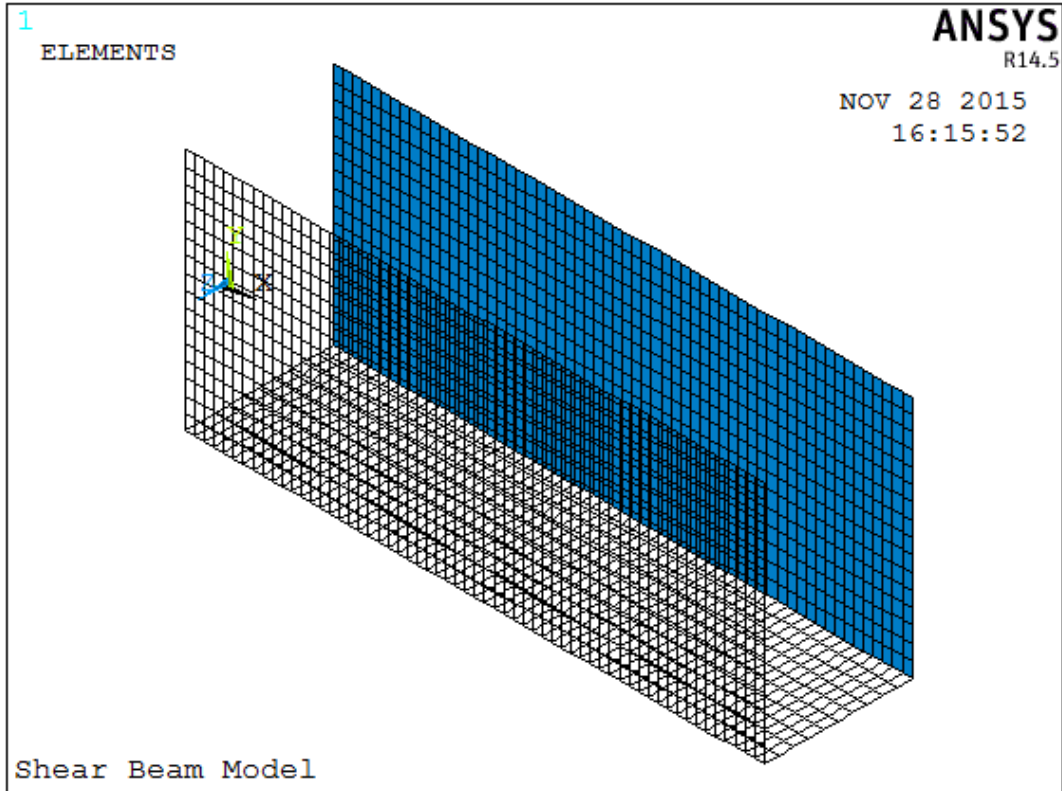


Fig. (4-19): Meshing of CFRP Layer in ANSYS – Shear Beam Model

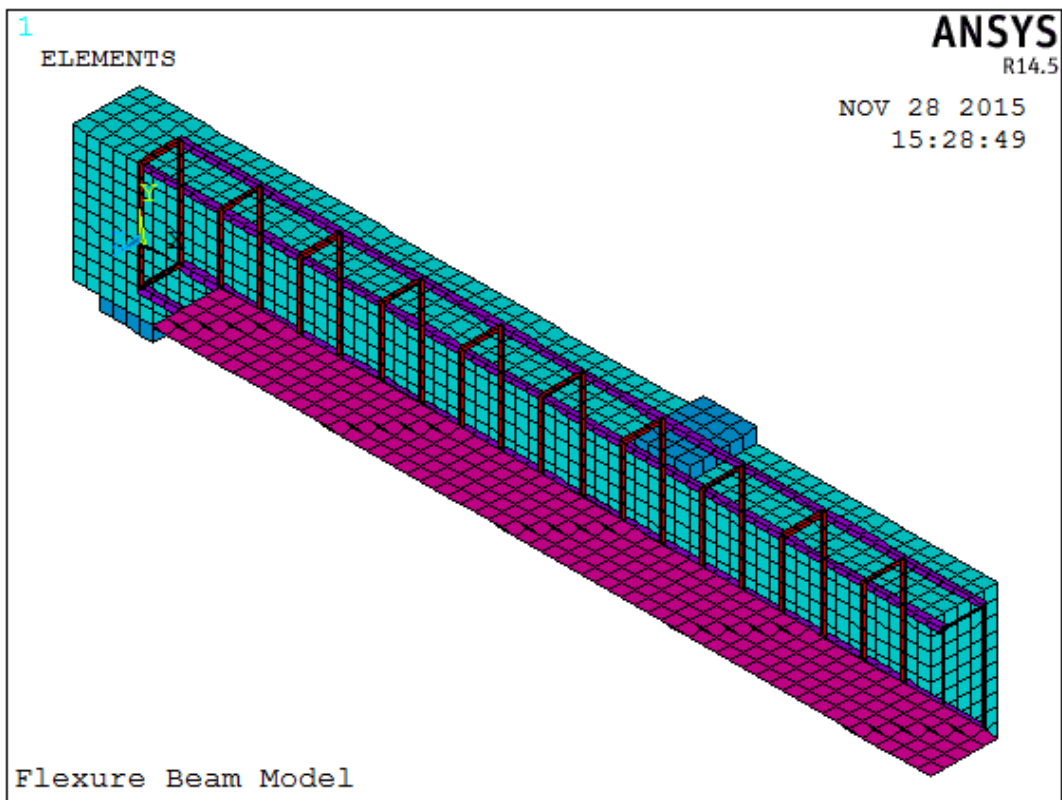


Fig. (4-20): The Overall Meshing of the Model – Flexure Beam Model

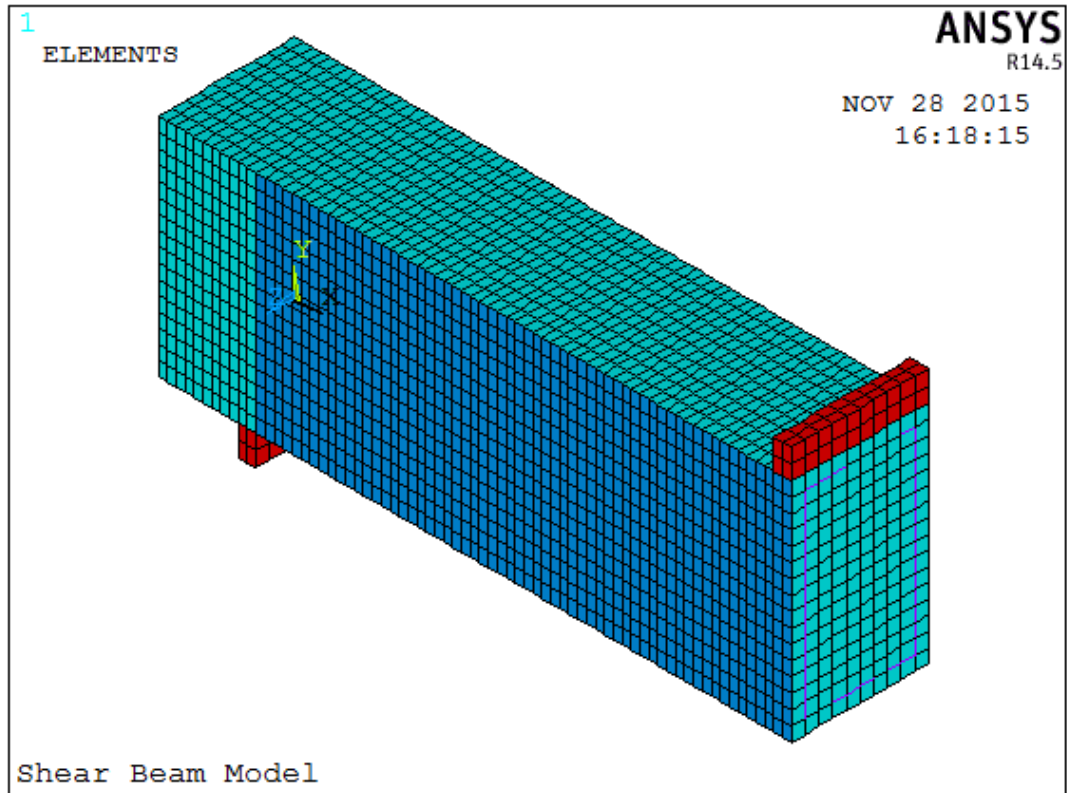


Fig. (4-21): The Overall Meshing of the Model – Shear Beam Model

4.9 Loads and Boundary Conditions

Displacement boundary conditions are needed to constrain the model to get a unique solution. To ensure that the model acts the same way as the experimental beam; boundary conditions need to be applied at points of symmetry, and where the supports and loadings exist, [Wolanski, 2004].

4.9.1 Planes of Symmetry

Because a half of each entire beam was used for the models, the models being used are symmetric about one plane. Nodes defining a vertical plane through the beam mid-section define a plane of symmetry. To model the symmetry, nodes on this plane must be constrained in the perpendicular direction. Therefore, these nodes have a degree of freedom constraint $UX = 0$, as shown in figures (4-22) and (4-23).

4.9.2 Support Plate

The support was modeled in such a way that a roller was created. A single line of nodes on the plate were given constraint in the UY , and UZ directions, applied as constant values of 0. By doing this, the beam will be allowed to rotate at the support, as shown in figures (4-24) and (4-25).

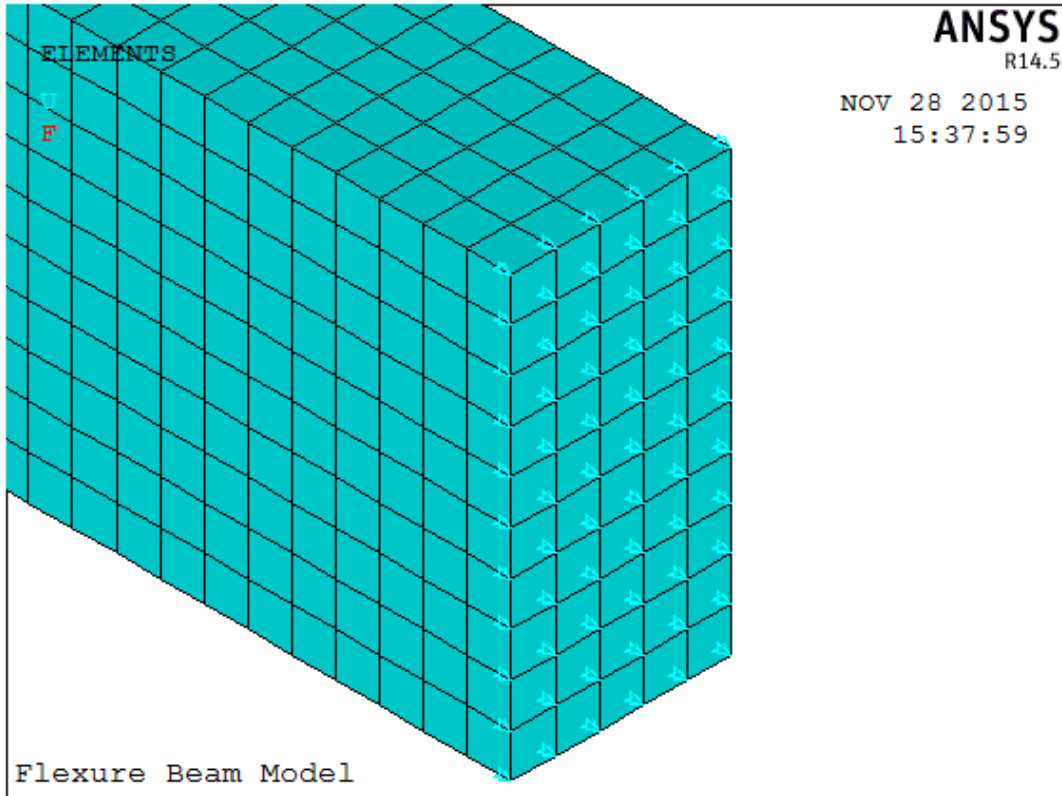


Fig. (4-22): Plane of Symmetry – Flexure Beam Model

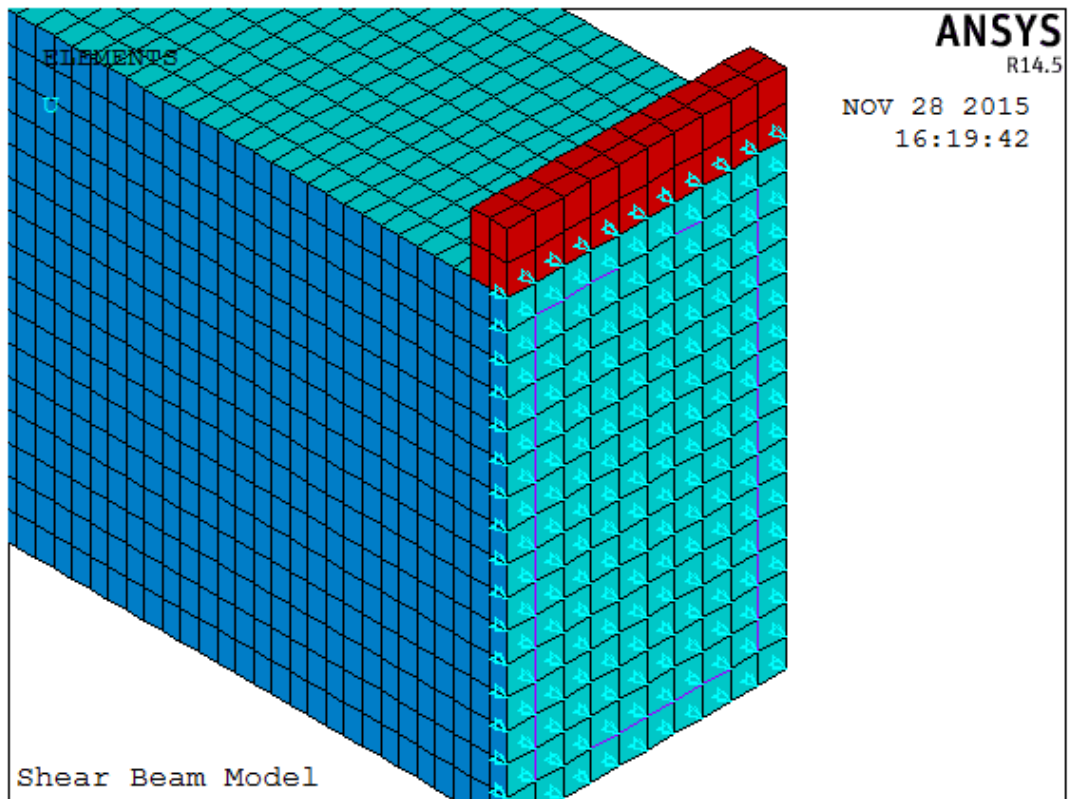


Fig. (4-23): Plane of Symmetry – Shear Beam Model

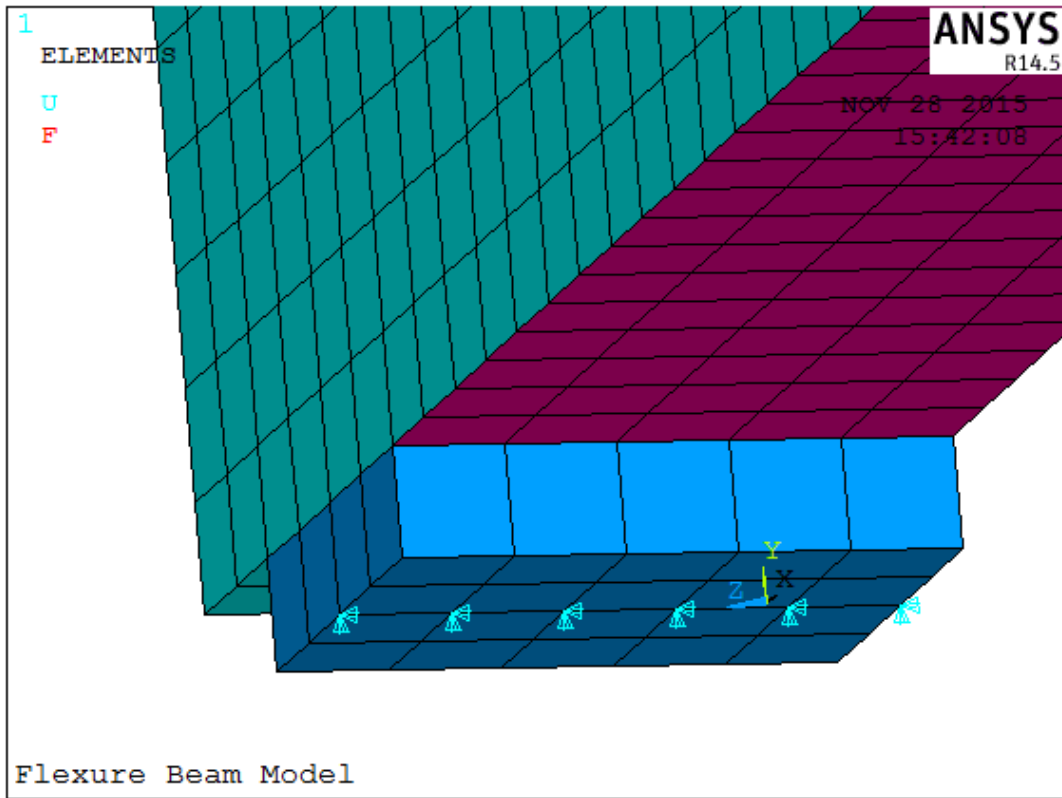


Fig. (4-24): Beam Support Plate – Flexure Beam Model

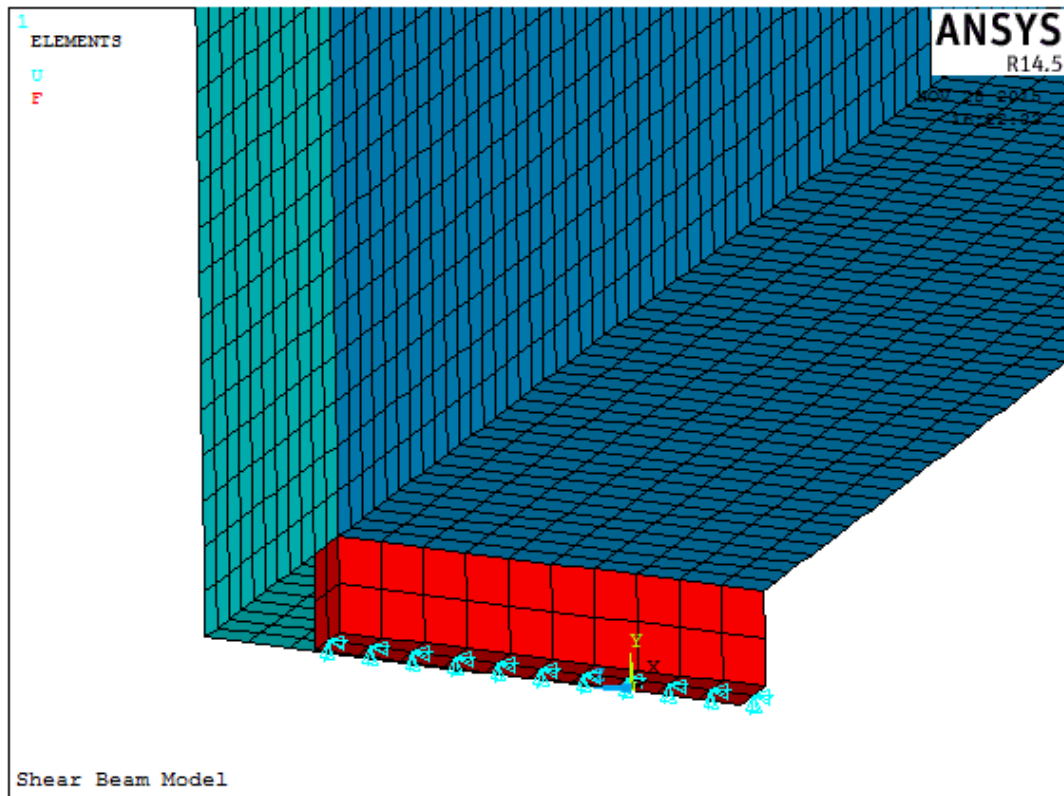


Fig. (4-25): Beam Support Plate – Shear Beam Model

4.9.3 Applied Loads

The force, P , applied at the steel plate is applied across the entire centerline of the loading plate, as shown in figures (4-26) and (4-27).

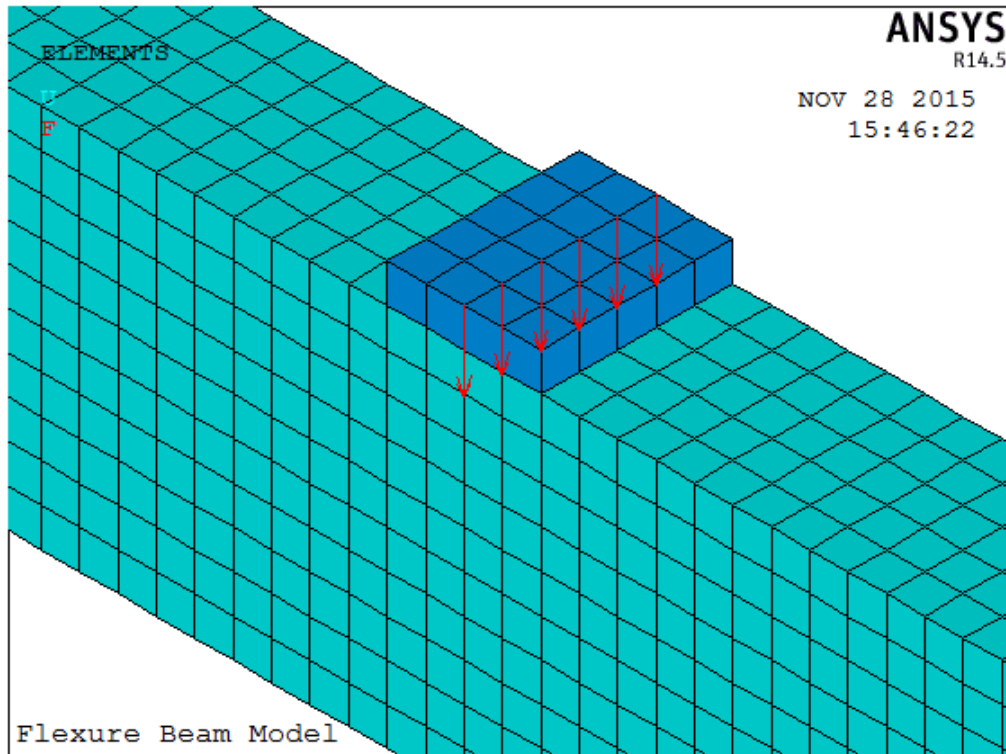


Fig. (4-26): Loading Plate – Flexure Beam Model

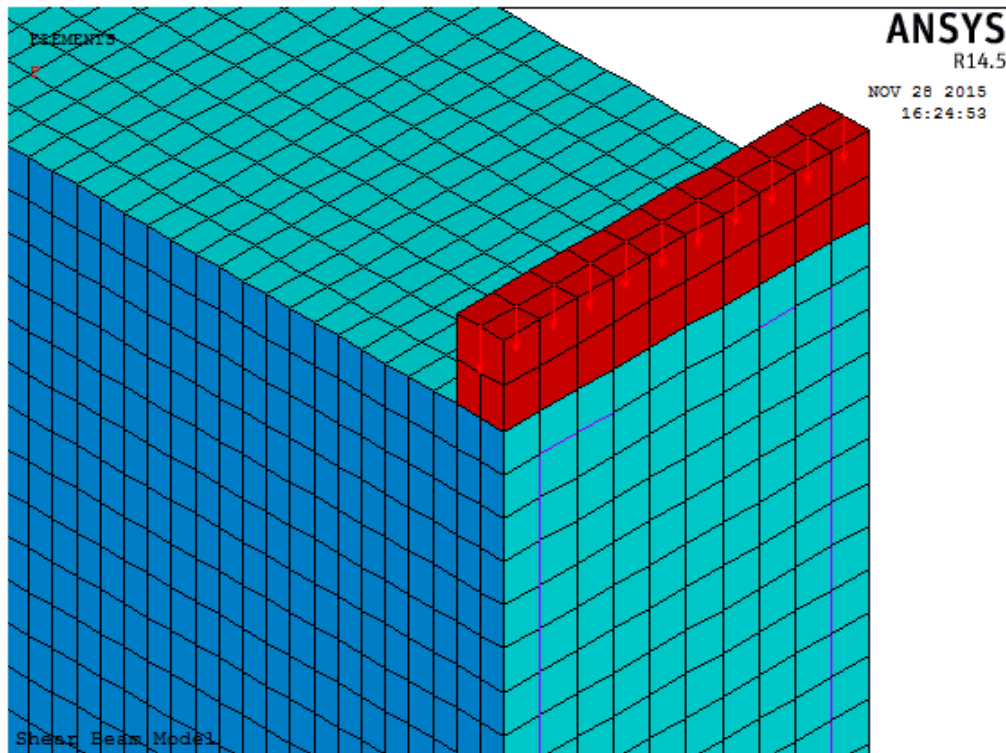


Fig. (4-27): Loading Plate - Shear Beam Model

4.10 Setting Nonlinear Solution Parameters

Setting solution parameters involves defining the analysis type and common analysis options for an analysis, as well as specifying load step options for it.

To ignore large deformation effects such as large deflection, large rotation, and large strain; the analysis option was set to (Small Displacement Static).

In nonlinear analysis, the load applied to the structures must be increased gradually to avoid non-convergence. The total load applied to a finite element model is divided into a series of load increments called load steps. At the completion of each incremental solution, the stiffness matrix of the model is adjusted to reflect nonlinear changes in structural stiffness before proceeding to the next load increment, [ANSYS, 2014]. The ANSYS program uses Newton–Raphson equilibrium iterations for updating the model stiffness.

Automatic time stepping in the ANSYS program predicts and controls load step sizes. Based on the previous solution history and the physics of the models, if the convergence behavior is smooth, automatic time stepping will increase the load increment up to a selected maximum load step size. If the convergence behavior is abrupt, automatic time stepping will bisect the load increment until it is equal to a selected minimum load step size. The maximum and minimum load step sizes are required for the automatic time stepping, [ANSYS, 2014].

Nonlinear Static Analysis type was utilized for both flexure beam and shear beam models. Typical commands utilized in the analysis are shown in Table (4-15).

Analysis Options	Small Displacement Static
Calculate Prestress Effects	No
Time at End of Load Step	1
Automatic Time Stepping	On
Time Step Size	0.05
Minimum Time Step	0.001
Maximum Time Step	0.05
Write Items to Results File	All Solution Items
Frequency	Write Every Sub Step

Table (4-15): Nonlinear Analysis Control Commands.

The commands used to control the solver and outputs are shown in Table (4-16).

Equation Solvers	Sparse Direct
Number of Restart Files	1
Frequency	Write Every Sub Step

Table (4-16): Output Control Commands.

The commands used for the nonlinear algorithm and convergence criteria are shown in Table (4-17). All values for the nonlinear algorithm are set to defaults.

Line Search	On
DOF solution predictor	Program Chosen
Maximum number of iteration	100
Cutback control	Cutback according to predicted number of iter.
Equiv. Plastic Strain	0.15
Explicit Creep ratio	0.1
Implicit Creep ratio	0
Incremental displacement	1,00,00,000
Points per cycle	13
Set Convergence Criteria	
Label	F U
Ref. Value	Calculated Calculated
Tolerance	0.005 0.05
Norm	L2 L2
Min. Ref.	Not applicable Not applicable

Table (4-17): Nonlinear Algorithm and Convergence Criteria Parameters.

Table (4-18) shows the command used for the advanced nonlinear settings. ANSYS program behavior upon non-convergence for this analysis was set such that the program will terminate but not exit. The rest of the commands were set to defaults.

Program Behavior Upon Non-convergence	Terminate but do not exit
Nodal DOF Sol'n	0
Cumulative Iterations	0
Elapsed time	0
CPU time	0

Table (4-18): Advanced Nonlinear Control Settings.

The properties of the used computer for models analysis are as follow:

Computer type: HP – ProBook 4530s

Processor: Intel (R) core i3 – 2350M – CPU @2.3 GHz

Installed Memory: 4.00 GB

System type: Window 7, 64-bit Operating System.

Table (4-19) shows analysis statistics and time required for nonlinear analysis for each model.

Model	Flexure Control Beam	Flexure Strengthened Beam	Shear Control Beam	Shear Strengthened Beam
Analysis Type	Static	Static	Static	Static
Number of Elements	3722	4248	11892	14420
Number of Nodes	4350	4410	13596	13662
Number of Keypoints	24	28	24	36
Number of Lines	36	40	36	48
Number of Areas	18	19	18	21
Number of Volumes	3	3	3	3
Number of Element Types	3	4	3	4
Number of Specified Constraints	78	78	209	209
Number of Nodal Loads	6	6	11	11
Analysis Time (min)	45	60	100	120

Table (4-19): ANSYS Analysis Statistics

CHAPTER 5

VERIFICATION OF ANSYS FINITE ELEMENT MODELS AND PARAMETRIC STUDY

5.1 Introduction

In this chapter, the finite element models developed in Chapter 4 for flexure and shear beams were verified by comparing results obtained from the FE analysis with results obtained from corresponding experimental tests. The verification process was based on the following criteria: load – mid span deflection curves, loads and deflection at failure, maximum stresses in CFRP fabric, and maximum strains in CFRP fabric. Having the finite element model validated, a parametric study was performed using ANSYS to evaluate the effect of the following parameters on the behavior of strengthened beams: number of CFRP layers, CFRP layer length, and CFRP layer inclination.

5.2 Verification of ANSYS Finite Element Models

5.2.1 Load - Mid Span Deflection Curves

5.2.1.1 Flexure Beam

Figure (5-1) shows a comparison of the load-deflection curve for the flexure control beam and strengthened beam as reported in the experimental investigation, [Balamuralikrishnan et. al, 2009].

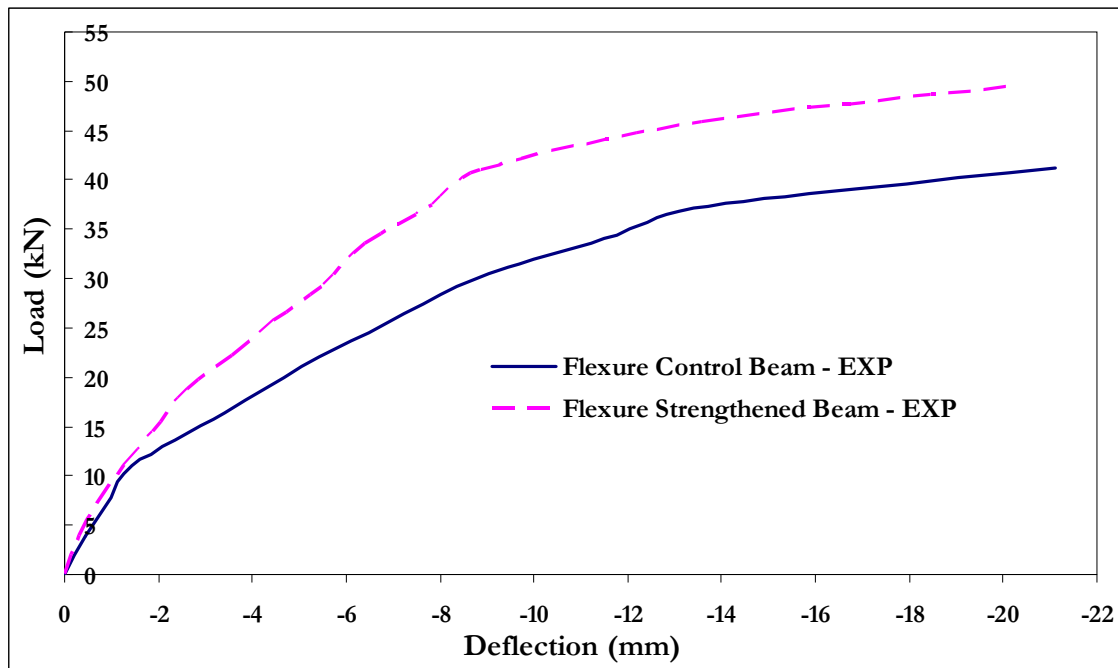


Fig. (5-1): Comparison of Experimental Load Deflection Curves for Flexure Beam.

Figure (5-2) shows a comparison of the load-deflection curve for the flexure control beam and strengthened beam as resulted from the finite element analysis (ANSYS).

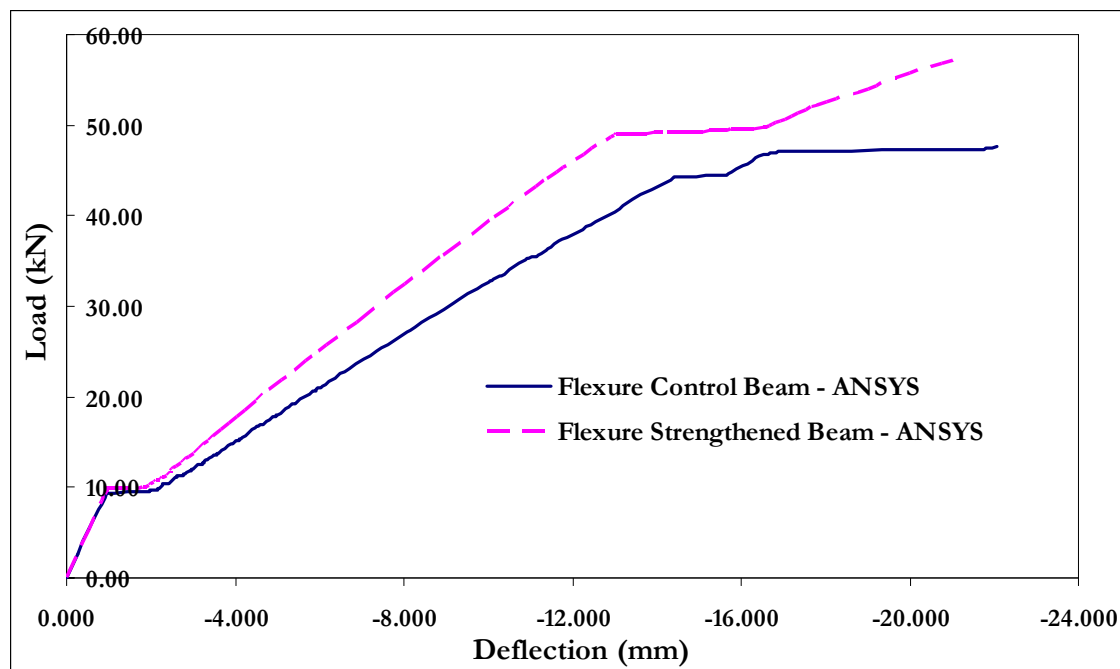


Fig. (5-2): Comparison of ANSYS Load Deflection Curves for Flexure Beam.

a- Flexure Control Beam

Figure (5-3) shows that the load-deflection curve obtained from the finite element analysis agrees well with the experimental data for the Flexure Control Beam. In the linear range, the load-deflection curve from the finite element analysis is stiffer than that from the experimental. The first cracking load for the finite element analysis is 9.4 kN, which is lower than the load of 15 kN from the experimental results by 37%. After first cracking, the stiffness of the finite element model is lower than the actual beam up to load 31 kN. The bottom steel reinforcement of the beam in the finite element model yields at 44 kN, which is higher than the load of 34.37 kN from the experimental results by 28%. At this load the elastic stress on the bottom reinforcement has exceeded the yield stress, Fig.(5-4). After steel yielding, the stiffness of the finite element model is higher than the actual beam. The final load of 47.7 kN from the model is higher than the ultimate load of 41.25 kN from the experimental data by 15.6 %.

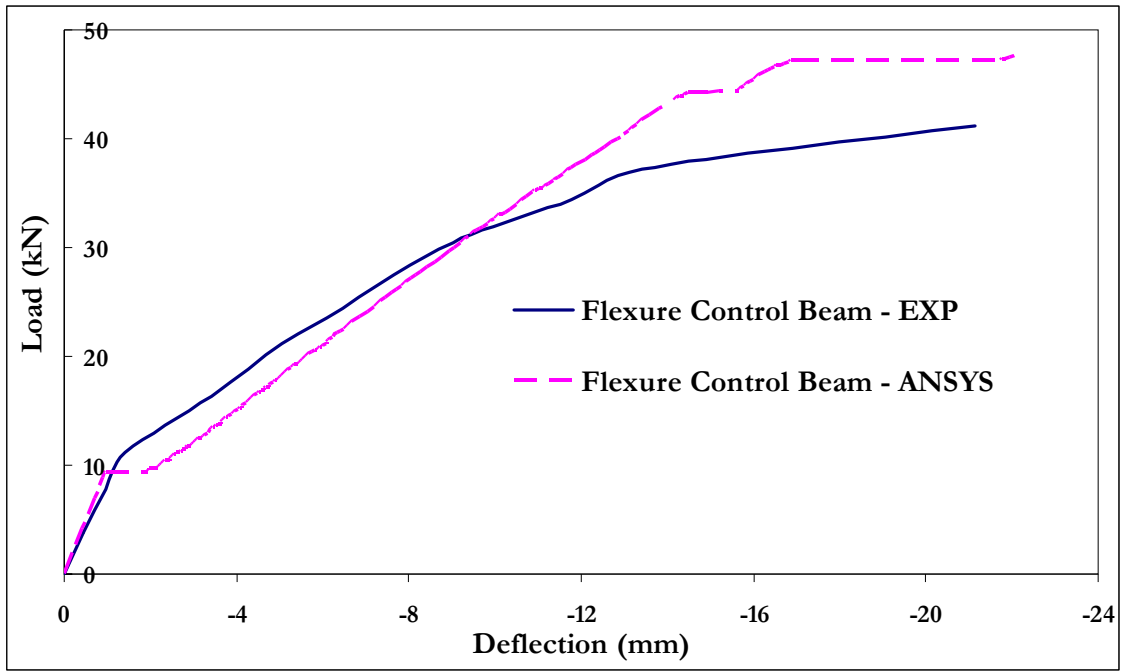


Fig. (5-3): Comparison of Experimental and ANSYS Load Deflection Curves – Flexure Control Beam.

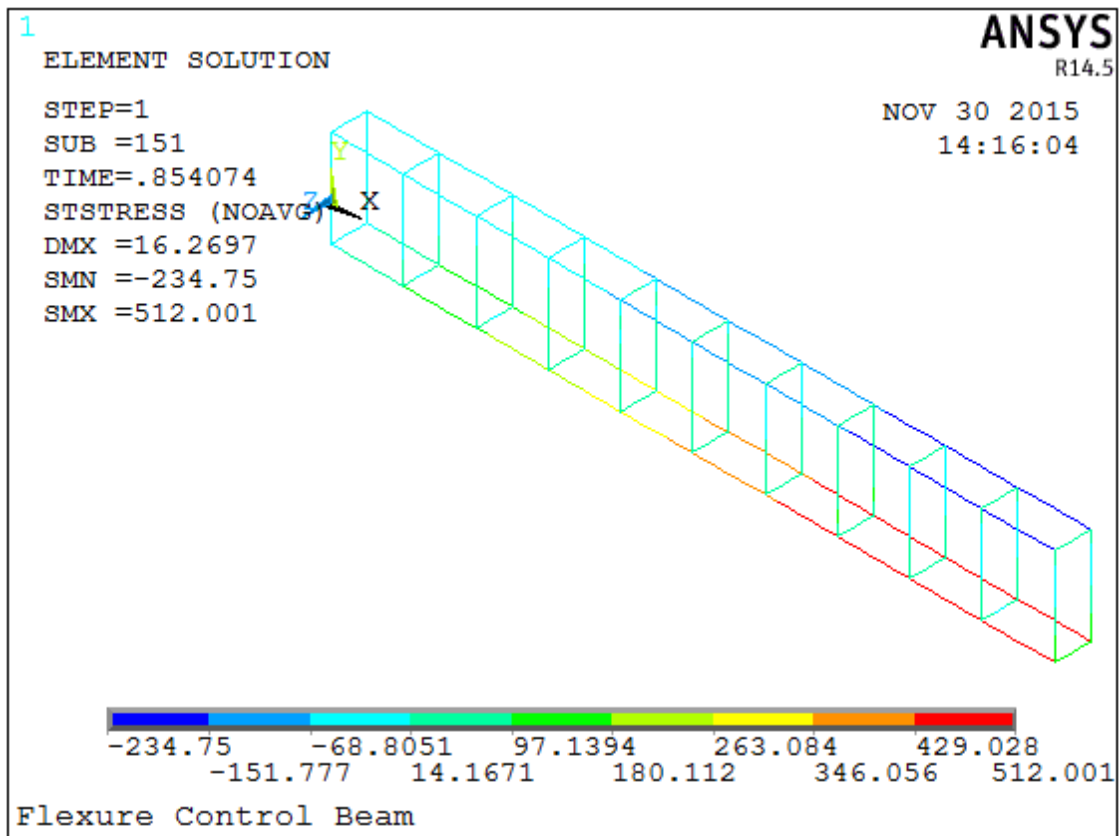


Fig. (5-4): Reinforcement Elastic Stress at Yielding Load– Flexure Control Beam.

b- Flexure Strengthened Beam

Figure (5-5) shows that the load-deflection curve obtained from the finite element analysis agrees well with the experimental data for the Flexure Strengthened Beam. In the linear range, the load-deflection curve from the finite element analysis is almost with the same stiffness as the experimental beam. The first cracking load for the finite element analysis is 10 kN, which is lower than the load of 16.25 kN from the experimental results by 38%.

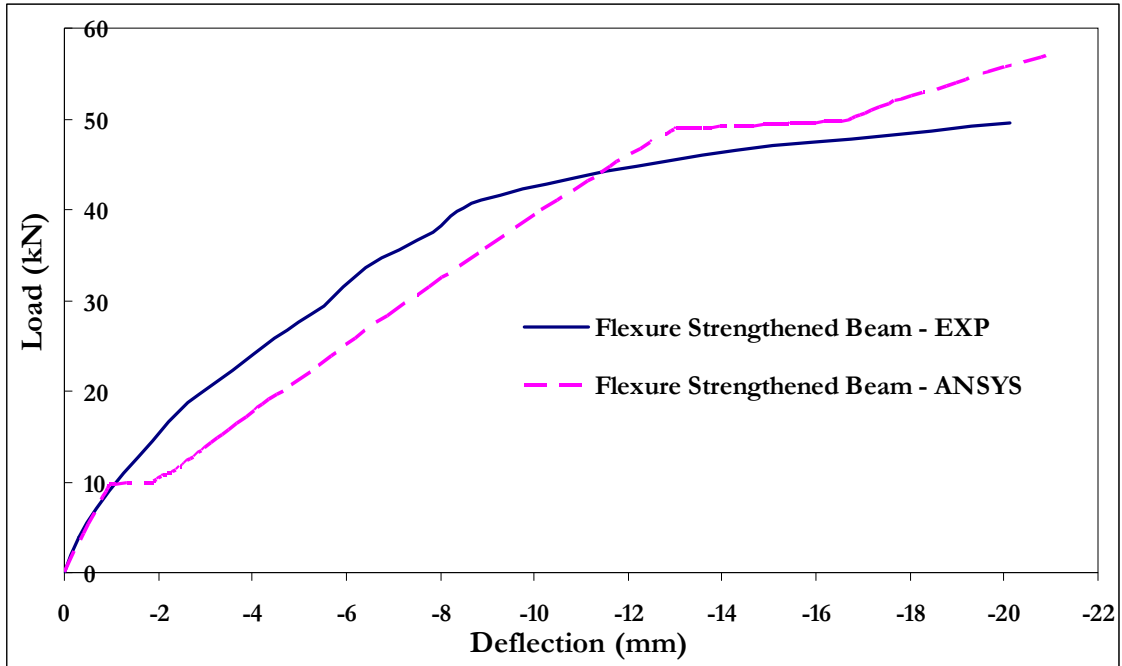


Fig. (5-5): Comparison of Experimental and ANSYS Load Deflection Curves – Flexure Strengthened Beam.

After first cracking, the stiffness of the finite element model is lower than the actual beam up to load 44kN. The bottom steel reinforcement of the beam in the finite element model yields at 48 kN, which is higher than the load of 40.63 kN from the experimental results by 15 %. At this load the elastic stress on the bottom reinforcement has exceeded the yield stress, Fig.(5-6). After yielding, the stiffness of the finite element model is higher than the actual beam. The final load of 57.3 kN from the model is higher than the ultimate load of 49.5 kN from the experimental data by 16%.

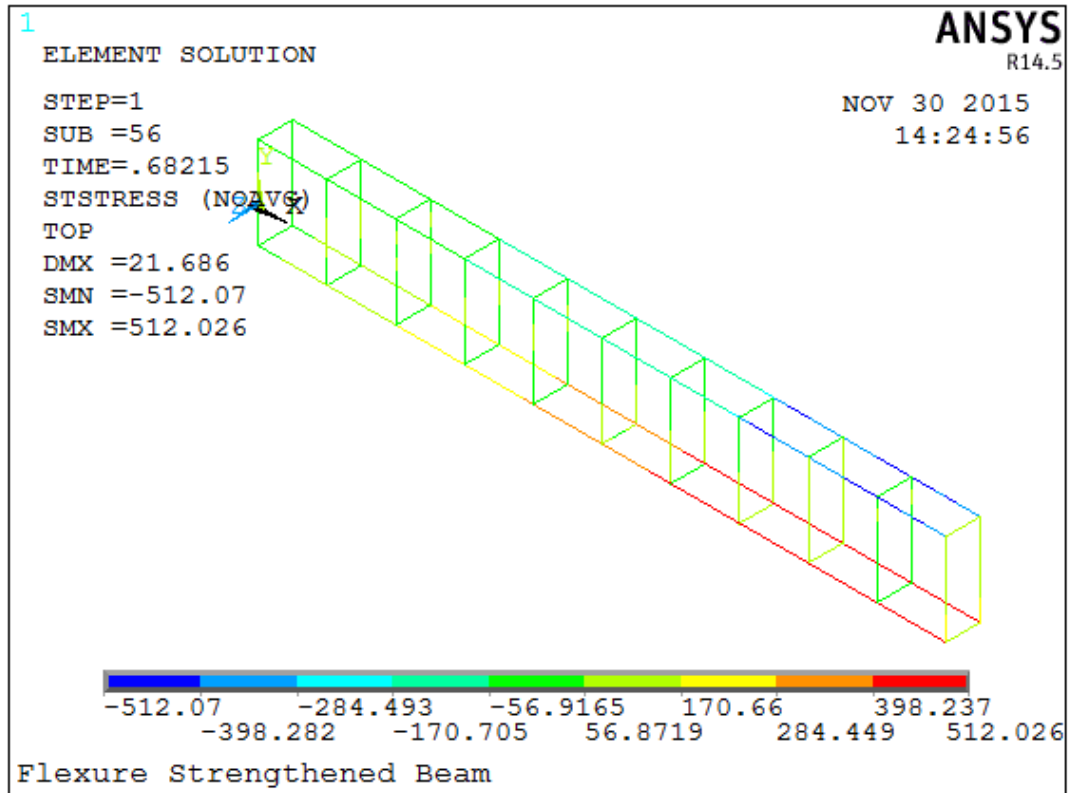


Fig. (5-6): Reinforcement Elastic Stress at Yielding Load – Flexure Strengthened Beam.

5.2.1.2 Shear Beam

Load deflection curve for shear control beam is not available in the experimental investigation, Alagusundaramoorthy et al. [2002]. The only available data is the failure load. Figure (5-7) shows a comparison of the load-deflection curve for the shear control beam and strengthened beam as resulted from the finite element analysis (ANSYS).

a- Shear Control Beam

Figure (5-8) shows the load-deflection curve obtained from the finite element analysis (ANSYS) for the Shear Control Beam. The first cracking load for the finite element analysis is 50 kN, The bottom steel reinforcement of the beam in the finite element model yields at 346.5 kN. At this load the elastic stress on the bottom reinforcement has exceeded the yield stress, Fig.(5-9). The final load of 359.6 kN from the model is lower than the ultimate load of 397 kN from the experimental data by 9.4 %.

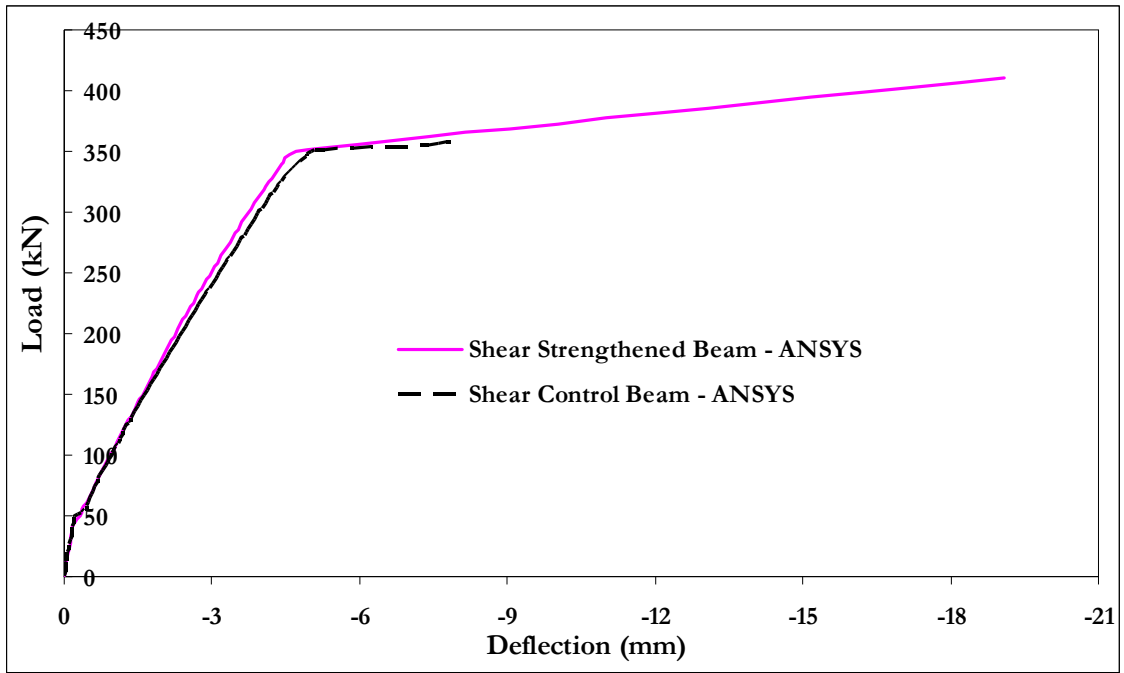


Fig. (5-7): Comparison of ANSYS Load Deflection Curves for Shear Beam.

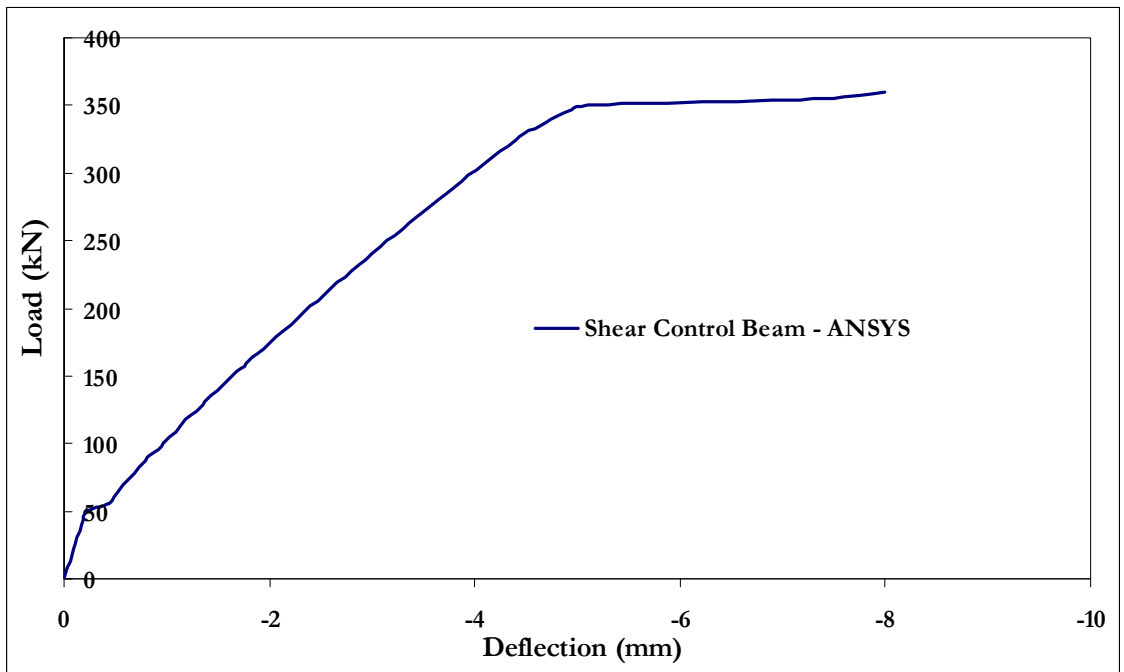


Fig. (5-8): Load Deflection Curve – Shear Control Beam.

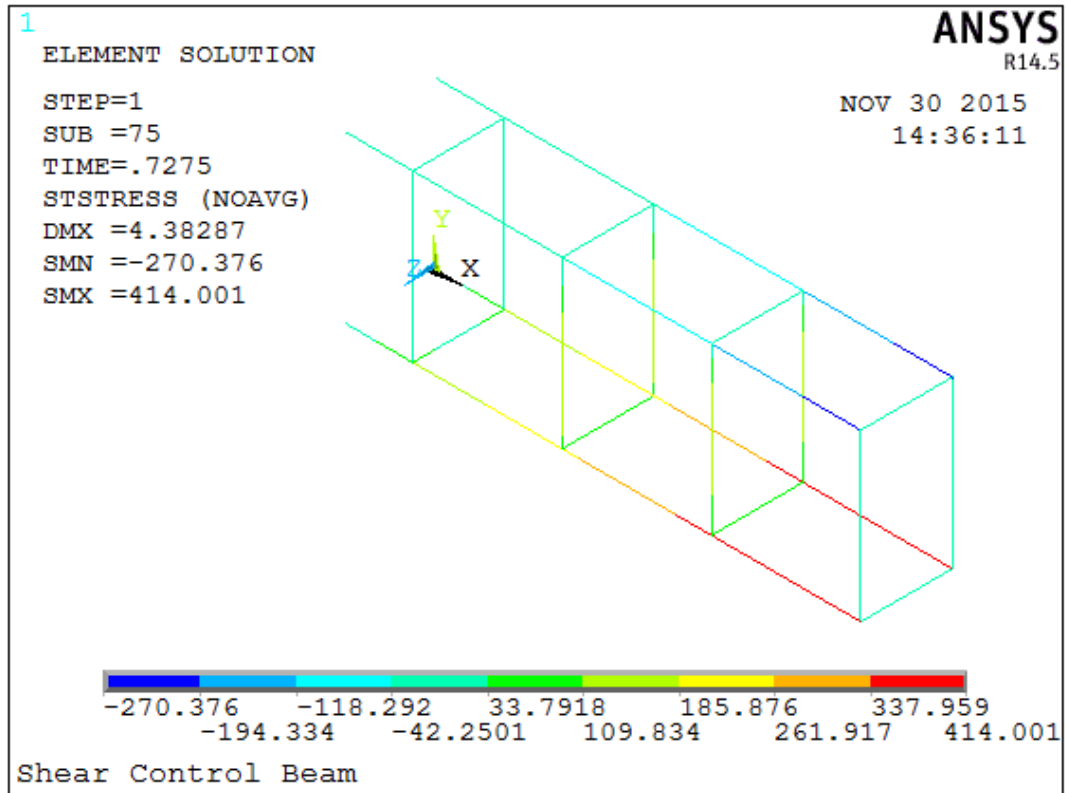


Fig. (5-9): Reinforcement Elastic Stress at Yielding Load – Shear Control Beam

b- Shear Strengthened Beam

Figure (5-10) shows that the load-deflection curve obtained from the finite element analysis agrees well with the experimental data for the Shear Strengthened Beam. In the linear range, the load-deflection curve from the finite element analysis is stiffer than that from the experimental. The first cracking load for the finite element analysis is 50 kN. After first cracking, the finite element model is stiffer than the actual beam. The bottom steel reinforcement of the beam in the finite element model yields at 350 kN. At this load the elastic stress on the bottom reinforcement has exceeded the yield stress, Fig.(5-11). Lastly, the final load of 410 kN from the model is lower than the (average) ultimate load of 421 kN from the experimental data by 2.6 %.

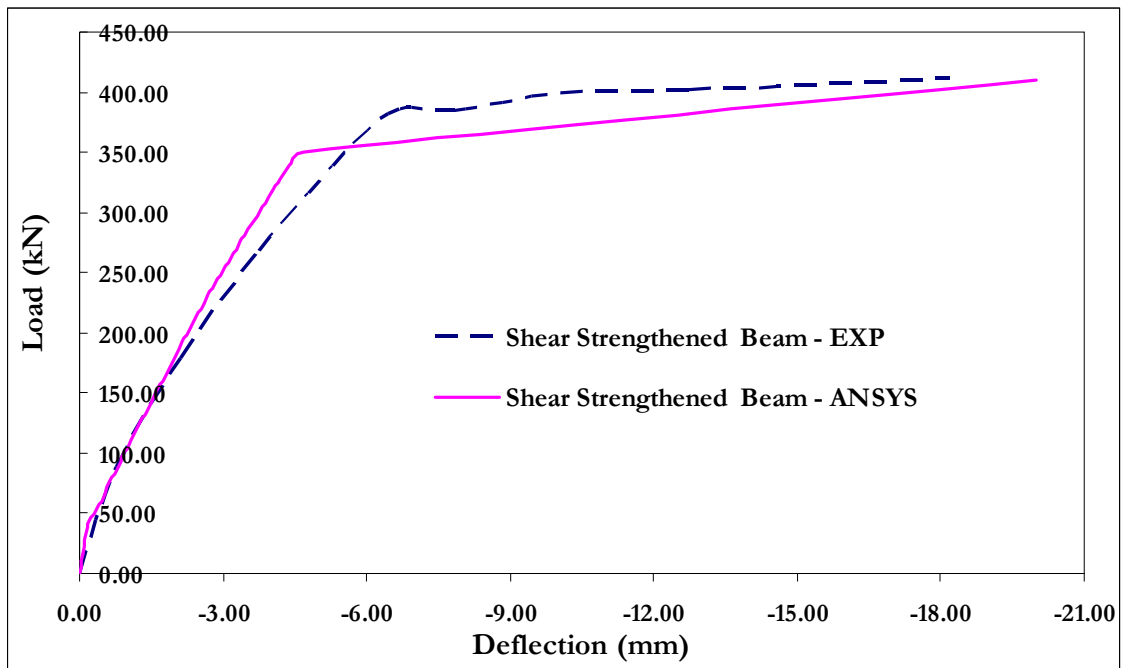


Fig. (5-10): Comparison of Experimental and ANSYS Load Deflection Curves – Shear Strengthened Beam.

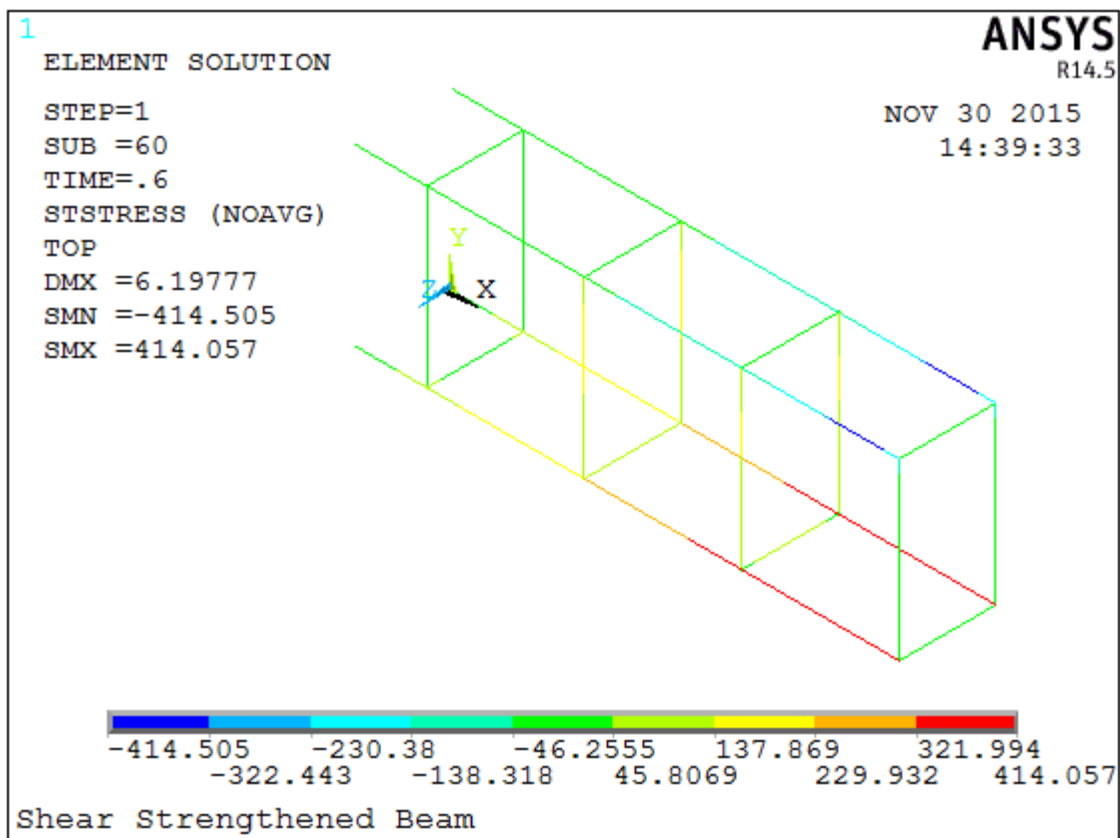


Fig. (5-11): Reinforcement Elastic Stress at Yielding Load – Shear Strengthened Beam.

5.2.3 Crack Patterns

ANSYS records a crack pattern at each applied load step. ANSYS displays circles at locations of cracking or crushing in concrete elements. Cracking is shown with a circle outline in the plane of the crack, and crushing is shown with an octahedron outline. The first crack at an integration point is shown with a red circle outline, the second crack with a green outline, and the third crack with a blue outline, [ANSYS, 2014].

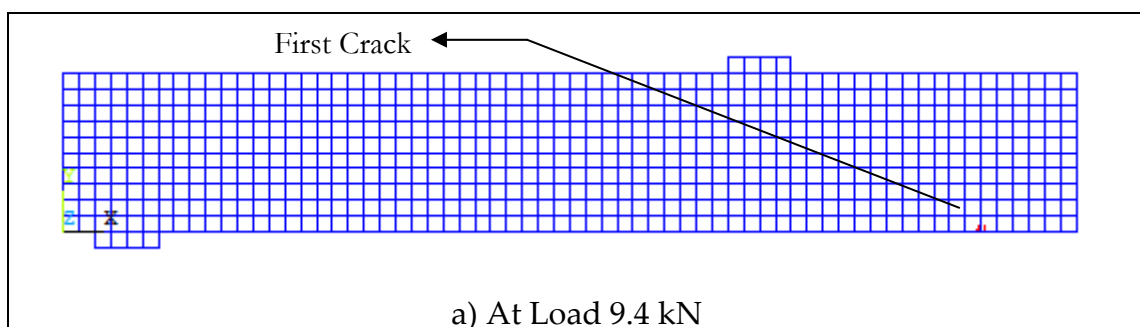
In ANSYS, stresses and strains, are calculated at integration points of the concrete solid elements. A cracking sign represented by a circle appears when a principal tensile stress exceeds the ultimate tensile strength of the concrete. The cracking sign appears perpendicular to the direction of the principal stress, [ANSYS, 2014]. Figures (5-12) to (5-15) show evolutions of crack patterns developing for each beam at different loading steps.

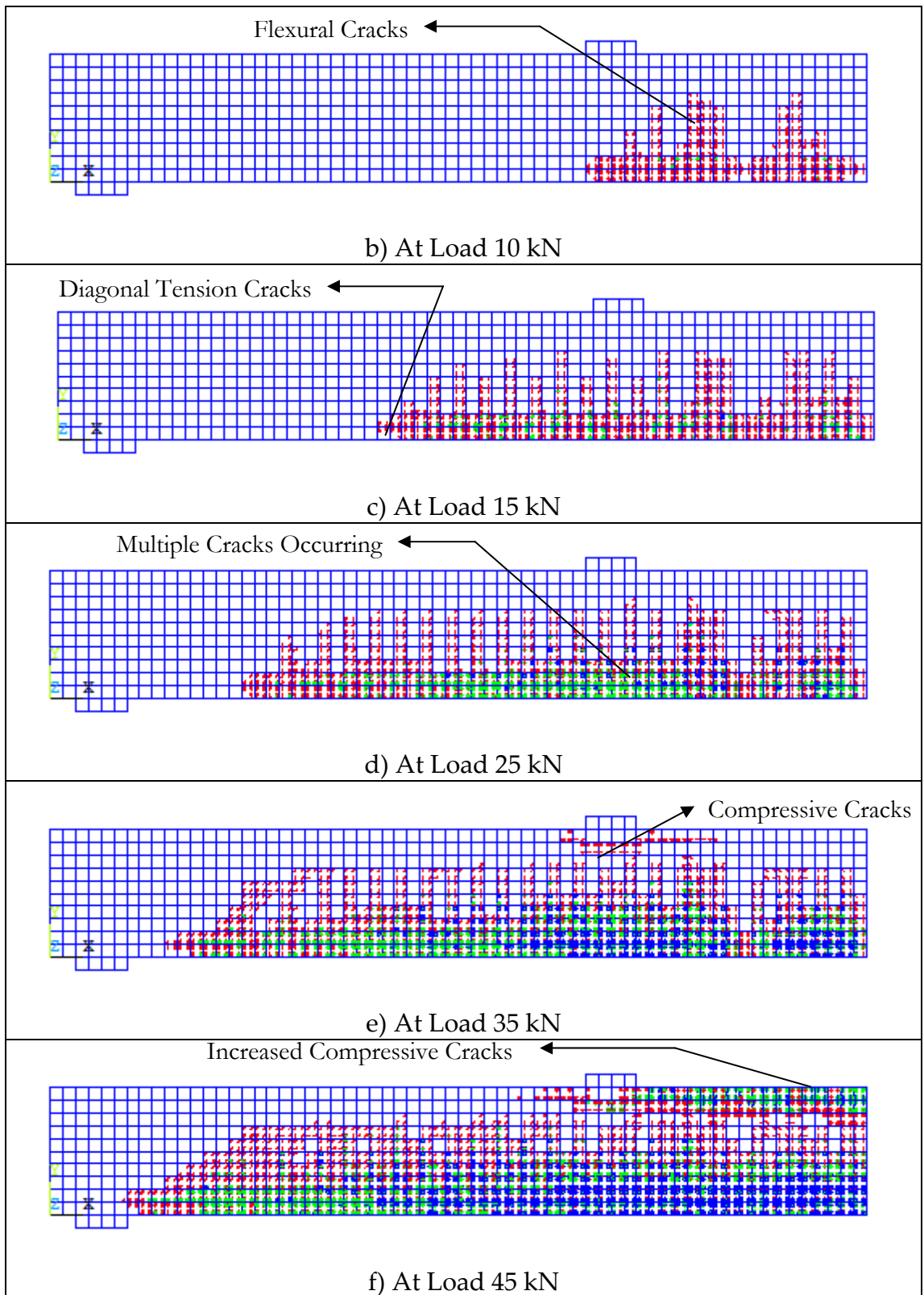
5.2.3.1 Crack Patterns for Flexure Beam

The propagation of cracks at different load steps for flexure control and strengthened beams is shown in the figures (5-12) and (5-13). Flexural cracks occur early at mid-span. When applied loads increase, vertical flexural cracks spread horizontally from the mid-span to the support. At a higher applied load, diagonal tensile cracks appear. Increasing applied loads induces additional diagonal and flexural cracks. Finally, compressive cracks appear at nearly the last applied load steps. The appearance of the cracks defines the failure mode for the beams.

a- Flexure Control Beam

The propagation of cracks at different load steps for flexure control beam is shown figures (5-12), (a), (b), (c), (d), (e), (f), (g) and (h)





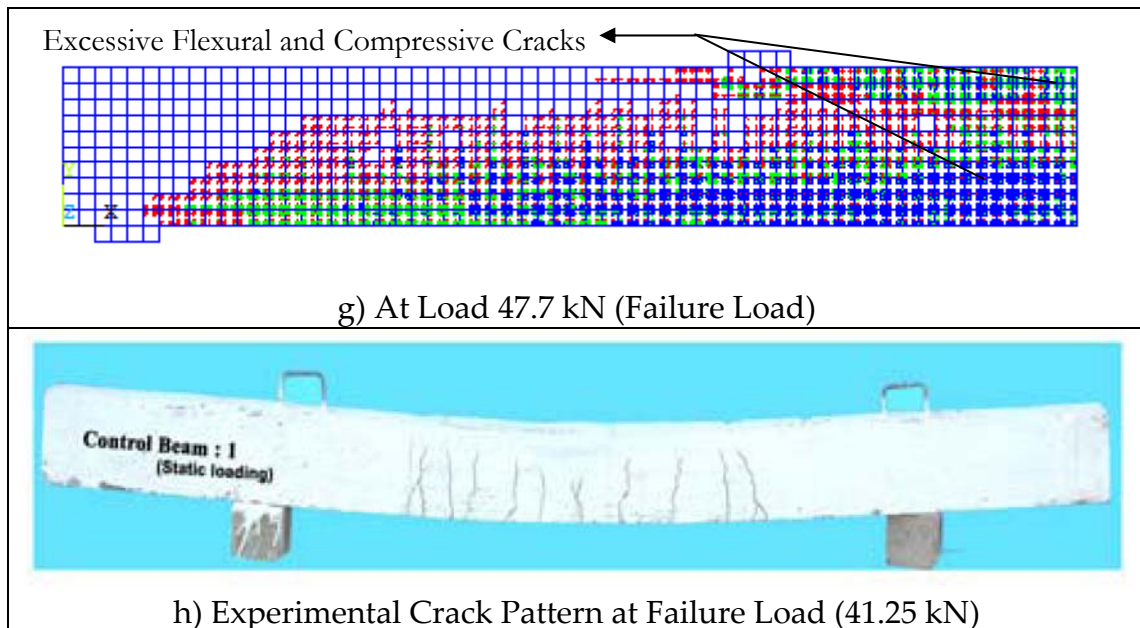
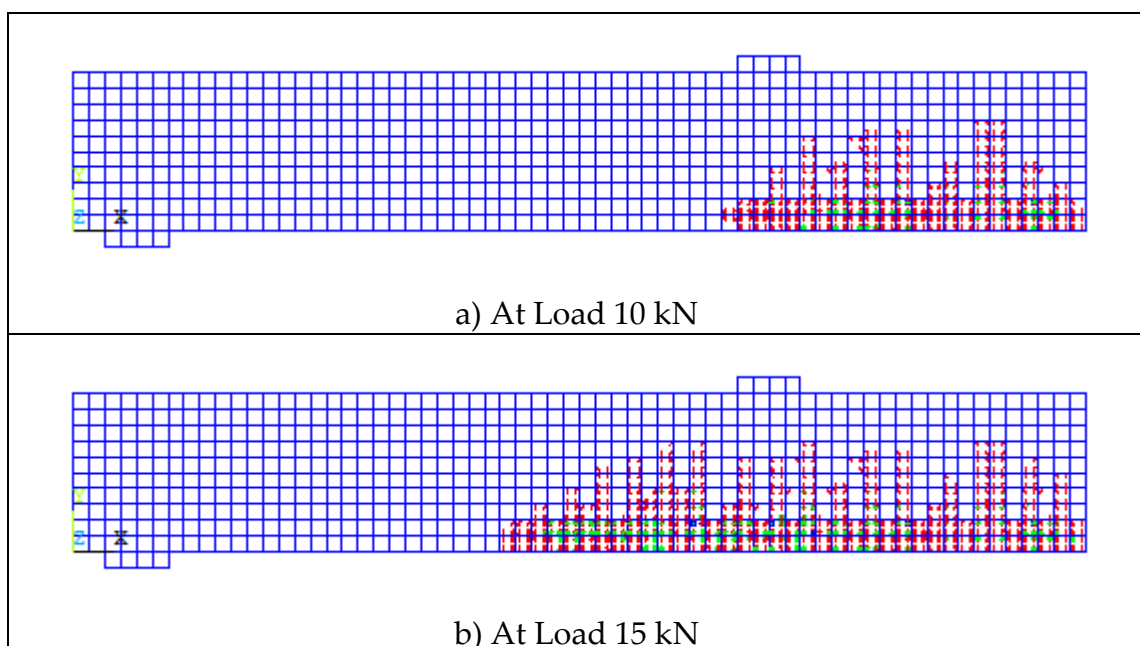


Fig. (5-12): Crack Propagations – Flexure Control Beam.

Comparing crack pattern obtained from the finite element analysis (ANSYS) at the last converged load step (Fig.5-12/g) with failure photographs from the actual beam (Fig.5-12/h), shows that the crack pattern from ANSYS and the actual beam agree very well. The flexure control beam failed in flexure at the mid-span, with yielding of the steel reinforcement, followed with a compression failure at the top of the beam.

b- Flexure Strengthened Beam

The propagation of cracks at different load steps for flexure strengthened beam is shown figure (5-13) (a), (b), (c), (d), (e), (f), and (g).



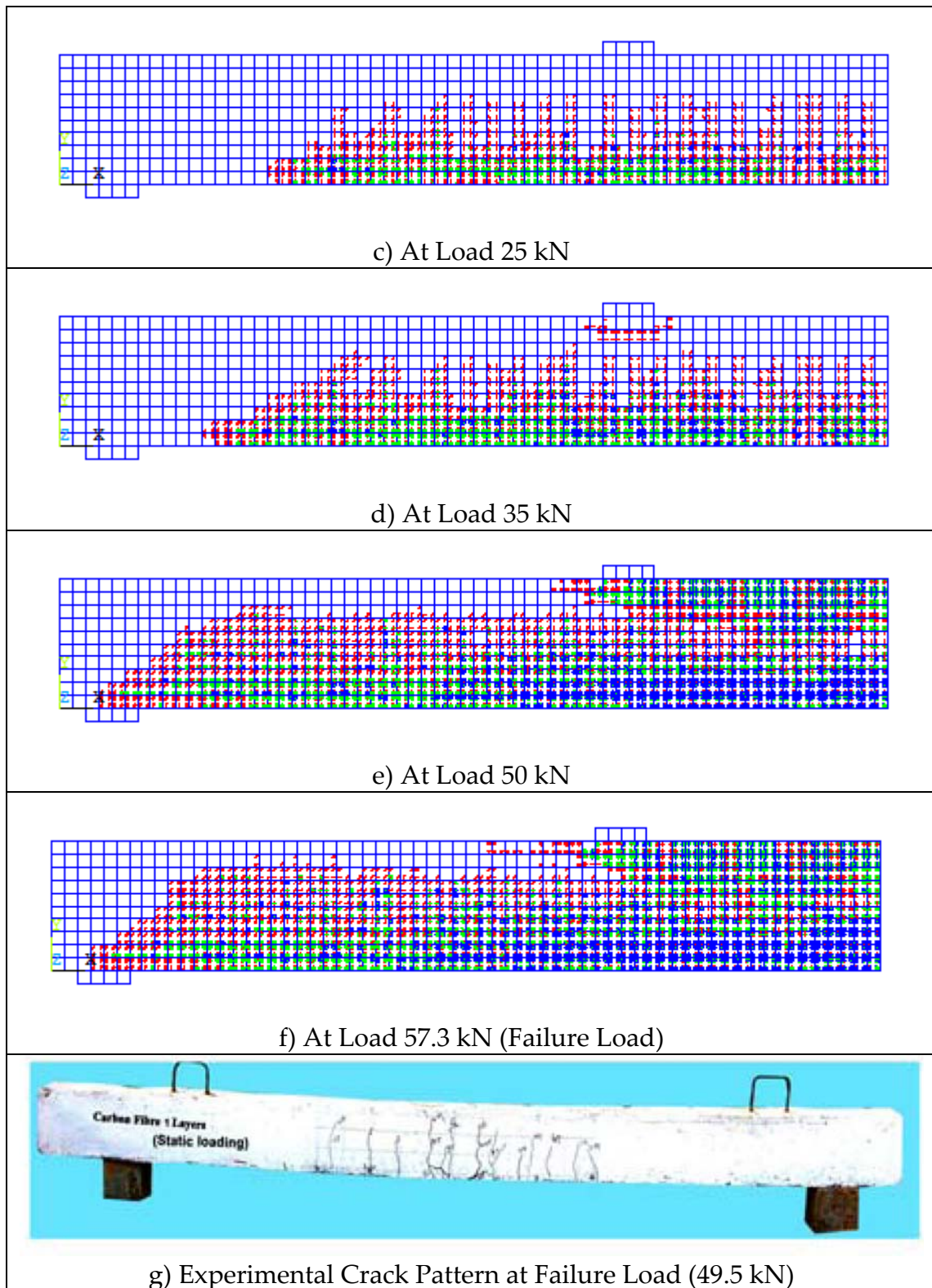


Fig. (5-13): Cracks Propagation – Flexure Strengthened Beam.

Comparing crack pattern obtained from the finite element analysis (ANSYS) at the last converged load step (Fig.5-13/f) with failure photographs from the actual beam (Fig.5-13/g), shows that the crack pattern from ANSYS and the actual beam agree very well. The flexure strengthened beam failed in flexure at

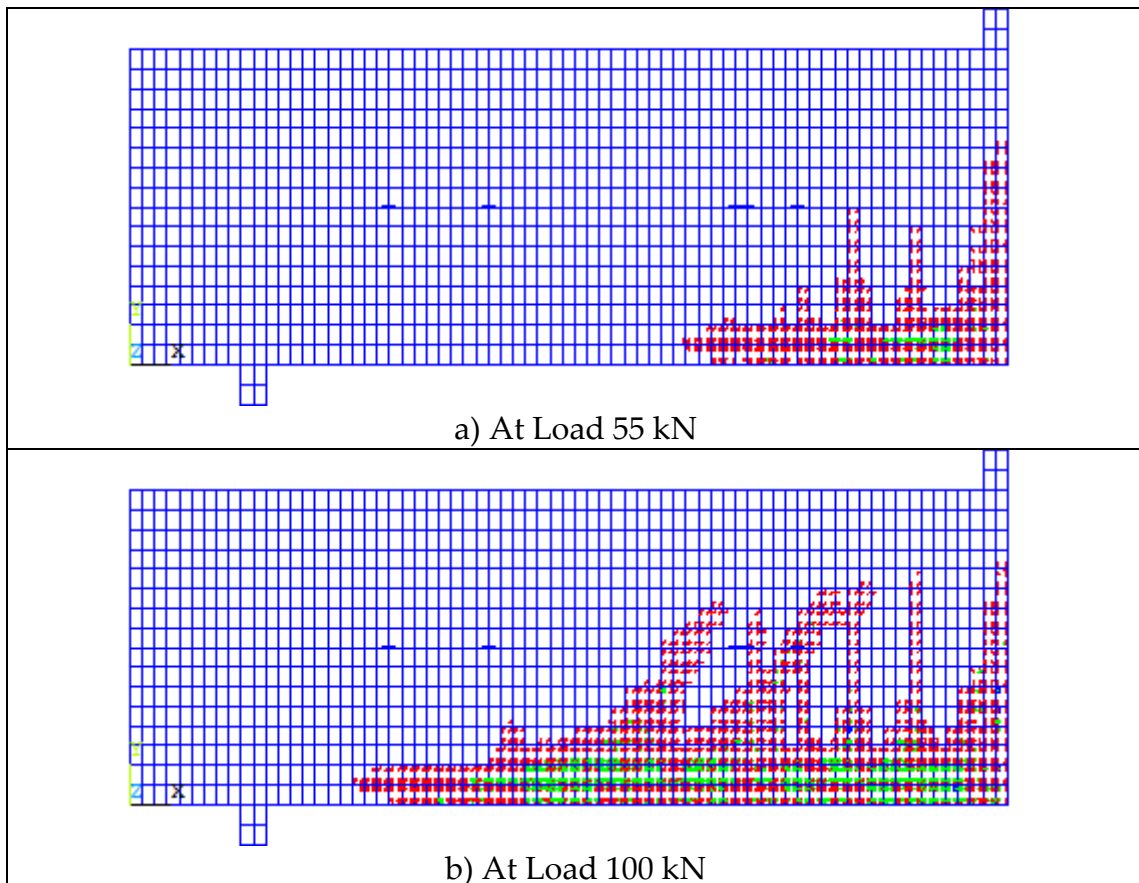
the mid-span, with yielding of the steel reinforcement, followed with a compression failure at the top of the beam.

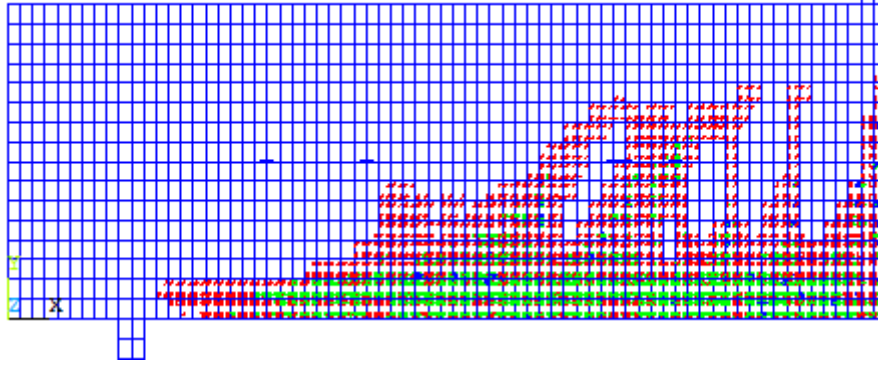
5.2.3.2 Crack Patterns for Shear Beam

The propagation of cracks at different load steps for shear control and strengthened beams is shown in the figures (5-14) and (5-15). Flexural cracks occur early at mid-span. When applied loads increase, vertical flexural cracks spread horizontally from the mid-span to the support. At a higher applied load, diagonal tensile cracks appear. Increasing applied loads induces additional diagonal and flexural cracks. Finally, compressive cracks appear at nearly the last applied load steps. The appearance of the cracks defines the failure mode for the beams.

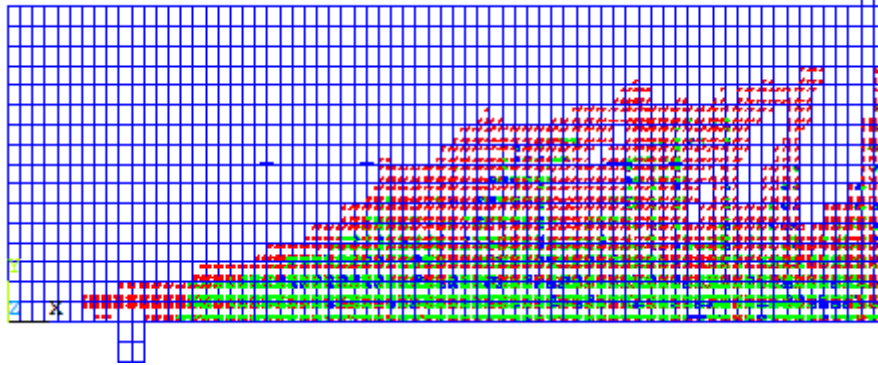
a- Shear Control Beam

The propagation of cracks at different load steps for shear control beam is shown figure (5-14) (a), (b), (c), (d), (e), (f), (g) and (h).

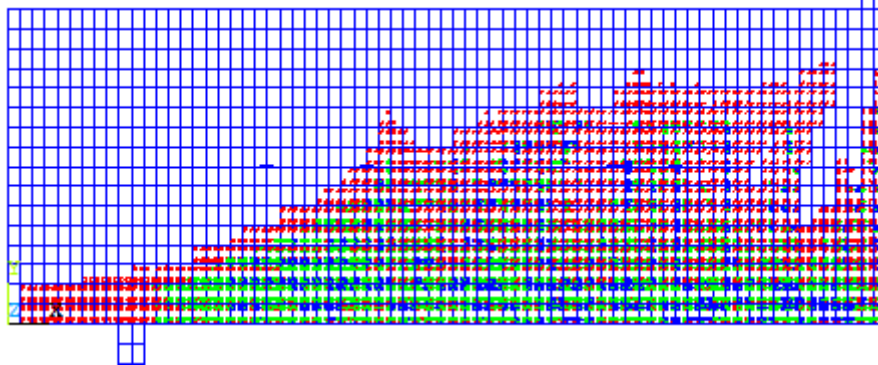




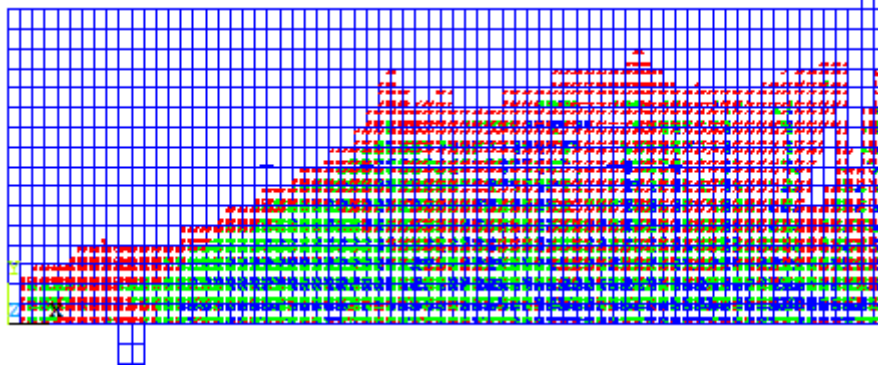
c) At Load 150 kN



d) At Load 200 kN



e) At Load 250 kN



f) At Load 300 kN

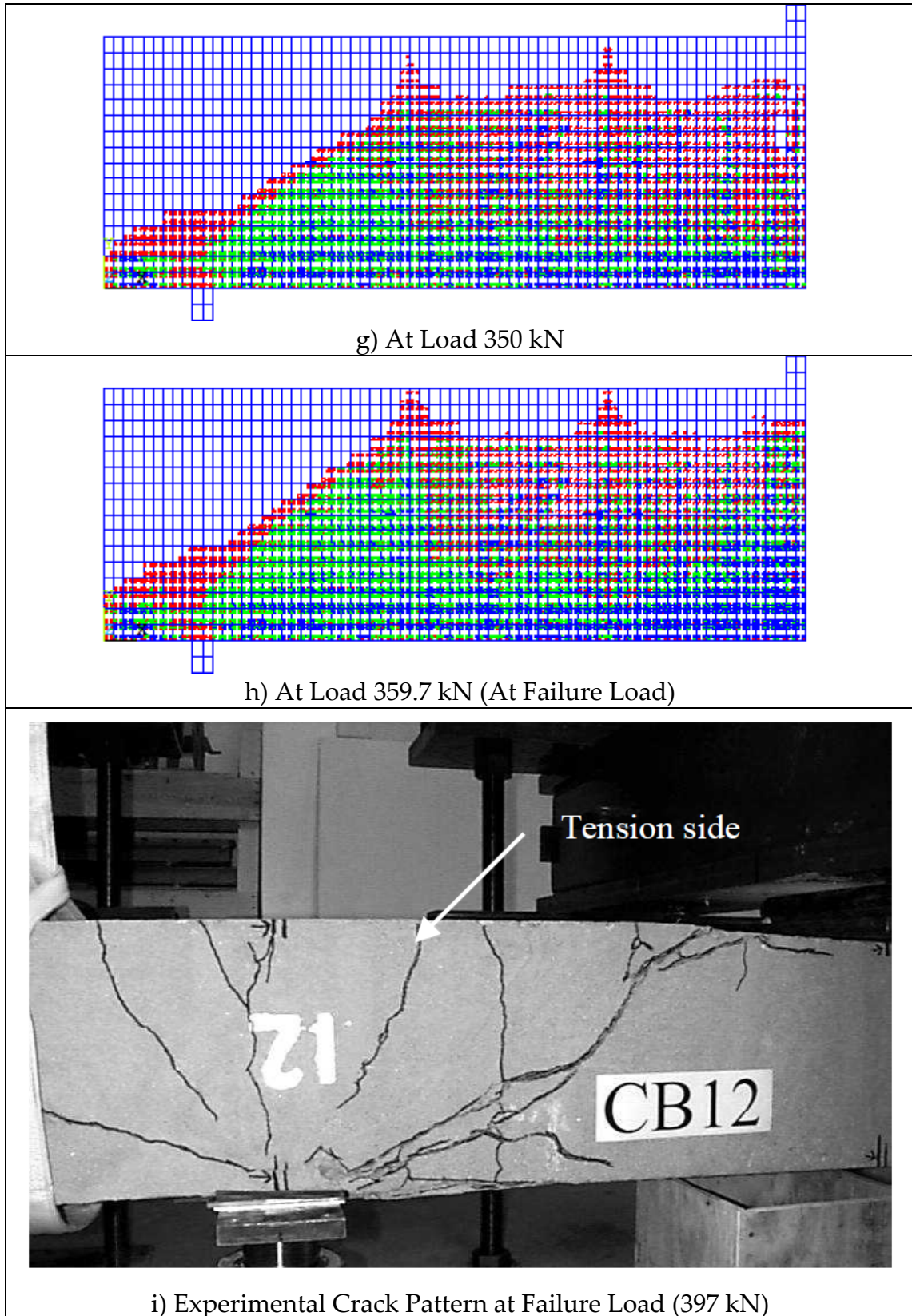


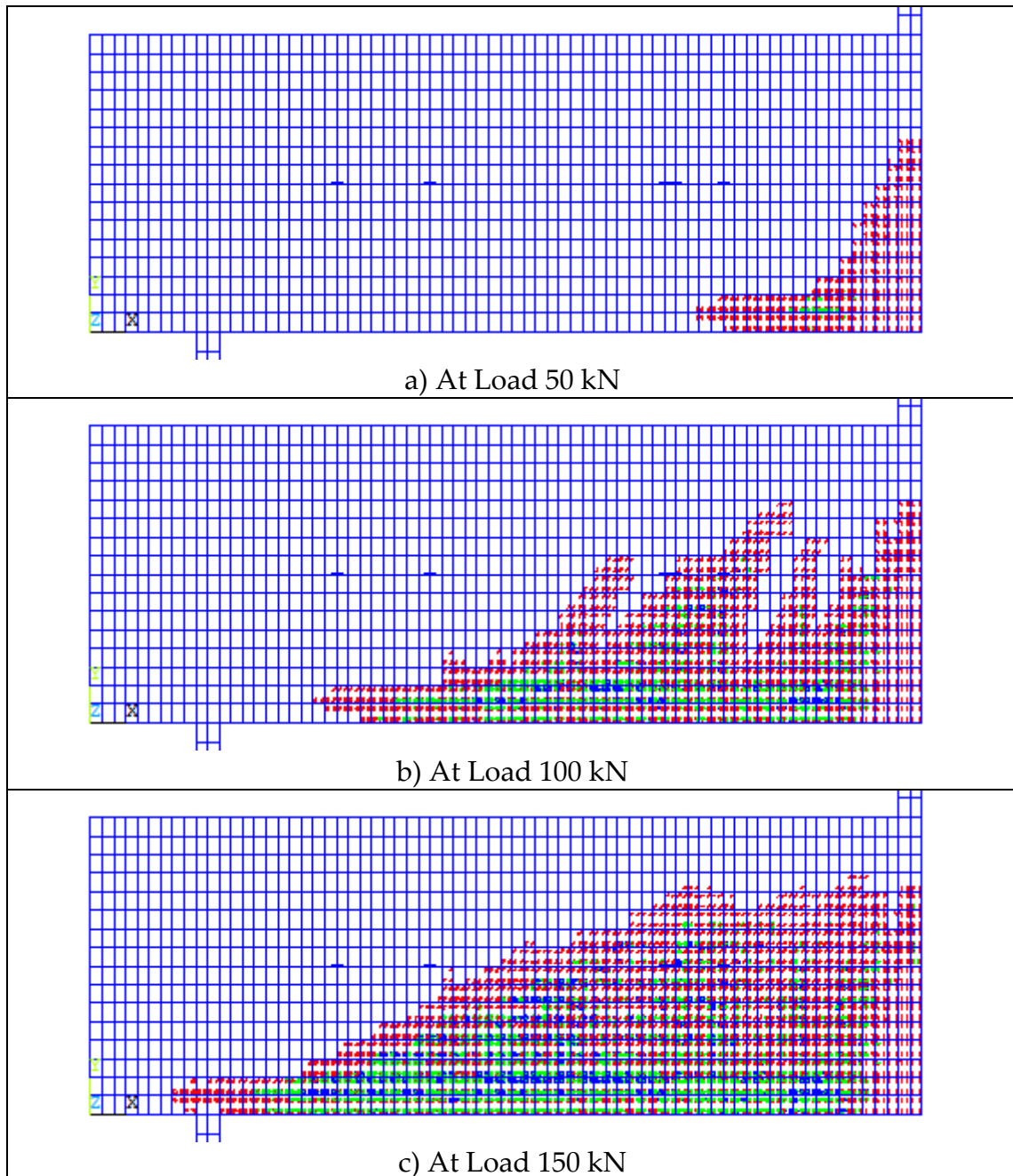
Fig. (5-14): Cracks Propagation- Shear Control Beam.

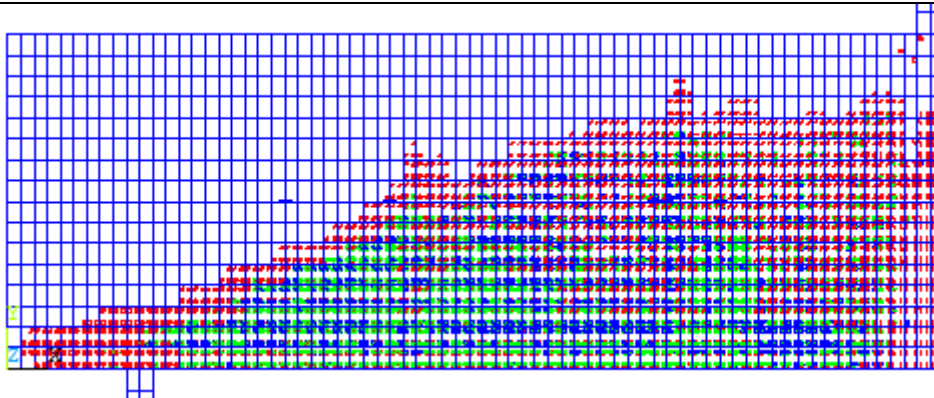
Comparing crack pattern obtained from the finite element analysis (ANSYS) at the last converged load step (Fig.5-14/h) with failure photographs from the actual beam (Fig.5-14/i), shows that the crack pattern from ANSYS and the

actual beam agree very well. The shear control beam failed in shear. Diagonal tensile cracks propagate from the loading area toward the support. The cracks occur excessively in the high shear stress region.

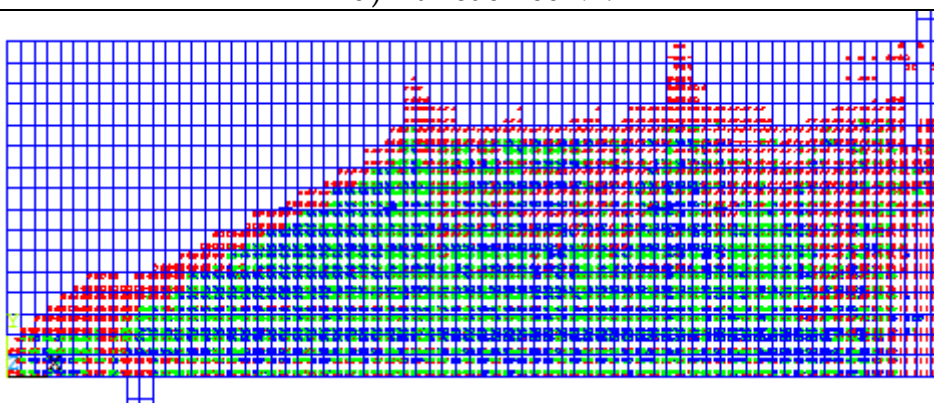
b- Shear Strengthened Beam

The propagation of cracks at different load steps for shear strengthened beam is shown figure (5-15) (a), (b), (c), (d), (e), (f), (g) and (h).

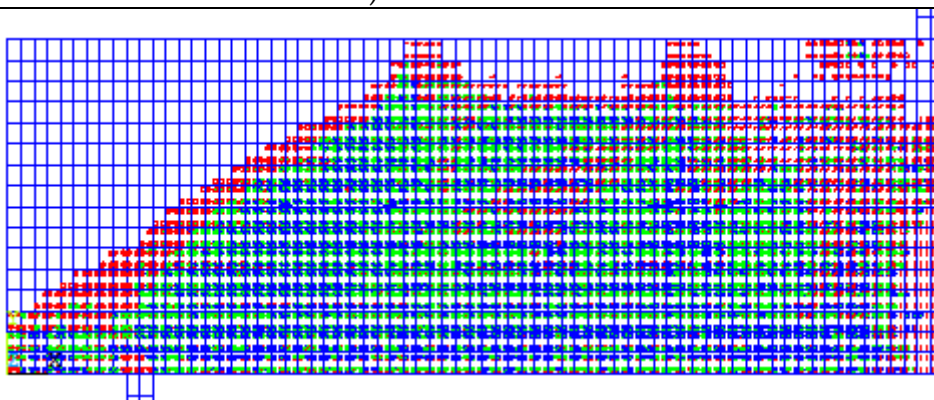




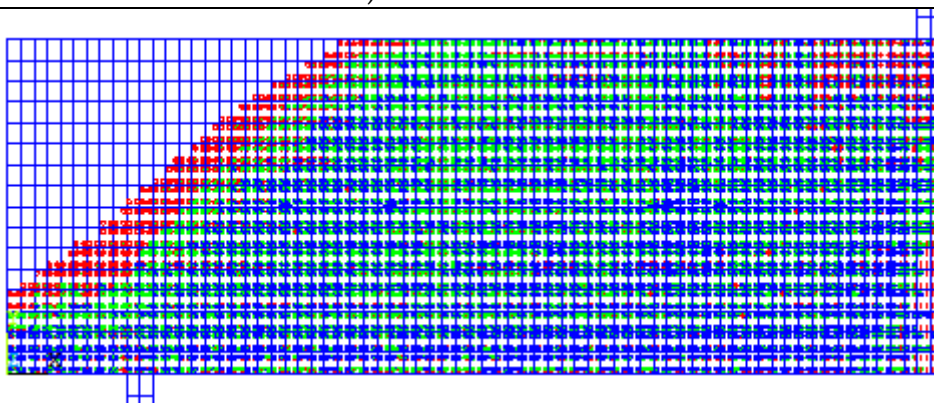
d) At Load 200 kN



e) At Load 250 kN



f) At Load 300 kN



g) At Load 350 kN

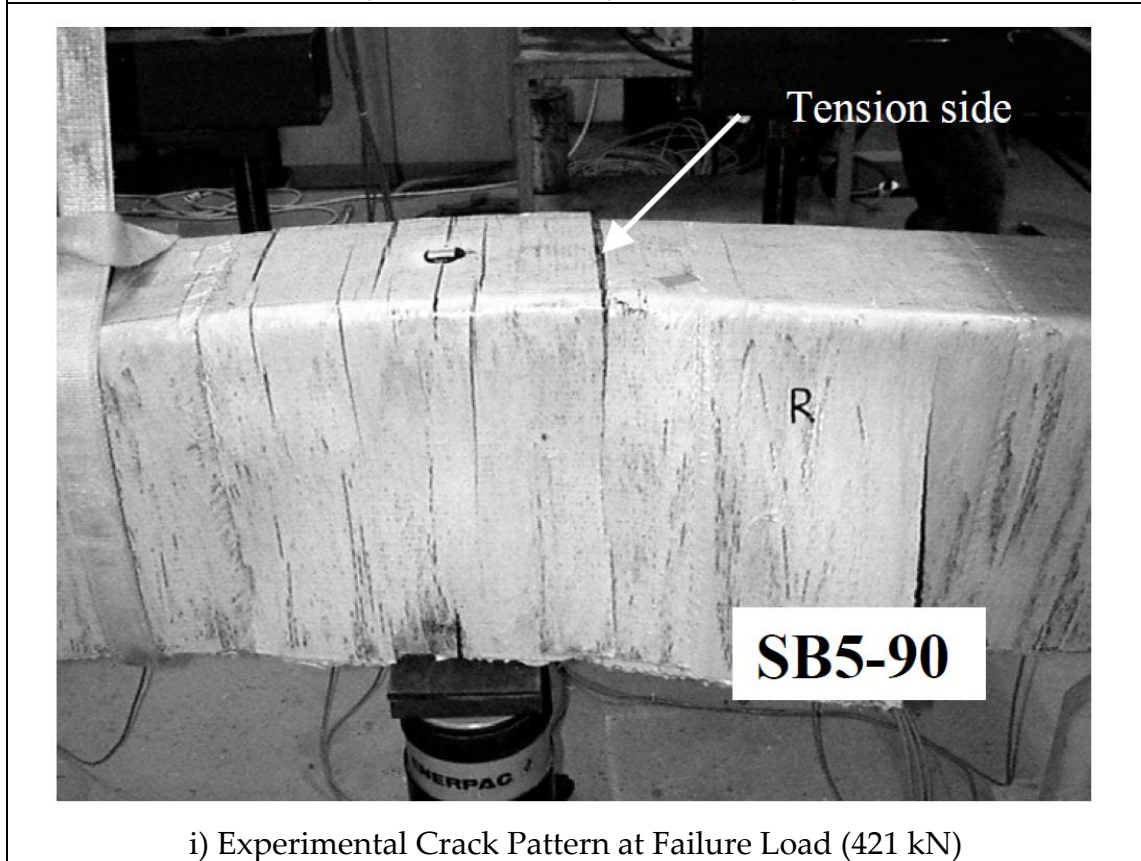
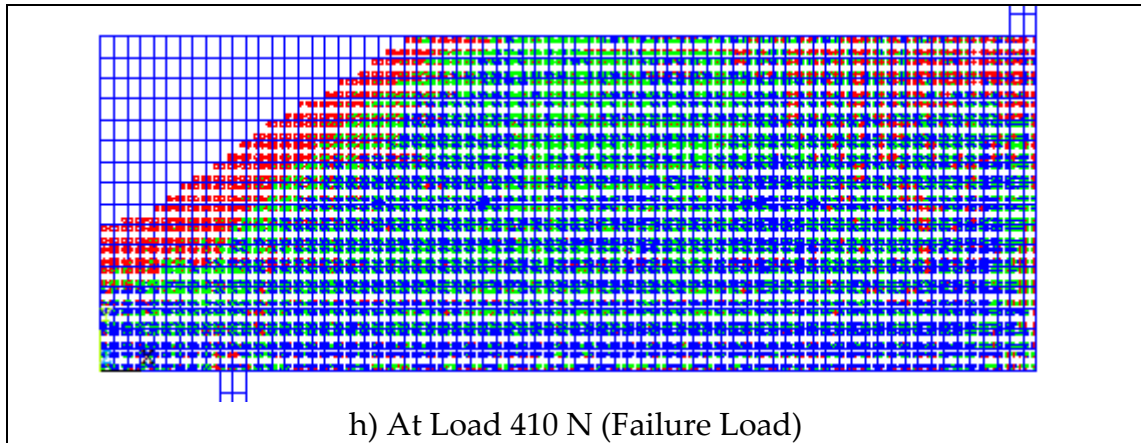


Fig. (5-15): Cracks Propagation – Shear Strengthened Beam.

As reported in the experimental investigation, [Alagusundaramoorthy et al. 2002], shear strengthened beam was failed in a shear-compression failure mode. Rupture and delamination of CFRP fabric was noticed at the final stages. Comparing crack pattern obtained from the finite element analysis (ANSYS) at the last converged load step (Fig.5-15/h) with failure photographs from the actual beam (Fig.5-15/i), shows that the crack pattern from ANSYS and the actual beam agree very well with respect to failure mode. Rupture and delamination of CFRP fabric would not appear in the ANSYS model, since the model was basically built on a perfect bond assumption.

5.2.4 Loads and Deflection at Failure

Table (5-1) shows a comparison between experimental and finite element ultimate loads, and ultimate capacity of the strengthened beams with ultimate capacity of the control beams.

Beam	Failure Load (EXP) kN	Failure Load (ANSYS) kN	Difference (%)	Increased Strength (EXP) (%)	Increased Strength (ANSYS) (%)
Flexure Control Beam	41.25	47.7	15.15	-	-
Flexure Strengthened Beam	49.5	57.3	15.76	20	20.13
Shear Control Beam	397	359.7	- 9.40	-	-
Shear Strengthened Beam	421 (Avg)	410	-2.6	6.05	14

Table (5-1): Comparisons Between Experimental and ANSYS Results – Failure Loads

Table (5-2) shows a comparison between experimental and finite element mid-span deflection at failure.

Beam	Mid-Span Deflection at Failure (EXP) mm	Mid-Span Deflection at Failure (ANSYS) mm	Difference (%)
Flexure Control Beam	21.13	22.10	4.59
Flexure Strengthened Beam	20.13	21.64	7.50
Shear Control Beam	Not Reported	8.1	-
Shear Strengthened Beam	18.25	19.3	5.75

Table (5-2): Comparisons Between Experimental and ANSYS Results – Mid-Span Deflection

Figure (5-16) shows the deflection results obtained from the finite element analysis (ANSYS) for the flexure control beam at failure. Figure (5-17) shows the deflection results obtained from the finite element analysis (ANSYS) for the flexure strengthened beam at failure.

Figure (5-18) shows the deflection results obtained from the finite element analysis (ANSYS) for the shear control beam at failure. Figure (5-19) shows the deflection results obtained from the finite element analysis (ANSYS) for the shear strengthened beam at failure.

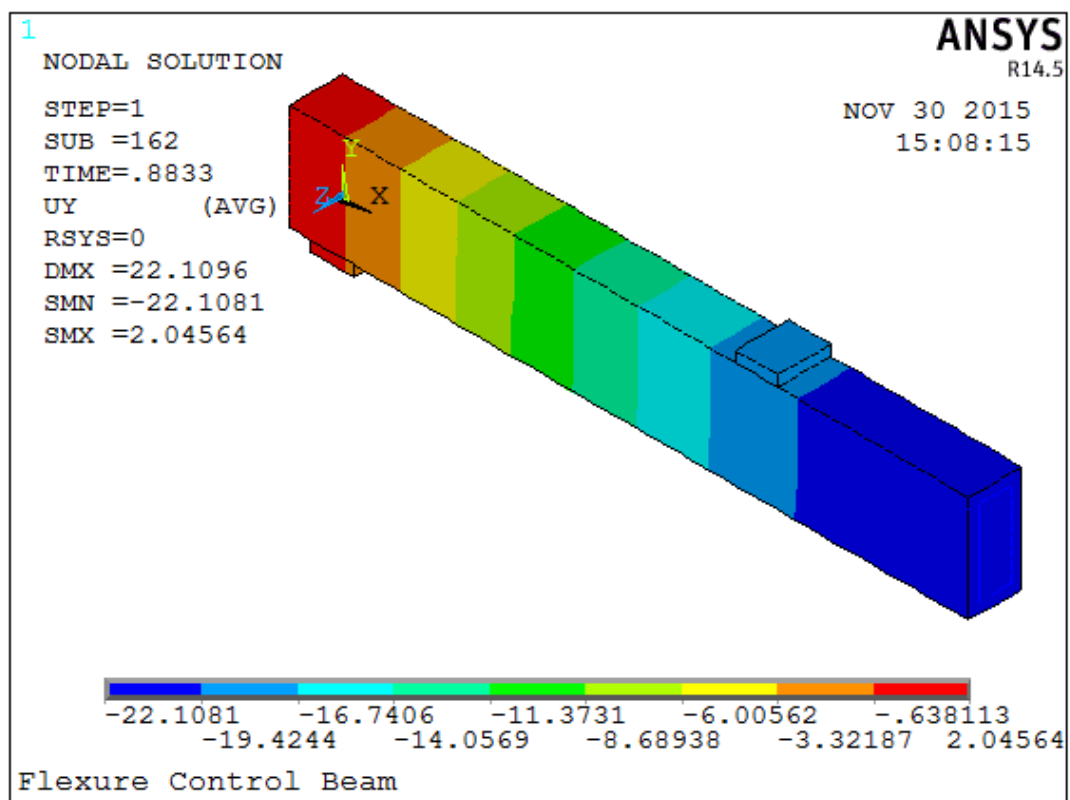


Fig. (5-16): Deflection Contour Results at Failure – Flexure Control Beam.

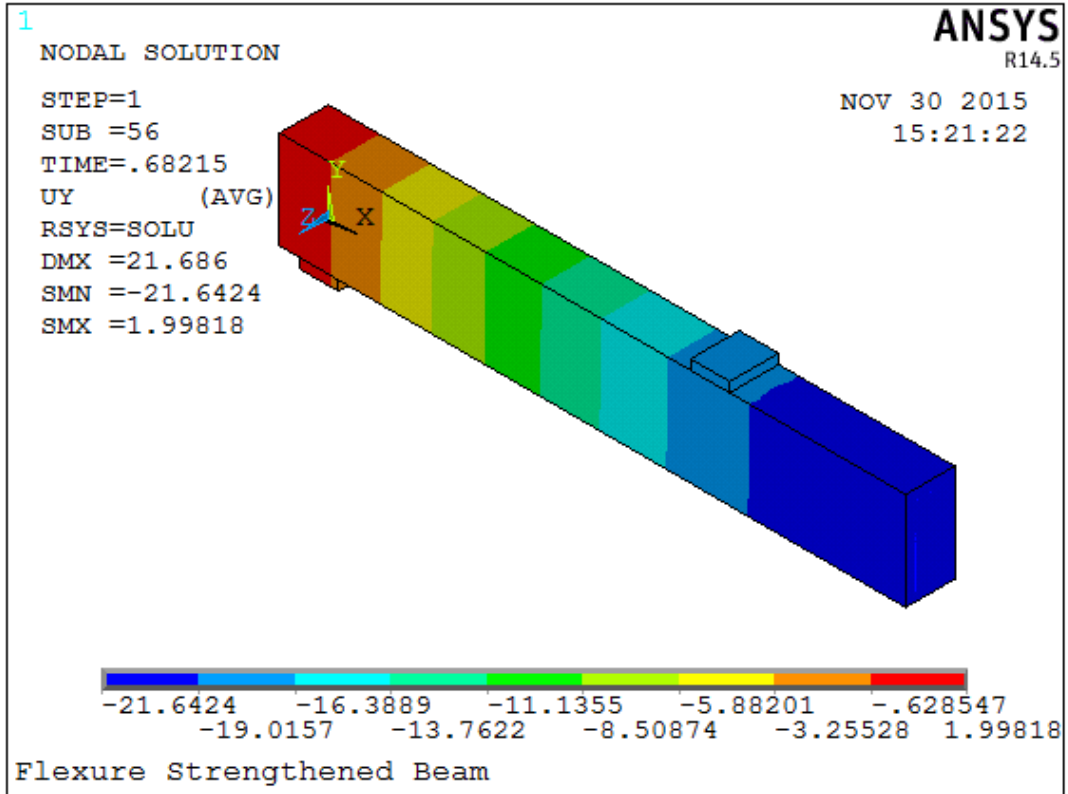


Fig. (5-17): Deflection Contour Results at Failure – Flexure Strengthened Beam.

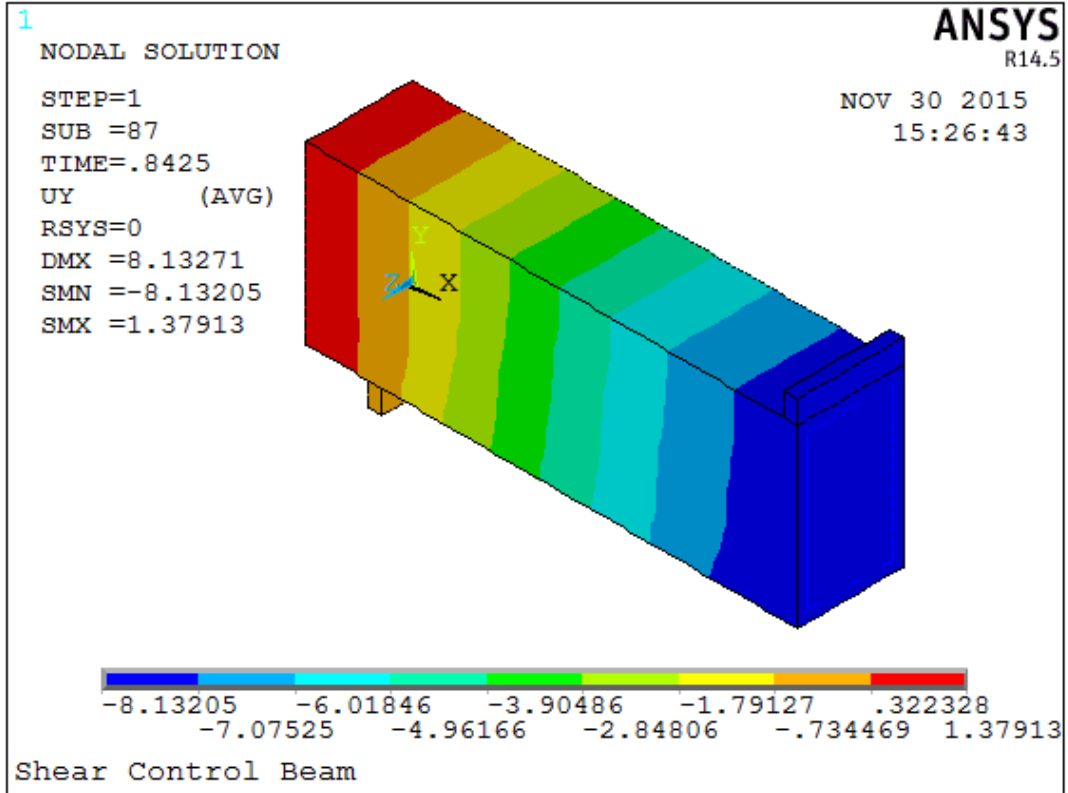


Fig. (5-18): Deflection Contour Results at Failure – Shear Control Beam.

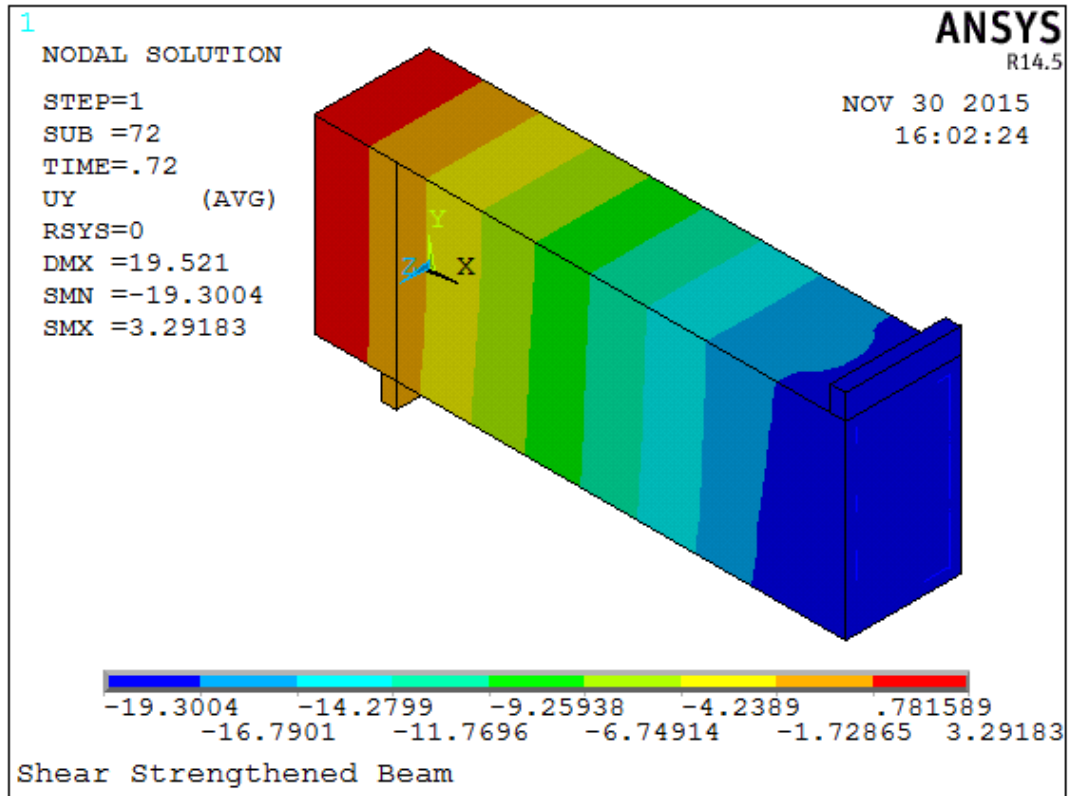


Fig. (5-19): Deflection Contour Results at Failure – Shear Strengthened Beam.

5.2.5 Maximum Stresses in CFRP Fabric

Figure (5-20) shows the tensile stress results of CFRP fabric obtained from the finite element analysis (ANSYS) for the flexure strengthened beam at failure. The maximum tensile stress in the model is 1474.11 N/mm^2 , which is lower than the manufacturer ultimate tensile strength of CFRP fabric which equals to 3500 N/mm^2 .

Figure (5-21) shows the tensile stress results of CFRP fabric obtained from the finite element analysis (ANSYS) for the shear strengthened beam at failure. The maximum tensile stress in the model is 1993.3 N/mm^2 , which is lower than the manufacturer ultimate tensile strength of CFRP fabric which equals to 2722.22 N/mm^2 .

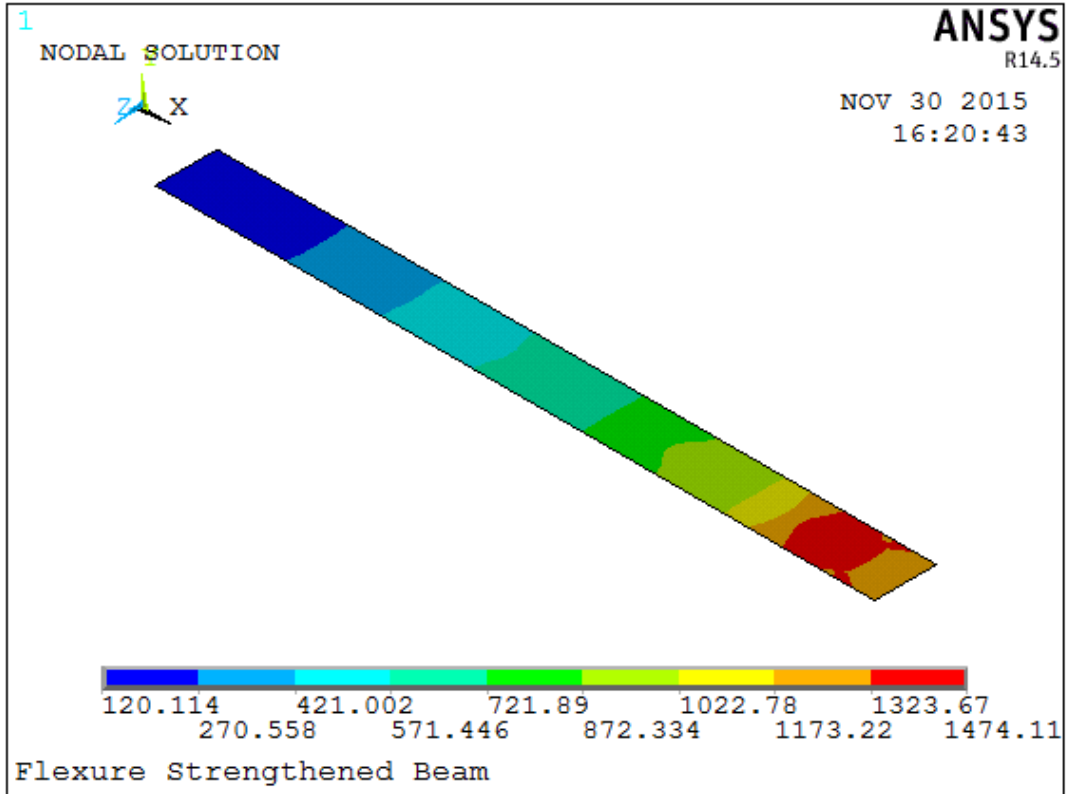


Fig. (5-20): Stress of CFRP Fabric at Failure – Flexure Strengthened Beam

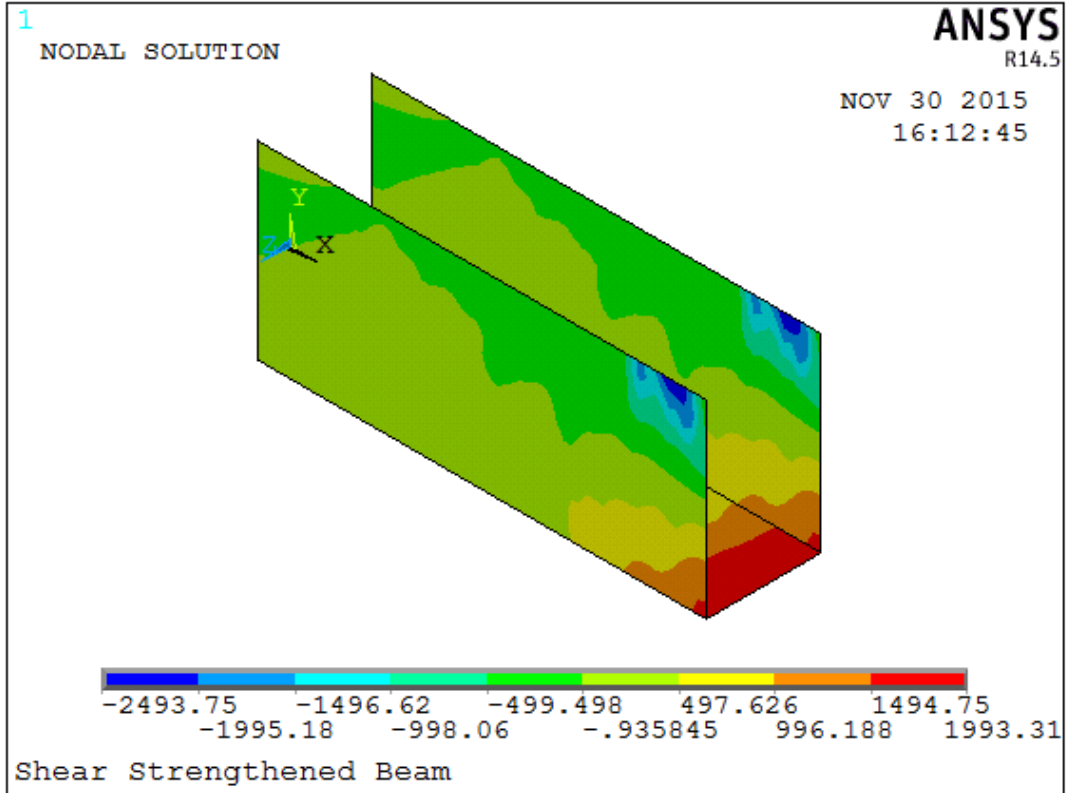


Fig. (5-21): Stress of CFRP Fabric at Failure – Shear Strengthened Beam.

5.2.6 Maximum Strain in CFRP Fabric

Figure (5-22) shows the strain results of CFRP fabric obtained from the finite element analysis (ANSYS) for the flexure strengthened beam at failure. The maximum strain in the model is 0.0051, which is lower than the manufacturer ultimate strain of CFRP fabric 0.015.

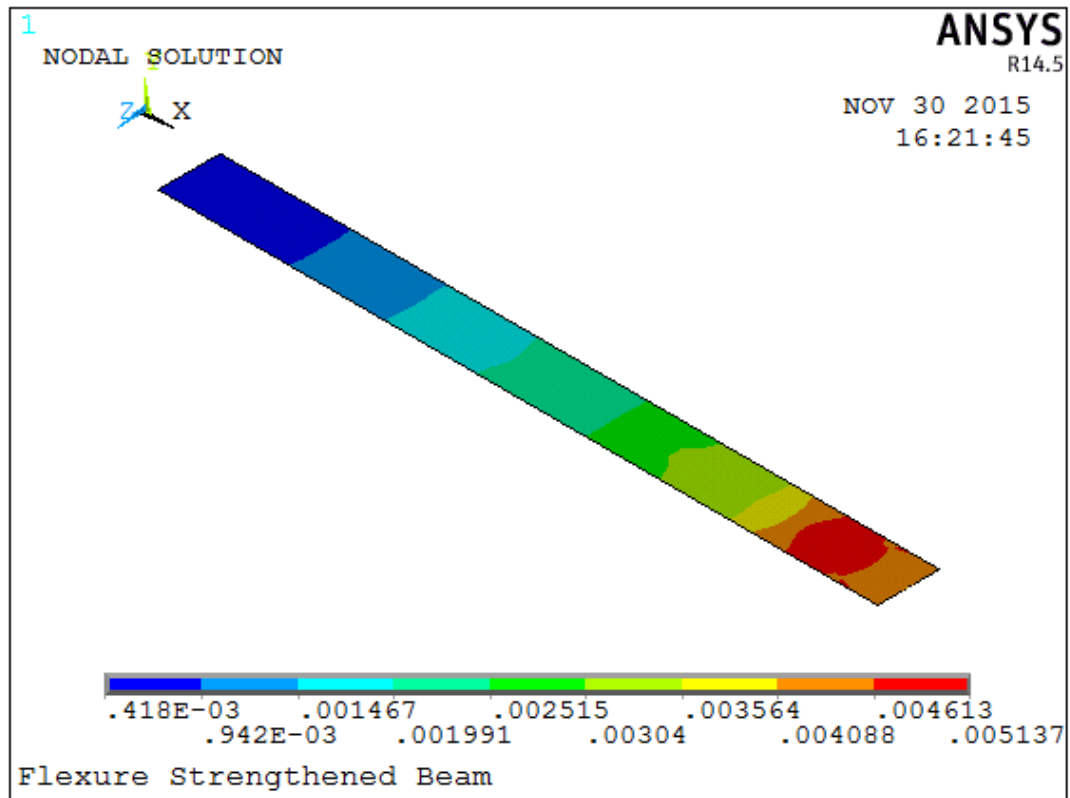


Fig. (5-22): Strain of CFRP Fabric at Failure – Flexure Strengthened Beam.

Figures (5-23) shows the strain results of CFRP fabric obtained from the finite element analysis (ANSYS) for the shear strengthened beam at failure. The maximum strain in the model is 0.0106, which is lower than the manufacturer ultimate strain of CFRP fabric 0.018.

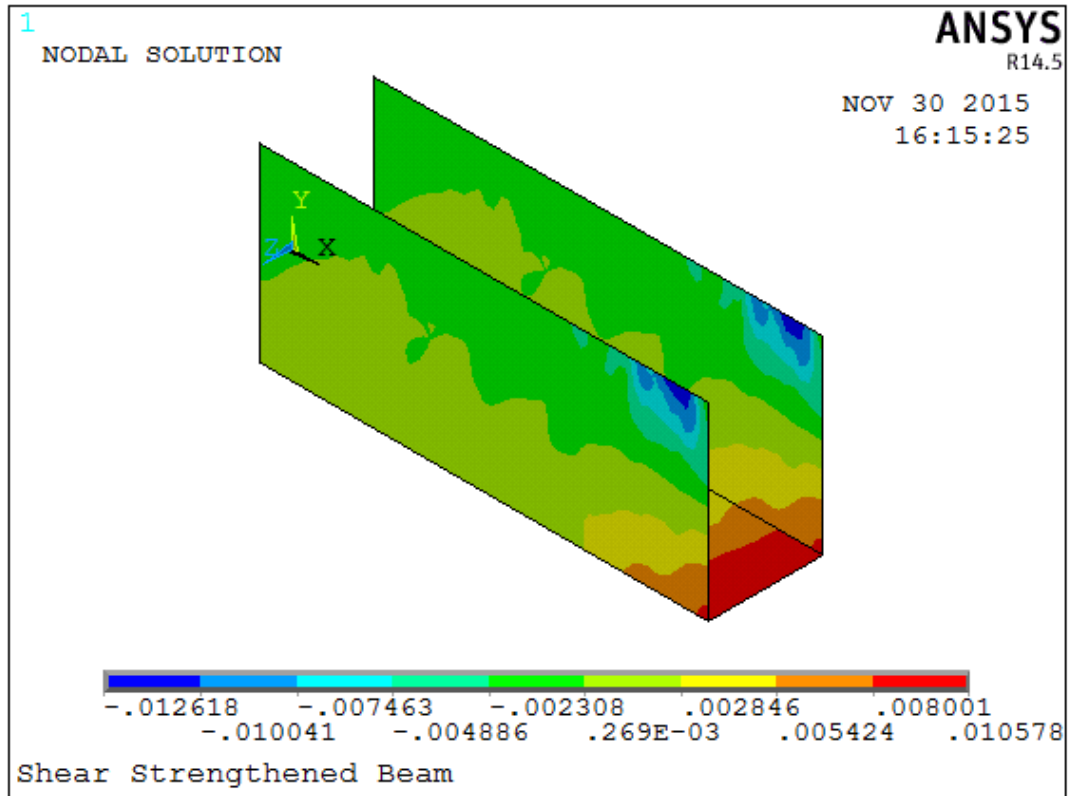


Fig. (5-23): Strain of CFRP Fabric at Failure – Shear Strengthened Beam.

5.3 Parametric Study

5.3.1 Effect of Number of CFRP Layers – Flexure Beam

Figure (5-25) shows a comparison of load-deflection curve as resulted from finite element analysis using ANSYS for the flexure beam, strengthened with different number of CFRP layers (Fig. 5-24). As it is shown in the figure, bonding of additional layers of CFRP to the beam soffit increases stiffness of the beam, increases its ultimate capacity, and decreases mid-span deflection at failure.

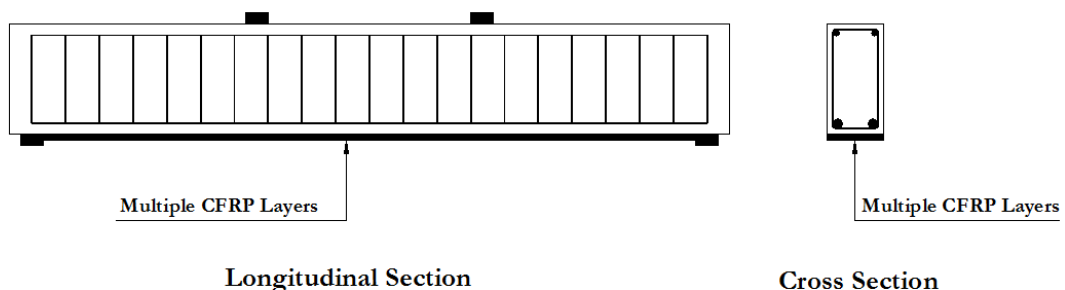


Fig. (5-24): Bonding Multiple CFRP Layers to the Flexure Beam

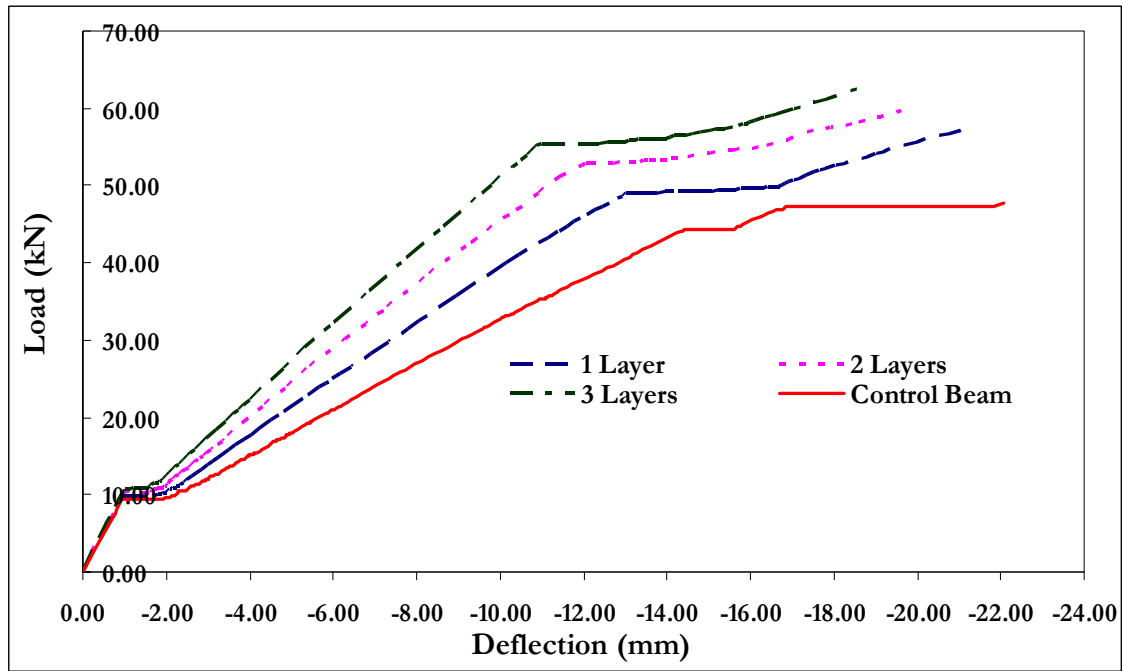


Fig. (5-25): Effect of Increasing Number of CFRP Layers Bonded to the Flexure Beam– Load Deflection Curves.

Table (5-3) shows a comparison of the effect of additional CFRP layers on the beam ultimate load and mid-span deflection as resulted from FE analysis using ANSYS.

Beam	Failure Load (kN)	Increased Strength (%)	Mid-Span Deflection at Failure (mm)	Decreased Deflection at Failure (%)
Control Beam	47.7	-	22.08	-
Strengthened Beam (One Layer)	57.3	20.1	21.17	4.12
Strengthened Beam (Two Layers)	59.8	25.4	19.64	11.1
Strengthened Beam (Three layers)	63	32.1	18.83	14.7

Table (5-3): Effect of Increasing Number of CFRP Layers – Comparison of ANSYS Results

5.3.2 Effect of CFRP Length – Flexure Beam

Figure (5-26) shows a comparison of load-deflection curve as resulted from finite element analysis using ANSYS for the flexure beam, strengthened with different lengths of CFRP layer. As it is shown in the figure, and knowing that (L) is half of the length of the CFRP layer - as tested in the experimental investigation- representing the distance between the beam end support and the center line of the beam (due to using symmetry in modeling, Fig. (5-27); decreasing the length of the CFRP layer bonded to the flexure beam soffit decreases the ultimate load of the beam, with a slight increase in mid-span deflection of the beam at failure.

The figure shows load-deflection curves for the flexure beam strengthened with four different lengths of CFRP layer; full length, 80% of full length, 70% of full length, and 50% of full length. Comparing with Control Beam; the FE analysis result shows that the length of CFRP fabric when reach 50% of span length, the increase of ultimate strength of the beam becomes worthless.

Table (5-4) shows the effect of CFRP layer length on the beam ultimate load, as resulted from FE analysis using ANSYS.

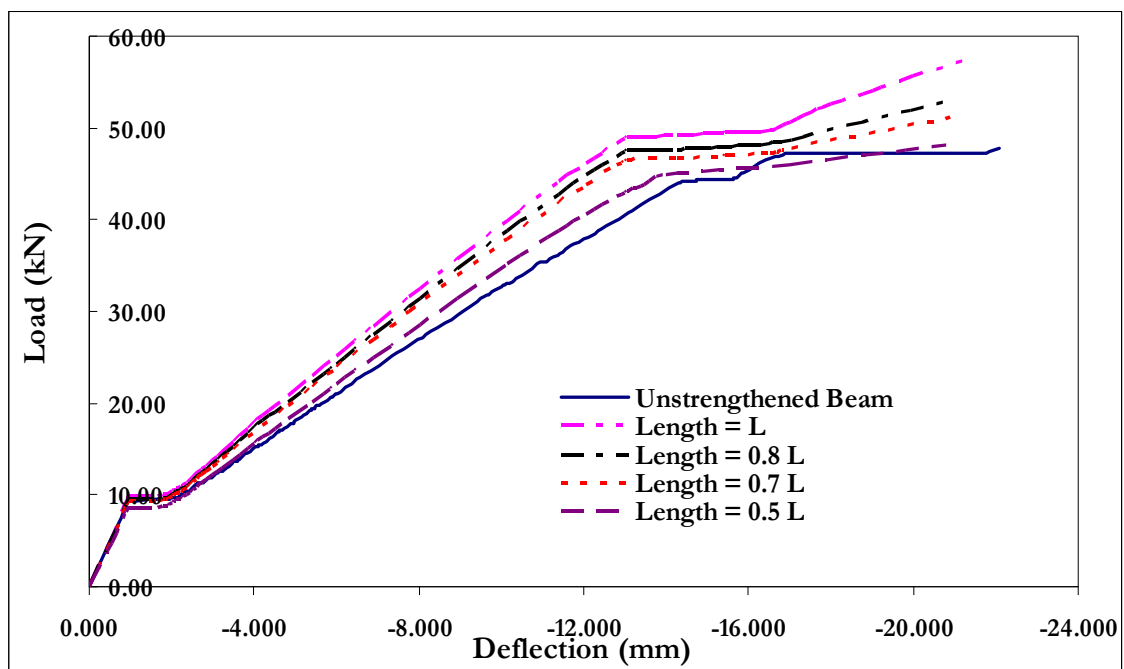


Fig. (5-26): Effect of Changing Length of CFRP Layer – Load Deflection Curves.

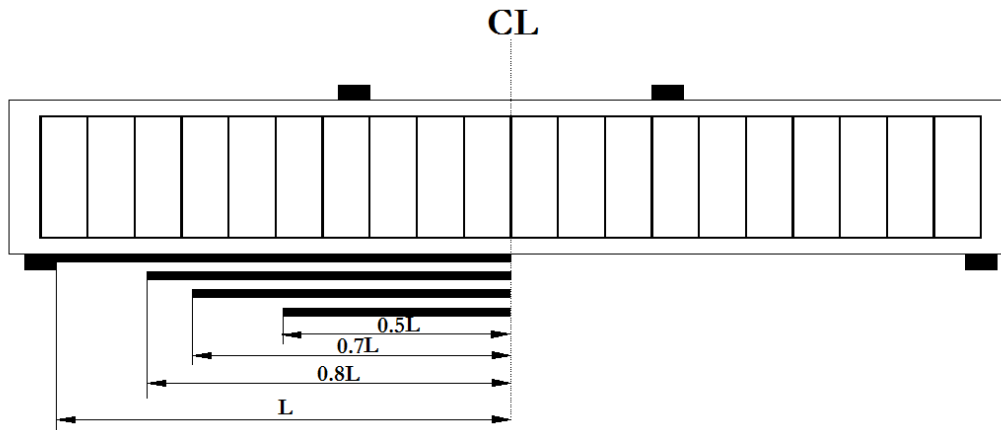


Fig. (5-27): Decreasing length of CFRP Layer Bonded to Flexure Beam

Beam	Failure Load (kN)	Increased Strength (%)
Control Beam	47.7	-
Strengthened Beam (CFRP length = L)	57.3	20.1
Strengthened Beam (CFRP length = 0.8 L)	53.1	11.3
Strengthened Beam (CFRP length = 0.7 L)	51.2	7.3
Strengthened Beam (CFRP length = 0.5 L)	48.1	0.8

Table (5-4): Effect of CFRP Length – Comparison of ANSYS Results

5.3.3 Effect of CFRP Inclination – Shear Beam

To evaluate the effect of CFRP orientation with the longitudinal axis of the beam on the shear strength of the beam, four different strengthening configurations were tested using ANSYS, these configuration are shown in figures (5-28) to (5-31):

- 1- Strengthened beam with one layer of U-wrap CFRP fabric, inclined at an angle of 90° to the longitudinal axis of the beam, Fig. (5-28).

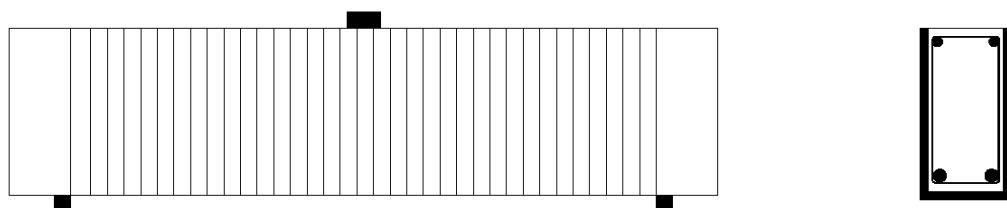


Fig. (5-28): Effect of CFRP Inclination – First Configuration

- 2- Strengthened beam with one layer of U-wrap CFRP fabric inclined at an angle of 90° with an additional layer of CFRP fabric on both sides of the web inclined at an angle of 0° , Fig. (5-29).

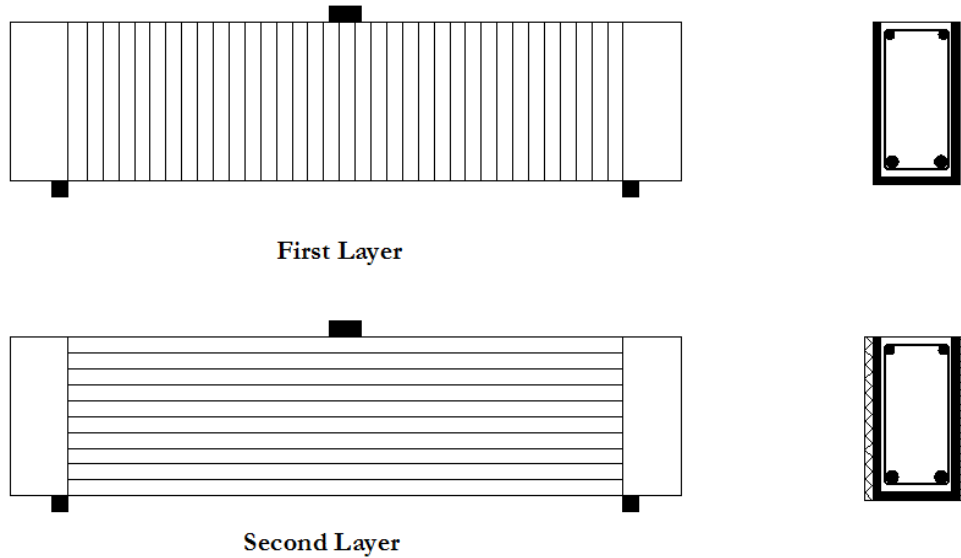


Fig. (5-29): Effect of CFRP Inclination – Second Configuration

- 3- Strengthened beam with one layer of U-wrap CFRP fabric, inclined at an angle of 45° to the longitudinal axis of the beam, Fig. (5-30).

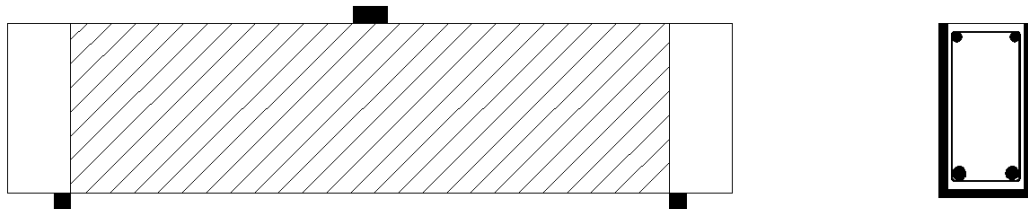


Fig. (5-30): Effect of CFRP Inclination – Third Configuration

- 4- Strengthened beam with one layer of U-wrap CFRP fabric inclined at an angle of 45° with an additional layer of CFRP fabric on both sides of the web inclined at an angle of 0° , Fig. (5-31).

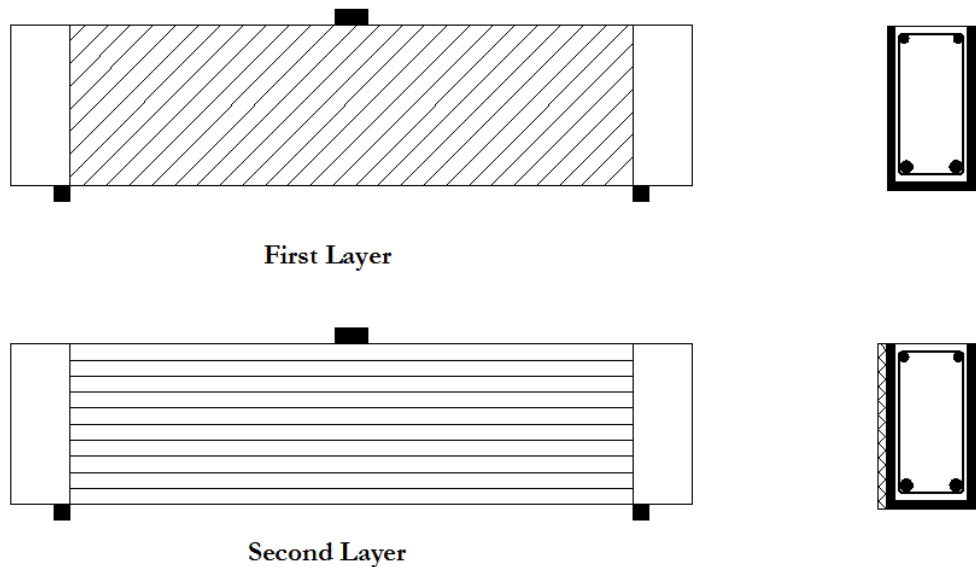


Fig. (5-31): Effect of CFRP Inclination – Fourth Configuration

Figure (5-32) shows a comparison of load-deflection curves as resulted from finite element analysis using ANSYS for previous strengthening configurations. Table (5-5) shows the ultimate load and mid-span deflection for each strengthening configuration, as resulted from FE analysis using ANSYS:

As it is shown in Fig.(5-32) and Table (5-5), strengthening the control beam with one U-wrap CFRP layer inclined at an angle of 90° with the beam axis (1st configuration) increases the beam ultimate load by 14% and increases the mid-span deflection at failure by 138.3%. While, strengthening the control beam with one U-wrap CFRP layer inclined at an angle of 45° with the beam axis (3rd configuration) increases the beam ultimate load by 11.5% and increases the mid-span deflection at failure by 38.3%

This indicates that the beam with 90° U-wrap CFRP layer (1st configuration) is more ductile than beam with 45° U-wrap CFRP layer (3rd configuration), and gives sufficient warning before failure, and that the beam has a higher load capacity with this configuration. So, shear strengthening of RC beams with one layer of CFRP fabric inclined at an angle of 90° with the beam axis is more efficient than strengthening the beam with one layer of CFRP fabric inclined at an angle of 45° .

Further, strengthening the control beam with one layer of U-wrap CFRP fabric inclined at an angle of 90° with an additional layer of CFRP fabric on both sides of the web inclined at an angle of 0° (2nd configuration) increases the beam ultimate load by 25.5% and increases the beam mid-span deflection by 65.4%. While strengthening the control beam with one layer of U-wrap CFRP fabric inclined at an angle of 45° with an additional layer of CFRP fabric on both sides of the web inclined at an angle of 0° (4th configuration) increases the beam ultimate load by 46.3 % and increases the beam mid-span deflection by 34.6%.

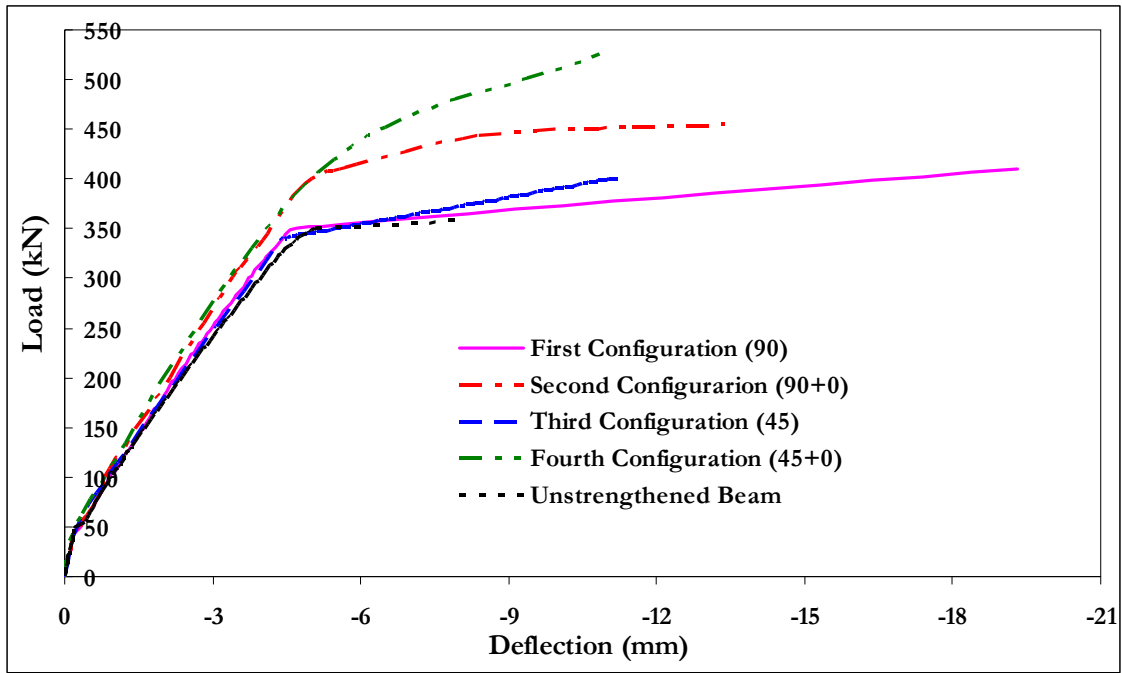


Fig. (5-32): Effect of CFRP Inclination – Load Deflection Curves.

Beam	Failure Load (kN)	Increased Strength (%)	Mid-Span Deflection at Failure (mm)	Increased Deflection at Failure (%)
Control Beam	359.7	-	8.1	-
1 st Configuration (90)	410	14	19.3	138.3
3 rd Configuration (45)	401.2	11.5	11.2	38.3
2 nd Configuration (90+0)	455	25.5	13.4	65.4
4 th Configuration (45+0)	526.3	46.3	10.9	34.6

Table (5-5): Effect of CFRP Inclination – Comparison of ANSYS Results.

This indicates that strengthening the control beam with one layer of U-wrap CFRP fabric inclined at an angle of 45° with an additional layer of CFRP fabric on both sides of the web inclined at an angle of 0° (4th configuration) is more efficient - in terms of load capacity - than strengthening the beam with one layer of U-wrap CFRP fabric inclined at an angle of 90° with an additional layer of CFRP fabric on both sides of the web inclined at an angle of 0° (2nd configuration).

CHAPTER 6

CONCLUSIONS AND RECOMMENDATIONS

6.1 Introduction

The aim of this research is to develop nonlinear finite element models of reinforced concrete beams externally strengthened with carbon fiber reinforced polymers (CFRP) using the commercial Finite Element Modeling software (ANSYS); in order to investigate the effect of different parameters on the behavior of these beams. In this section, the important conclusions drawn from this study and research recommendations are presented.

6.2 Conclusions

The important conclusions drawn from the study are listed below:

1. Finite element models using ANSYS were successfully verified comparing with previously published experimental test results. Therefore, ANSYS can be confidently used in analysis of RC Beams externally strengthened with Carbon Fiber Reinforced Polymers (CFRP) fabrics.
2. The ultimate load carrying capacity of all the strengthened RC beams in flexure and shear are higher when compared to the control (unstrengthened) beams.
3. The general behavior of the finite element models represented by the load-deflection curves at mid-span shows good agreement with the test data from the full-scale beam tests. However, the finite element models show slightly more or less stiffness than the test data. The effects of bond slip between the concrete and steel reinforcing and microcracks occurring in the actual beams were excluded in the finite element models, contributing to the difference in stiffness of the finite element models.
4. The final loads from the finite element analyses are higher than the ultimate loads from the experimental results of flexure beam by 15 %, and lower than the ultimate loads of shear beam by 2.6%- 9.4%. This is probably due to using assumed materials properties values instead of measured values.

5. Strengthening the RC beam by bonding a single layer of CFRP to the tension face of the beam increases the flexural strength of the beam by 20%, and reduces the mid-span deflection at failure slightly by 4%.
6. Increasing number of CFRP layers bonded to the beam soffit increases the stiffness of the beam, increases its ultimate capacity, and decreases mid-span deflection at failure.
7. Strengthening the RC beam by bonding two layers of CFRP to the tension face of the beam increases the flexural strength of the beam by 25%, and reduces the mid-span deflection at failure slightly by 11%.
8. Strengthening the RC beam by bonding three layers of CFRP fabric to the tension face of the beam increases the flexural strength of the beam by 32%, and reduces the mid-span deflection at failure slightly by 15%.
9. Decreasing the length of the CFRP layer bonded to the flexure beam soffit decreases the ultimate load of the beam, with a slight decreasing in mid-span deflection of the beam at failure. Length of CFRP fabric when reaches 50% of beam span length, the increase of ultimate strength of the beam becomes worthless.
10. Strengthening the RC beam by bonding a single layer of U-wrap CFRP fabric, inclined at an angle of 90° to the longitudinal axis of the beam increases the shear strength of the beam by 14 %, and increases the mid-span deflection at failure by 138 %.
11. Strengthening the RC beam by bonding a single layer of U-wrap CFRP fabric, inclined at an angle of 45° to the longitudinal axis of the beam increases the shear strength of the beam by 11.5 %, and increases the mid-span deflection at failure by 38 %.
12. Shear strengthening of beams with one layer of CFRP fabric inclined at an angle of 90° to the beam axis is more efficient than strengthening with one layer of CFRP fabric inclined at an angle of 45° .
13. Strengthening the shear control beam with one layer of U-wrap CFRP fabric inclined at an angle of 90° with an additional layer of CFRP fabric on both sides of the web inclined at an angle of 0° increases the shear strength of the beam by 25.5% and increases the beam mid-span deflection by 65 %.

14. Strengthening the control beam with one layer of U-wrap CFRP fabric inclined at an angle of 45° with an additional layer of CFRP fabric on both sides of the web inclined at an angle of 0° increases the shear strength of the beam by 46.3% and increases the beam mid-span deflection by 34.6%.
15. Strengthening the control beam with one layer of U-wrap CFRP fabric inclined at an angle of 45° with an additional layer of CFRP fabric on both sides of the web inclined at an angle of 0° is more efficient than strengthening with one layer of U-wrap CFRP fabric inclined at an angle of 90° with an additional layer of CFRP fabric on both sides of the web inclined at an angle of 0° .

6.3 Recommendations

1. In this study, the commercial Finite Element analysis software (ANSYS) was used in the analysis process. Comparative studies using other available Finite Element softwares can be conducted to investigate which one can give more precise results comparing with experimental investigations.
2. In this study, the external strengthening of RC beam with CFRP was investigated. Strengthening with other available Fiber Reinforced Polymer (FRP) materials like Glass Fiber Reinforced Polymer (GFRP) can be studied to investigate the efficiency of the strengthening technique using different materials with different properties.
3. In this study, the bond between concrete and CFRP fabric was assumed to be perfect. Although this assumption did not cause a significant error in the obtained results comparing with experimental investigations; the behavior of the concrete-CFRP bond and de-bonding issues can be studied analytically to get more precise results especially regarding failure modes.
4. In this study, the influence of some parameters on the overall response of the strengthened RC beams has been investigated. These parameters are: effect of number of CFRP layers, effect of CFRP length, and effect of CFRP inclination. Effect of other parameters as beam stiffness, beam geometry, CFRP stiffness, and CFRP width on the behavior of the strengthened RC beams can be also studied.

5. In this study, environmental factors that may affect the efficiency of RC beams strengthened with CFRP as seasonal temperature variation, creep, and shrinkage were not considered. Effect of these parameters during the beam life span can be studied.

REFERENCES

- 1- Alagusundaramoorthy, P., Harik, I.E. and Choo, C.C., (2002), "Shear Strengthening of R/C beams Wrapped with CFRP Fabric", Research report KTC-02-14/SPR 200-99-2F, University of Kentucky, Kentucky Transportation Center.
- 2- Abbas, A., (2010), "Non-linear Analysis of Reinforced Concrete Beams Strengthened with Steel and CFRP Plates", Diyala Journal of Engineering Sciences, pp. 249-256.
- 3- ACI 440R-07 (2007), "Report on Fiber-Reinforced Polymer (FRP) Reinforcement for Concrete Structures".
- 4- Amer, I.; and Wissam, S., (2009), "Finite Element Analysis of Reinforced Concrete Beams Strengthened with CFRP in Flexure", Diyala Journal of Engineering Sciences, Vol.2, No.2, pp.88-104.
- 5- Amer I.; and Mohammed, M., (2009), "Finite Element Modeling of Reinforced Concrete Beams Strengthened with FRP Laminates", European Journal of Scientific Research, Vol.30, No.4, pp.526-541.
- 6- ASTM A615, (1995), "Standard specification for deformed and plain billet steel bars for concrete reinforcing". American society for testing and material, Annual book of ASTM standard.
- 7- ANSYS Mechanical APDL Manual Set, (2012), Release 14.5, ANSYS, Inc., USA, Southpointe.
- 8- Balamuralikrishnan, R.; and Jeyasehar, A., (2009), "Flexural Behavior of RC Beams Strengthened with Carbon Fiber Reinforced Polymer (CFRP) Fabrics", Department of Civil and Structural Engineering, Annamalai University, Annamalainagar, The Open Civil Engineering Journal, Volume 3, 102-109.
- 9- Barbero, E. J., (2014), " The Finite Element Analysis of Composite Materials Using ANSYS", CRC Press, Taylor & Francis Group
- 10- Basappa, U.; and Rajagopal , A., (2013), " Modeling of CFRP Strengthened RCC Beam Using the Nonlinear Finite Element Method" , Department of civil engineering, Indian institute of technology Hyderabad, India, Journal of Structural Engineering, Vol. 40, no. 2, pp. 169-184.

- 11-Camata, G., Spacone, E. and Zarnic, R., (2007), "Experimental and Nonlinear Finite Element Studies of RC beams Strengthened with FRP plates", *Composites: Part B.*, 38: 277- 288.
- 12-Chansawat, K., Potisuk, T., Miller, T.H., Yim, S.C., and Kachlakev, D.I., (2009), "FE Models of GFRP and CFRP Strengthening of Reinforced Concrete Beams".
- 13-Chong, K. T., (2004), "Numerical Modeling of Time-dependent Cracking and Deformation of Reinforced Concrete Structures", Doctoral Thesis, University of New South Wales, Sydney, Australia.
- 14-Concrete Society Committee, Technical Report No.55, (2000), "Design Guidance for Strengthening Concrete Structures Using Fiber Composite Materials".
- 15-Elyasian, I.; Abdoli, N.; Ronagh, H.R., (2006), "Evaluation of Parameters Effective in FRP Shear Strengthening of RC Beams Using FE Method", *Asian Journal of Civil Engineering*, Vol.7, No.3, pp.249-257.
- 16-Fathelbab, F.; Ramadan, M.; Al-Tantawy, A., (2011), " Finite Element Modeling of Strengthened Simple Beams using FRP Techniques: A parametric Study", *Concrete Research (LETTERS)*, Vol.2 (2), pp.228-240.
- 17- FOSROC Constructive Solutions, Product Data.
- 18-Jayajothi, P.; Kumutha, R.; Vijai, K., (2013), "Finite Element Analysis of FRP Strengthened RC Beams Using ANSYS", *Asian Journal of Civil Engineering (BHRC)*, Vol.14, No.4, pp.631-642.
- 19-Hamedani, R.N., and Esfahani, M.S., (2012), " Numerical Evaluation of Structural Behavior of the Simply Supported FRP-RC Beams", Master Thesis, Royal Institute of Technology (KTH), Stockholm, Sweden.
- 20-Hu, H.T., Lin, F.-M., and Jan, Y.Y., (2006), "Nonlinear Finite Element Analysis of Reinforced Concrete Beams Strengthened by Fiber-reinforced Plastics", *Cement and Concrete Composite*, 28: 102-114.
- 21-Isenburg, J., (1993), "Finite Element Analysis of Reinforced Concrete Structures II", ASCE, New York, NY, USA.
- 22- ISIS Educational Module 2, (2006), "An Introduction to FRP Composites for Construction", Canada.

- 23- ISIS Educational Module 4, (2004), "An Introduction to FRP Strengthening of Concrete Structures", Canada.
- 24- ISIS Educational Module 6, (2006), "Application and Handling of FRP Reinforcements for Concrete", Canada.
- 25- Kaufmann, W., (1998), "Strength and Deformations of Structural Concrete Subjected to In-Plane Shear and Normal Forces," PhD Thesis, Swiss Federal Institute of Technology, Zurich, Switzerland
- 26- Kaw, A. K., (2006), "Mechanics of Composite Materials", CRC Press LLC, Boca Raton, Florida.
- 27- Kostovos, M. D., and Pavlovic, M.N., (1995), "Structural Concrete: Finite Element Analysis for Limit-State Design", Thomas Telford Publications, London.
- 28- Lawrence, K. L., (2012), "ANSYS Tutorial, Release 14, Structural and Thermal Analysis Using the ANSYS Mechanical APDL Release 14 Environment", Schroff Development Corporation.
- 29- MacGregoe, J.G., (1997), " Reinforced Concrete: Mechanics and Design", 3rd Edition, Prentice Hall.
- 30- Moaveni, S., (2008), " Finite Element Analysis: Theory and Application with ANSYS", 3rd Edition, Pearson Prentice Hall, USA.
- 31- Nakasone, Y.; Yoshimoto, S.; and Stolarski, T. A., (2006) "Engineering Analysis with ANSYS Software", Elsevier Butterworth-Heinemann, MPG Books Ltd., Bodmin, Cornwall.
- 32- Neale, K., Ebead, U., Abdel Baky, H., Elsayed, W. and Godat, A., (2005), "Modeling of Debonding Phenomena in FRP-Strengthened Concrete Beams and Slabs", Proceedings of the International Symposium on Bond Behavior of FRP in Structures (BBFS).
- 33- Madenci, E.; and Guven, I., (2006) " The Finite Element Method and Applications in Engineering Using ANSYS", Springer Science and Business Media, LLC, USA.
- 34- Piggott M., (2002), "Load Bearing Fiber Composites", 2nd Edition, London: Kluwer Academic Publishers.

- 35- Santhakumar, R.; Chandrasekaran, E.; and Dhanaraj, R., (2004), "Analysis of Retrofitted Reinforced Concrete Shear Beams using Carbon Fiber Composites", *Electronic Journal of Structural Engineering (eJSE)*, Vol.4, pp.66-74.
- 36- Supaviriyakit, T., Pornpongsaroj, P. and Pimanamas, A., (2004), "Finite Element Analysis of FRP Strengthened RC Beam", 26(4): 497-507.
- 37- Vijayakumar, A.; Venkatesh B.; and Jayaprakash, R., (2012), "Analytical Study on Various Types of FRP Beams by using AVSYS", *Engineering Research and Applications (IJERA)*, Vol.2, Issue 5, pp.593-598.
- 38- Willam, K.J., and Warnke, E.P., (1974), "Constitutive Model for Triaxial Behavior of Concrete". *International Association of Bridge and Structural Engineering Conference*, pp 174–204.
- 39- Zihai, S., (2009), "Crack Analysis in Structural Concrete: Theory and Applications", Elsevier Ltd., UK.